Groundwater Residence Time Distributions within the Nevada Environmental Response Trust (NERT) Site, Henderson, Nevada

Rosemary W.H. Carroll
Susan Rybarski
Ronald L. Hershey
Chuck Russell

July 2023

Publication No. 41294

Prepared by
Division of Hydrologic Sciences, Desert Research Institute

Prepared for
Nevada Division of Environmental Protection

THIS PAGE LEFT INTENTIONALLY BLANK

Groundwater Residence Time Distributions within the Nevada Environmental Response Trust (NERT) Site, Henderson, Nevada

Rosemary W.H. Carroll
Susan Rybarski
Ronald L. Hershey
Chuck Russell

July 2023

Publication No. 41294

Prepared by
Division of Hydrologic Sciences, Desert Research Institute

Prepared for
Nevada Division of Environmental Protection

THIS PAGE LEFT INTENTIONALLY BLANK

EXECUTIVE SUMMARY

The Nevada Environmental Response Trust (NERT) site is within the Black Mountain Industrial (BMI) Complex located in Henderson, Nevada, and in the vicinity of the Las Vegas Wash (Wash). The NERT is focused on remediation of perchlorate and other legacy chemicals. As part of remediation efforts, a physically based groundwater model (Phase 6) was developed. The research presented here uses observed groundwater age tracers (δ^2H, $\delta^{18}O$, ^3H, SF_6, CFCs, and ^{14}C) to (i) independently assess the Phase 6 model's ability to replicate observed groundwater ages, (ii) improve conceptual understanding of subsurface flow paths and mixing behavior from source to discharge locations across the site, and (iii) qualitatively address the efficiency and duration of management alternatives needed to meet remedial action objectives. Through an iterative process of backward particle tracking from 130-plus wells and conversations with the Nevada Division of Environmental Protection (NDEP) and NERT, 25 wells were identified for age tracer collection. These wells fell along principal groundwater flow paths, at variable depths, and supported adequate yield for sampling needs as determined in previous NERT monitoring campaigns (>100 mL/min). Wells were also completed in the primary lithologic units represented within the Phase 6 model domain, with eight wells selected near the Wash to capture the age distribution of water discharging into the surface water. Ultimately, lower than expected flow rates at several locations reduced the number of wells actually sampled for age tracers from 25 to 19.

An initial assessment of the young water fraction (age <70 years) in sampled wells relied on ^3H, SF_6, CFCs, and the presence of chemical contaminants. The amount of old water (>1,000 years) relied on ^{14}C, major ion chemistry and water-rock reaction modeling (*NETPATH*). *NETPATH* was used to correct groundwater ^{14}C ages for carbon isotopic changes related to CO_2 gas, calcite, and dolomite dissolution, as well as precipitation and CO_2 degassing. Lumped parameter models (LPM) were used to explore the range in groundwater ages as a function of travel time distribution (e.g., piston flow, exponential mixing, and dispersion) and choice of tracer used for calibration. These age distributions were compared to Phase 6 model estimated age distributions using backward particle tracking. One thousand particles were released from each of the sampled wells and tracked back to their source. Each particle was weighted by the volume of water contributing to their flow path. Sourced water included groundwater basin inflows (GBF), surface recharge, and water seepage from Las Vegas Wash. A sensitivity analysis explored the effect of independent adjustments to three GBF zones, five porosity zones, four vertical hydraulic conductivity zones, and four horizontal hydraulic conductivity zones on simulated age distributions for each of the 19 sampled wells. The simulated age distribution of groundwater discharging into the Wash was determined in a similar fashion as for the sampled wells. Ten particles were released from each gaining Las Vegas Wash stream cell and tracked back to their source. Ages for these particles were grouped into five reaches defined by U.S. Geological Survey stream gage locations and a sixth reach defined by Duck Creek. Age distributions into the Wash reaches are presented for the Phase 6 baseline model (no model parameters adjusted) and using the suite of model parameter adjustments that best mimic the tracer-based age distributions in the sampled wells.

Overall, the Phase 6 model replicates the tracer-based groundwater age distributions in two-thirds of the sampled wells with either the Phase 6 model in its current state (i.e., baseline) or through parameter adjustments tested as part of the sensitivity analysis. Wells

adequately simulated with the current Phase 6 model structure are primarily located in operatable unit-1 (OU-1) and operatable unit-2 (OU-2) (the southern and mid portions of the model domain). Parameter adjustments that improved estimated Phase 6 age distributions were based on reducing southern boundary inflows and increasing the speed of transport. No adjustment was done with respect to surface recharge estimates. The Phase 6 model was unable to capture the tracer-based age distributions in one-third of the wells sampled with or without parameter adjustments. These wells primarily occur in operatable unit-3 (OU-3) (the northern portion of the model domain), as well as east of the NERT facility and proximal to the eastern edge of the Las Vegas Wash (reach 4). In all cases, observed tracers indicate some or all water in the well is modern, whereas the Phase 6 model predictions are overly reliant on deep, old water upwelling to the surface with limited/no inputs of modern water from surface recharge.

The simulated Phase 6 model baseline age distribution for water inflow to the Las Vegas Wash is primarily young with 96.7 percent by volume <10 years and 2.7 percent >100 years. Shifting model parameters to better estimate the fraction of young water observed in sampled wells significantly shifts simulated age distributions in reach 3 and reach 4 toward much younger water but has little effect on the other stream reaches. Flux-weighted particle tracking in the steady-state groundwater model indicates reach 3 contributes <1 percent of the water volume into the Wash. Its volumetric contribution remains unchanged with parameters adjusted in the Phase 6 model. Flux-weighted particles suggest reach 4 contributes 1.3 percent of the simulated Wash volume. With parameter adjustments from the sensitivity analysis, this volumetric contribution increases to 7.3 percent making reach 4 potentially more impactful on the global surface water budget. Additionally, even after parameter adjustments, 30 percent of the water entering reach 4 remains >100 years. This “heavy tail” of older water could have implications on remediation efforts into the far future. However, it is noted that the Phase 6 model is unable to replicate the tracer-based age distributions in wells adjacent to reach 4 and the predicted age distribution into reach 4 is highly uncertain. Improvements to reach 4 groundwater ages could be achieved by increasing localized influences of surface water inputs, including the circulation of Las Vegas Wash surface water through the adjacent gravels. Additional improvement of predicted ages in wells near reach 4 will also require limiting the amount of deeper water upwelling into surface alluvial units by limiting influxes of water from the southern boundary. Given the limited number of age tracer observations and the uncertainty associated with these data, we also recommend a coupled approach using observed age tracers and perchlorate mass balance to better constrain groundwater inputs to the Las Vegas Wash.

ACKNOWLEDGMENTS

We would like to acknowledge the Nevada Division of Environmental Protection (NDEP) and the Nevada Environmental Response Trust (NERT) for project funding and data sharing, as well as insights and logistical coordination for well sampling of groundwater age tracers. We would also like to thank our internal and external reviewers for their time and expertise. This includes Jim Thomas (DRI), Jenny Chapman (DRI), Weiquan Dong (NDEP), and Alka Singhal (Ramboll).

THIS PAGE LEFT INTENTIONALLY BLANK

CONTENTS

LIST OF FIGURES

LIST OF TABLES

LIST OF ACRONYMS

BMI	Black Mountain Industrial Complex
BMM	binary mixing model
CDF	cumulative distribution function
CERCLA	Comprehensive Environmental Response
CFC	chlorofluorocarbon
DIC	dissolved inorganic carbon
DM	dispersion model
DO	dissolved oxygen
DP	dispersion parameter
DRI	Desert Research Institute
EC	electrical conductivity
EMM	exponential mixing model
EPA	Environmental Protection Agency
ET	evapotranspiration
fY	fraction of young water
GBF	groundwater basin inflow
GMWL	Global Meteoric Water Line
^{3}H	tritium
HK	horizontal hydraulic conductivity
ID	inside diameter

LMWL	Local Meteoric Water Line
LPM	lumped parameter model
MDPE	medium density polyethylene
NDEP	Nevada Division of Environmental Protection
NERT	Nevada Environmental Response Trust
OD	outside diameter
ORP	oxidation-reduction potential
OSSM	Olin Chlor Alkali Products, Montrose Chemical Corporation of California, and Stauffer Management Company
OU-1	operatable unit-1
OU-2	operatable unit-2
OU-3	operatable unit-3
PFM	piston flow model
pmC	percent modern carbon
Por	porosity
SF_6	sulfur hexafluoride
SFR	streamflow routing
STOR	groundwater storage
TDS	total dissolved solids
TTD	travel time distribution
TU	tritium units
UMCf	Upper Muddy Creek Formation
USGS	United States Geological Survey
VK	vertical hydraulic conductivity
VOC	volatile organic compound
WEL	specified flux (e.g., groundwater pumping, interbasin groundwater flow)

THIS PAGE LEFT INTENTIONALLY BLANK

1.0 INTRODUCTION

1.1 Purpose and Scope

The Nevada Environmental Response Trust (NERT) is one of five ongoing environmental cleanups being conducted at the Black Mountain Industrial Complex (BMI) that was originally built by the Anaconda Copper Company in 1941 to produce magnesium for the Allied war effort during World War II. The BMI began operation from 1941 to 1945 as the largest magnesium plant in the world at the time. Later, the BMI site was home to the Western Electrochemical Company (1945 to 1967), the American Potash and Chemical Company (1956 to 1967), the Kerr-McGee Corporation (1967 to 2005), and lastly Tronox Inc. (2005 to 2009). Hexavalent chromium and perchlorate were discovered in groundwater in the early 1980s and late 1990s, respectively. Following the bankruptcy of Tronox in 2009, the NERT was established as part of the bankruptcy reorganization, with NERT-focused site remediation of perchlorate, chromium, and volatile organic compound (VOC) contamination. The BMI cleanup is regulated by the Nevada Division of Environmental Protection (NDEP) and the Environmental Protection Agency (EPA) and follows Comprehensive Environmental Response (CERCLA) processes. The NERT investigations conducted to date include, but are not limited to, health risk assessments; interim actions to remove contaminated soil and contaminants from groundwater; development of site conceptual models; implementation of field studies to characterize the subsurface conditions, extent of contamination, and nature of stream-aquifer interactions; and the development of numerical flow and transport models.

Desert Research Institute (DRI) faculty in the Division of Hydrologic Sciences have worked with personnel from the NDEP Bureau of Industrial Site Cleanup for more than four years to provide independent reviews of the NERT site groundwater flow and transport models. As part of this effort, DRI faculty identified a remedial investigation task to quantify groundwater movement and subsurface residence time distributions within the NERT Phase 6 modeling domain (Ramboll 2019). The primary objectives of this investigation are to independently evaluate the Phase 6 numerical flow model using observed groundwater age tracers and assess the age distribution of groundwater flowing into the Las Vegas Wash (Wash). The goal of this study is to improve the conceptual understanding of subsurface flow paths and groundwater mixing from source to discharge location across the modeled domain and to qualitatively address the efficiency and duration of management alternatives needed to meet remedial action objectives. The investigative task is divided into five components: (1) well selection for tracer sampling, (2) groundwater sampling and analysis, (3) lumped parameter models, (4) sensitivity analysis, and (5) Las Vegas Wash age distributions. This report provides insights from the analysis, future modeling recommendations, and addresses approach limitations based on the project's results.

1.2 Methodological Background

Groundwater circulation represents local, intermediate, and regional flow systems (Toth 1963) that can mix and generate a distribution of subsurface residence times. The fate of groundwater contaminants depends on this transit time distribution, which in turn depends on the location and timing of boundary fluxes (e.g., recharge, basin groundwater inflow, stream discharge) and the internal flow structure dictated by geologic considerations (Gleeson et al. 2018; Markovich et al. 2019). Groundwater residence time also indicates the degree of catchment memory of past inputs, and therefore reflects hydrologic sensitivity to

land use and changes in boundary fluxes (McGuire et al. 2005). There is growing awareness that the deeper parts of some aquifers are an important part of the hydrologically active system. These units can potentially store and transmit larger amounts of water and have a greater influence on streamflow exports than previously understood (Condon et al. 2020; Carroll et al. 2020). However, the true importance of these deeper groundwater flows remains largely unknown because the deeper parts of an aquifer system are difficult to characterize and information on hydraulic conductivity, porosity, and flow rates at depth are relatively scarce.

Lumped parameter models (LPMs) have been applied to numerous catchments lacking detailed hydrologic characterization to better understand subsurface flow paths as defined by observed age tracers (McGuire and McDonnell 2006). The age of groundwater at a discharge location (such as a well, spring, or stream water) is estimated by the convolution of time-varying inputs of an environmental tracer applied uniformly across a watershed and lagged through the subsurface by assuming a travel time distribution (TTD) (e.g., piston flow, exponential, dispersion). The TTD is adjusted to match observed tracer concentrations. A variety of environmental tracers exist for LPM calibration. Each tracer is applicable over a certain time range. The most commonly applied tracers for dating modern groundwater include stable isotopes of water (δ^2H and $\delta^{18}O$) for water ages <3 years and chlorofluorocarbons CFC-12, CFC-11, and CFC-113 that identify groundwater recharged since 1941, 1947, and 1955, respectively (<67 to 81 years). In addition, sulfur hexafluoride (SF_6) and tritium (^3H) are commonly used to assess water recharged since the mid-1960s, or <65 years (Solomon and Cook 2000). For the purposes of this study, we generalize across all these tracers and define the young water fraction, or modern water, as groundwater with an age <70 years. We also rely on observed radiocarbon (^{14}C) to understand older groundwaters (>1,000 to 30,000 years). Groundwater ages up to one million years can be identified with ^{36}Cl and ^4He (Aggarwal et al. 2015) but are not included in this study. More recent advances in ultra-trace noble gas radioisotopes use ^{85}Kr, ^{39}Ar, and ^{81}Kr to date modern, intermediate, and old groundwater ages, respectively (Jiang et al. 2012; Yokochi 2016), with ^{39}Ar filling the gap between modern tracers and ^{14}C. However, these tracers are difficult to sample and costly to analyze and are also not included in our analysis.

In contrast to lumped parameter models, numerical mechanistic models and particle tracking can include complex boundary conditions and directly represent the pertinent physical and hydrological characteristics dictating catchment subsurface flow path distributions (Engdahl et al. 2016; Maxwell et al. 2016; Danesh-Yazdi et al. 2018). Numerical models are not limited to a predefined TTD shape as are LPMs. However, these models rely on detailed site characterization and hydrologic data for construction, calibration, and validation. Often data constraints make it difficult to test a conceptual understanding of groundwater flow paths and mixing history. To supplement hydrologic information (such as observed groundwater levels, stream discharge, etc.), recent studies have leveraged observed age tracers to inform numerical model estimates of groundwater flow paths and ages (Ameli et al. 2016; Carroll et al. 2020). The work presented here builds on these approaches in which age tracers are used to assess and inform Phase 6 estimated groundwater flow.

1.3 Site Description and Phase 6 Model Overview

The NERT site is located in southern Nevada near Las Vegas (Figure 1a) with observed perchlorate plumes originating from operatable unit-1 (OU-1) and migrating north-northeast along the principal groundwater flow path toward the Las Vegas Wash (Figure 1b). The OU-1 remediation efforts are focused on plume containment and source control. Operatable unit-2 (OU-2) is downgradient and off-site with remediation focused on mid-plume containment and mass removal. Operatable unit-3 (OU-3) is further downgradient and remediation efforts are focused on mitigating discharge into the Las Vegas Wash (Figure 1c). A second perchlorate plume is associated with American Pacific Corporation (AMPAC) and it occurs to the west of the NERT plume. The two plumes comingle just to the south of the Las Vegas Wash.

The groundwater flow model was constructed with MODFLOW-NWT (Niswonger et al. 2011) to support remediation investigation efforts pertaining to perchlorate (and other contaminants of potential concern) discharged from source areas into the Las Vegas Wash. A full description of the Phase 6 groundwater model is provided by Ramboll (2019) with a brief description provided here in the context of our analysis. The model domain is 23.6 mi^2 and encompasses the spatial extent of the observed contaminant plume and 4.5 miles of the Las Vegas Wash (Figure 1c). The model was developed using a 50 ft to 200 ft resolution grid and contains 10 model layers each ranging in thickness from 1.2 ft to 281 ft thick. There are nearly two-million active cells in the model.

The geology of the NERT site consists of three principal lithologic units (Figure 2). Quaternary alluvial deposits (Qal) occur along the surface and are dominated by a mixture of well-graded sand and gravels and lessor amounts of silt, clay, and caliche. Within this unit, paleochannel deposits occur. These were formed by intermittent flood events that formed narrow, uniform deposits of high permeability. The paleochannels trend north-northeast from the southern boundary of the model domain toward the Las Vegas Wash. Adjacent to the Las Vegas Wash, recent gravel deposits exist that are of very high permeability (Wash gravels). The second primary lithologic unit is the Upper Muddy Creek Formation (UMCf). It is a Pleistocene valley-fill deposit derived from the erosion of the Spring Mountains located to the west of the site that grade into fluvial, swamp, and lake deposits. The top of the UMCf is a thin layer of reworked sediments that are less consolidated (xMCf). Below the xMCf, and with some surface outcropping, is a fine-grained unit of clay and silt deposits (UMCf-fg). Interbedded into the UMCf-fg unit are two coarse-grained deposits. The shallower deposit (UMCf-cg1) is intermixed with the xMCf along the southern edge of the model domain. The deeper unit (UMCf-cg2) is located below the UMCf-fg and it grades upward as one moves north toward the Las Vegas Wash. Lastly, the Horse Springs Formation is situated in the northeast corner of the model domain adjacent to the Wash gravels. It is a dolomitic limestone interbedded with siltstone of lower permeability. It is not spatially extensive in the Phase 6 model domain. Figures 3 and 4 present model representations of these geologic units and their associated hydraulic conductivity and porosity, respectively.

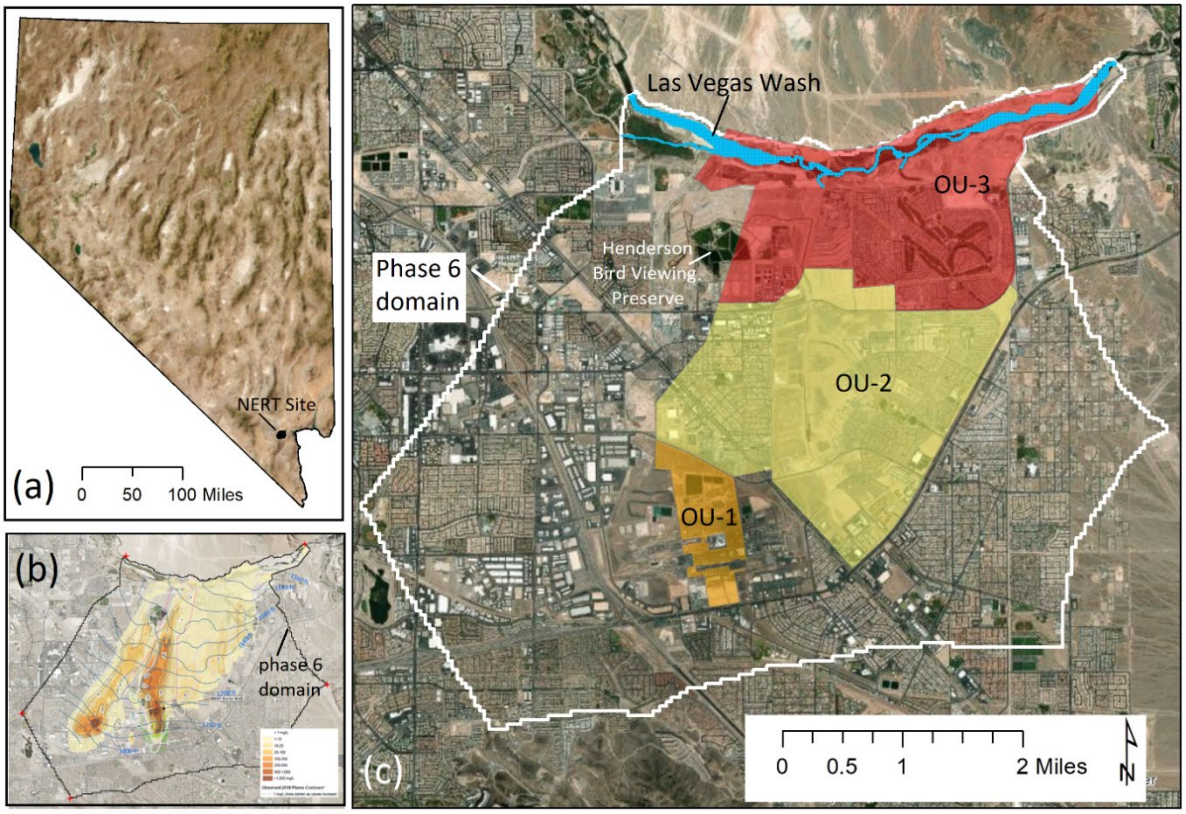

Figure 1. (a) The location of the NERT site in Nevada, (b) observed perchlorate plumes (1 to >1,000 mg/L) (modified from Ramboll [2019]), and (c) operational units within the Las Vegas Wash. Flow in the Las Vegas Wash is left to right. The Phase 6 model domain is identified in both (b) and (c).

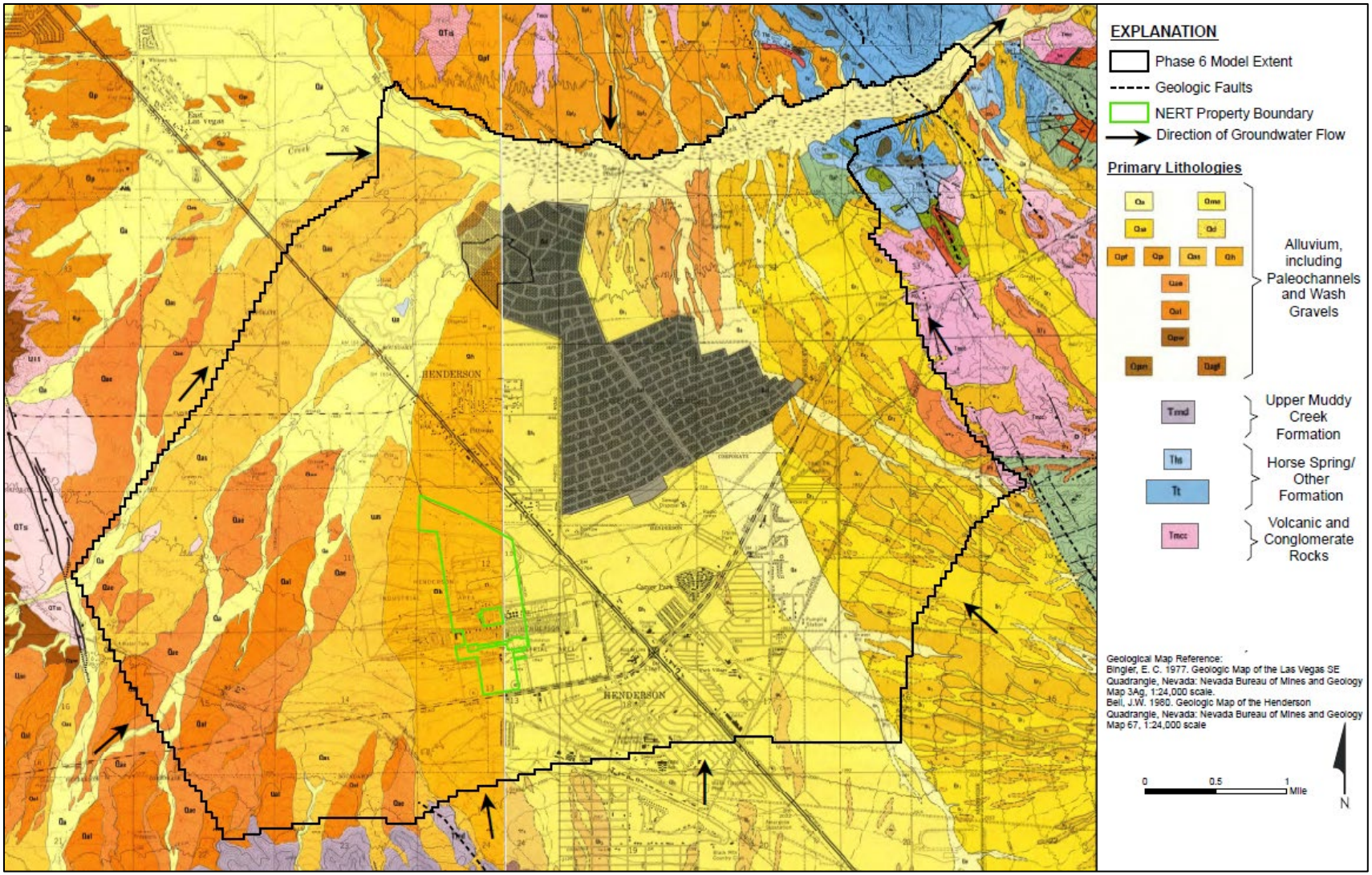

Figure 2. Surface geology for the Phase 6 model domain (modified from Ramboll [2019]).

Inflow to the Phase 6 model domain is dominated by groundwater basin inflows (GBF) shown in Figures 3 and 4. These occur along the southern, western, and northern edges of the model. Inflows were calibrated as part of matching observed water levels and compared to the range in recharge estimates based on both precipitation and elevation upgradient of the boundary (e.g., Maxey and Eakin [1949] and Epstein et al. [2010]). No flow boundaries are set where groundwater flow is parallel to the model domain (refer to Figure 2). Areal recharge into the basin from undeveloped areas is assumed to be negligible, whereas in residential and industrial areas it is defined. Likewise, irrigation recharge for the Chimera Golf Course, Henderson Bird Viewing Preserve, and focused recharge from a variety of effluent ponds and recharge trenches are included. Outflows from the model domain include surface outflows associated with the Las Vegas Wash, groundwater flow exiting the model under the Las Vegas Wash, evapotranspiration (ET) from phreatophytes, drain outflows, and groundwater extraction for industrial, commercial, and remediation efforts (e.g., well barrier walls). The Las Vegas Wash is simulated with the streamflow routing (SFR) package (Niswonger and Prudic 2005) to allow for gaining and losing conditions. Figure 5 depicts the six reaches of the Las Vegas Wash simulated with the SFR package, with gaining model cells color coded by reach. Reach definitions are taken from Ramboll (2019) and are based on U.S. Geological Survey (USGS) stream gages. Reach 1 has been subdivided into reach 1a from the model's western boundary to USGS stream gage Duck Creek Confluence (station ID 09419698) and reach 1b, which isolates Duck Creek contributions. Reach 2 is from the Duck Creek Confluence to Pabco Road (Station ID 09419700). Reach 3 is from Pabco Road to Bostick Weir (Station ID 09419747). Much of reach 3 is losing water to the groundwater system and the gaining cells are isolated to a short distance downstream from the Pabco Road station. Reach 4 is from Bostick Weir to Homestead Weir (Station ID 09419749). Reach 5 is from Homestead Weir to Three Kid Weir (Station ID 360549114564801).

Transient model simulations of the Phase 6 NERT model are for five years (2014 to 2018) at quarterly stress periods to allow for seasonality in ET and streamflow. Water balance terms are compared to the initial steady-state condition in Figure 6. Evapotranspiration and the Las Vegas Wash are tightly coupled in their seasonal oscillation with ET indirectly related to Wash outflows (SFR). Likewise, changes in groundwater storage (STOR) respond quickly to changes in groundwater pumping (WEL). The steady-state conditions approximate average conditions over the transient simulation if one ignores the short-term dewatering done for weir construction in the first and third quarters of 2018. The five-year transient model was deemed too short in duration for the groundwater age analysis. The transient model could have potentially been extended back in time, but the additional simulated years would have required significant effort for data assimilation and calibration. Therefore, running a transient model was considered out of scope of the investigation and steady-state conditions were assumed reasonable for the age analysis.

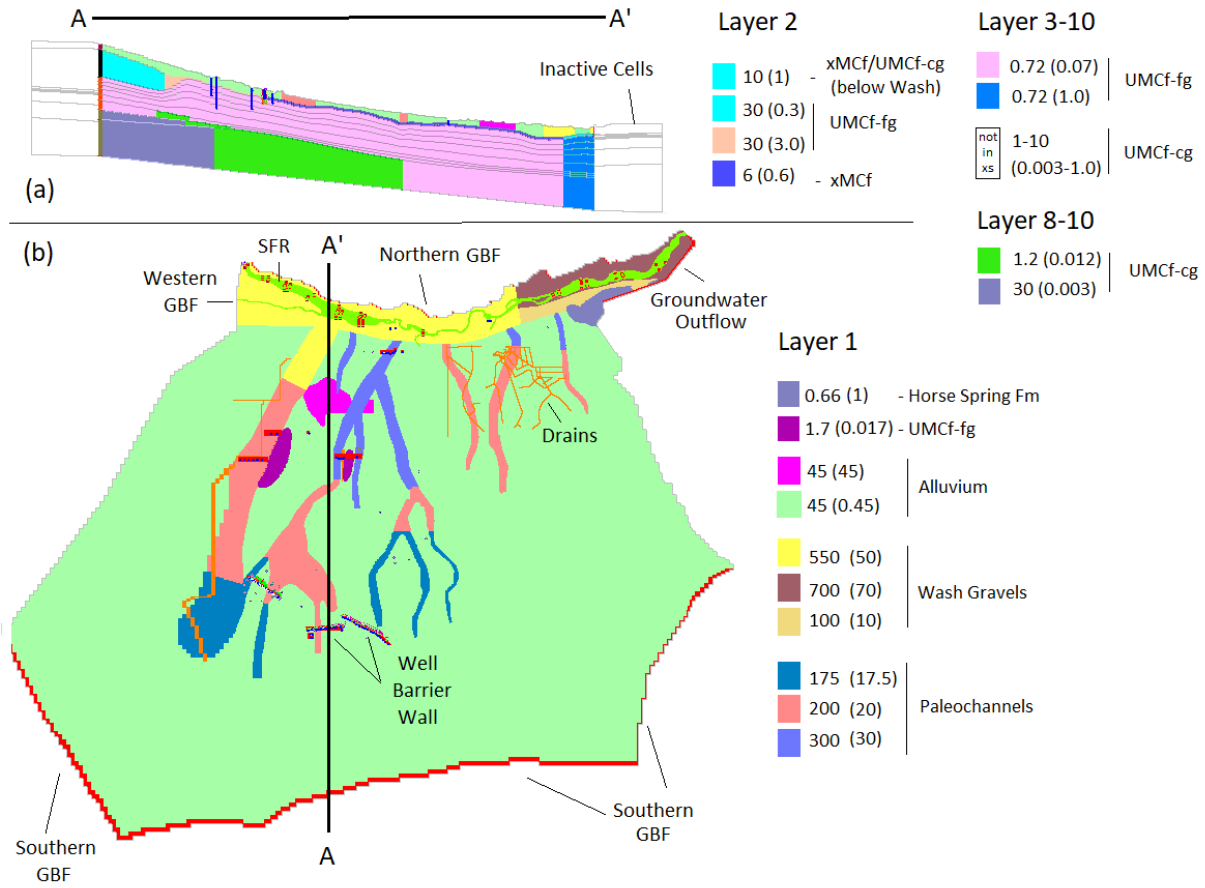

Figure 3. Hydraulic conductivity zones defined in the Phase 6 model. (a) Cross section A-A' with model layers shown and (b) layer 1 with location of A-A' identified. Cross section A-A' is in the vicinity of the NERT perchlorate plume (see Figure 1b). Hydraulic conductivity given as horizontal (vertical) in units of feet/day. Boundary conditions identified. Blue dots are the observation locations (in layer 1 or in the cross section). SFR = streamflow routing cells, GBF = groundwater basin inflow.

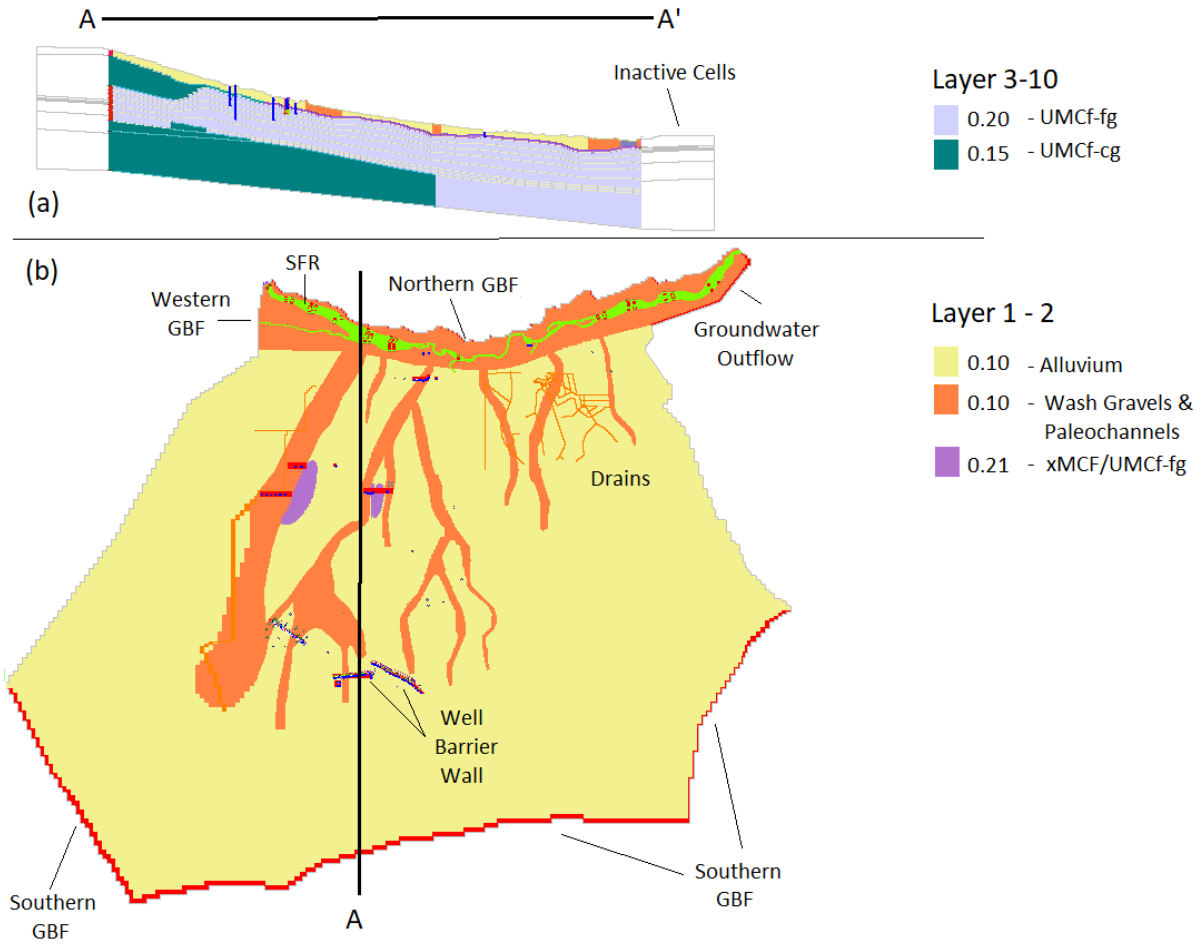

Figure 4. Porosity defined in the Phase 6 model. (a) Cross section A-A' with model layers shown and (b) layer 1 with location of A-A' identified. Boundary conditions identified. Blue dots are observation locations (in layer 1 or in the cross section). SFR = streamflow routing cells, GBF = groundwater basin inflow.

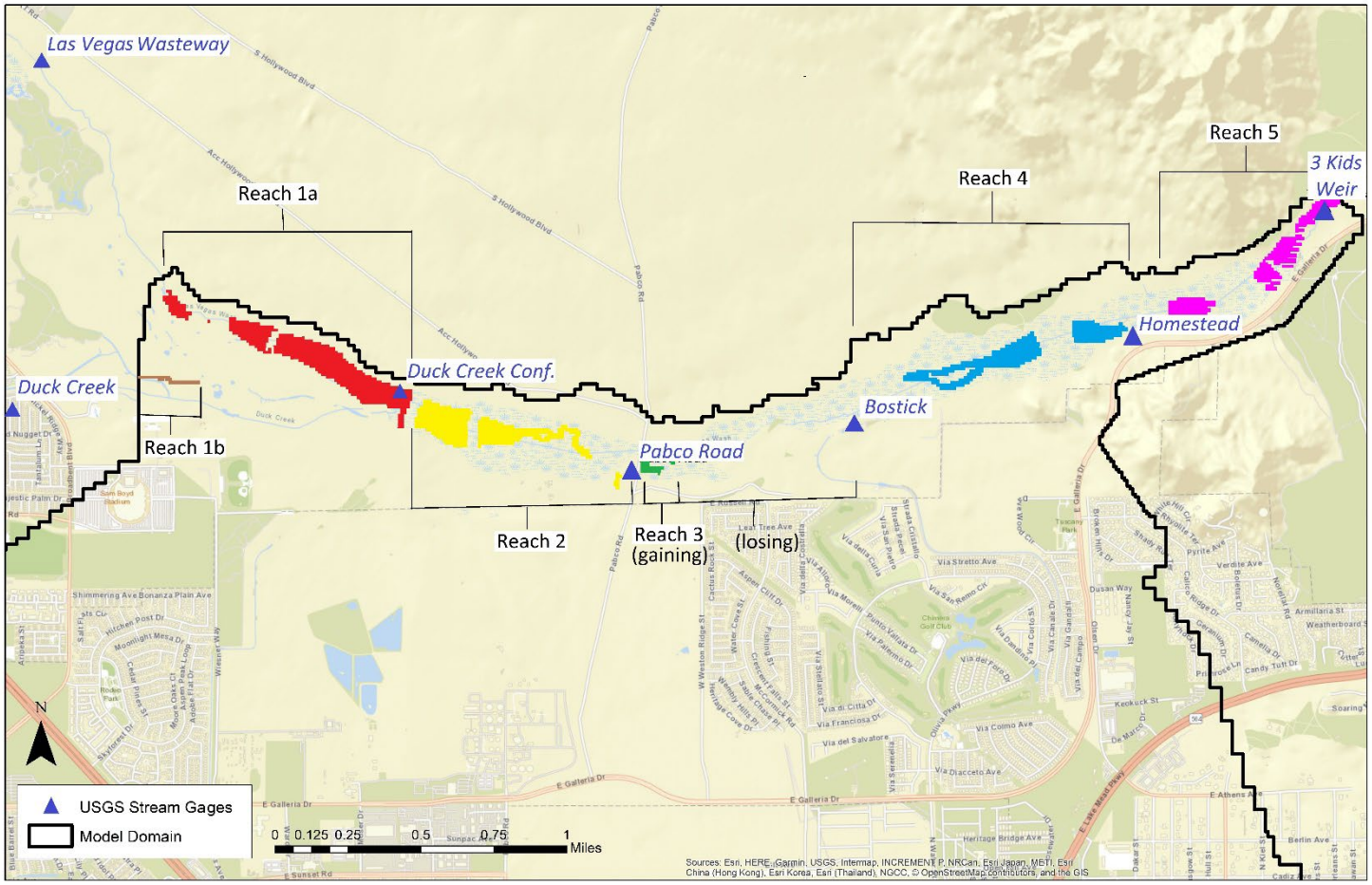

Figure 5. Phase 6 gaining streamflow cells in the steady-state model (using the SFR package) for simulating the Las Vegas Wash. The SFR cells are divided into reaches based on USGS stream gages that are identified with blue triangles and text. Modeled SFR cells are color coded by reach (e.g., red = reach 1a, brown = reach 1b, yellow = reach 2, green = reach 3, blue = reach 4, and pink = reach 5). Losing SFR cells are not shown. Reach 3 only contains a small gaining section.

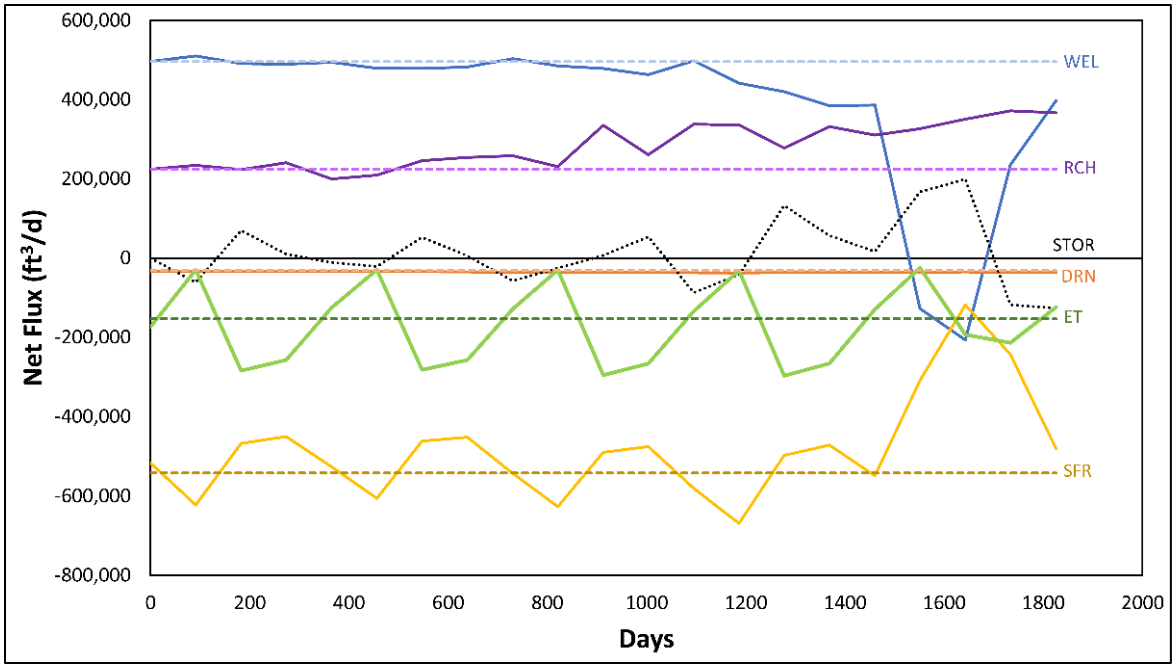

Figure 6. Modeled net transient fluxes (solid lines) and net steady-state fluxes (dashed lines) for the Phase 6 model. Net = inflows – outflows; WEL = simulated interbasin groundwater flows and groundwater pumping; RCH = surface recharge; STOR = changes in groundwater storage; DRN = drain outflow; ET = evapotranspiration; SFR = streamflow routing defining the Las Vegas Wash. Simulation period is 2014 to 2018, with large deviations in seasonal fluxes beginning in 2018 because of increased pumping for Las Vegas Wash weir construction.

2.0 METHODS

2.1 Well Selection

Using the steady-state solution, particles were placed at well screened locations and tracked back in time to assess different flow paths using MODPATH7 (Pollock 2016) in the Groundwater Vistas graphical interface. Approximately 130 wells were evaluated along transects at different depths in the Phase 6 model domain. Potential sampling locations were clustered based on geospatial location within the domain as upland (OU-1), midland (OU-2, OU-3), or proximal to the Las Vegas Wash, with clusters refined based on distinct flow paths and mixing regimes simulated within each of these locations. In addition, wells were selected based on their inclusion in the May 2022 sampling survey by Tetra Tech as containing no/low contamination and not residing in restricted access areas. The results were presented at the NERT Kickoff Meeting on March 2, 2022, for feedback on well selection. Twenty-five sampling wells were identified as possible sites for the groundwater tracer sampling and analysis.

In April 2022, the initial 25-well selection was modified to exclude wells with too small a pumping yield (<100 mL/min) as determined in the spring 2021 NERT sampling campaign. Additional particle tracking was conducted to evaluate flow path configurations for alternatives. During the DRI groundwater tracer sampling campaign in May 2022

(Section 2.2), real-time modifications to well selection using modeled particle tracking was necessary because on-site observations revealed several previously identified wells had lower than expected pumping yields.

2.2 Geochemical Sampling and Analysis

2.2.1 Groundwater Samples

Groundwater sampling was conducted in conjunction with Tetra Tech during the NERT 2022 annual sampling event from May 2 to May 11, 2022. Tetra Tech inspected the wells, measured depth to water, installed new bladders in the bladder pump for each well, purged the well using low-flow purging techniques, and monitored field parameters (temperature, pH, electrical conductivity [EC], dissolved oxygen [DO], turbidity, and oxidation-reduction potential [ORP]). Once water levels and field parameters stabilized, Tetra Tech collected their samples, and then DRI commenced with their sampling. Several wells had dedicated bladder pumps; bladders were not replaced in these pumps prior to sampling.

Less than 1 m of 6.35 mm (0.25 inch) inside diameter (ID) Tygon tubing was slipped over the 6.35 mm (0.25 inch) outside diameter (OD) medium density polyethylene (MDPE) pump discharge tubing and secured with a stainless-steel hose clamp. Initially, a 0.45 µm groundwater filter cartridge was installed at the end of the Tygon tubing with a barbed fitting. Approximately 200 mL of groundwater was flushed through the tubing and filter cartridge, and then discarded to purge the tubing and filter. Samples were collected in the following order: δ^2H and $\delta^{18}O$, cations, anions, and dissolved inorganic carbon (DIC) ^{14}C. The filter cartridge was then removed and samples for SF_6, ^3H, and dissolved gases (N_2 and Ar) were collected. The Tygon tubing was removed and <1 m of 6.35 mm (0.25 inch) OD refrigerator-grade copper tubing was connected to the MDPE pump discharge tubing with a 6.35 mm (0.25 inch) OD plastic SharkBite connector. Samples for CFCs were then collected. Samples were collected in appropriate bottles, as listed in Table 1. Bottles for δ^2H and $\delta^{18}O$, cations, anions, DIC ^{14}C, and ^3H were rinsed with groundwater prior to filling. Bottles for SF_6, dissolved gases, and CFCs were flushed with groundwater prior to capping, as described in the U.S. Geological Survey's Reston Groundwater Dating Laboratory procedure for each analyte (https://water.usgs.gov/lab/sf6/sampling/, https://water.usgs.gov/lab/dissolved-gas/sampling/, https://water.usgs.gov/lab/chlorofluorocarbons/sampling/bottles/) and listed in Table 1.

The δ^2H and $\delta^{18}O$ samples were analyzed at the Nevada Stable Isotope Laboratory in Reno, Nevada (https://www.unr.edu/geology/research/labs-and-facilities). Cations and anions were analyzed at Silver State Analytical in Las Vegas, Nevada (https://www.ssalabs.com/). Dissolved inorganic carbon ^{14}C was analyzed at the University of Arizona Accelerator Mass Spectrometer Lab (https://ams.arizona.edu/radiocarbon) in Tucson, Arizona. The University of Utah Dissolved and Noble Gas Service Center (https://noblegaslab.utah.edu/) in Salt Lake City, Utah, analyzed ^3H. The U.S. Geological Survey's Reston Groundwater Dating Laboratory (https://water.usgs.gov/lab/) in Reston, Virginia, analyzed SF_6, dissolved gases, and CFCs.

Table 1. Sample bottle type, volume, cap type, rinsing or flushing, filtering, and/or preservative requirements for each analyte.

Analyte	Bottle Type	Volume (mL) [#]	Cap	Rinse or Flush	Filtered	Preservative
d^2H and $d^{18}O$	glass	30 [2]	Polycone	no rinse	0.45 mm	none
Cations	plastic	250 [1]	plastic	rinse	0.45 mm	HNO_3 ice
Anions	plastic	500 [1]	plastic	rinse	0.45 mm	ice
^{14}C	glass	1,000 [2]	Polycone	rinse	0.45 mm	ice
^{3}H	glass	500 [2]	Polycone	rinse	no	none
SF_6	amber glass	1,000 [2]	Polycone	flush	no	none
Dissolved Gases	glass	150 [2]	stopper	flush	no	none
CFCs	glass	125 [4]	aluminum foil lined	flush	no	none

2.2.2 Geochemical and Isotopic Modeling of Groundwater Travel Times

Water-rock reaction modeling was used to correct ^{14}C ages for carbon isotopic changes in groundwater caused by water-rock reactions along a flow path, specifically CO_2 gas, calcite, and dolomite dissolution, precipitation, or degassing. Typically, a set of water-rock reactions and the carbon isotopic changes caused by these reactions are modeled either along a groundwater flow path from one well to another or by mixing different upgradient groundwaters to produce the observed downgradient groundwater using the *NETPATH* modeling software (https://wwwbrr.cr.usgs.gov/projects/GWC_coupled/netpath/). The average time it takes (in years) for the water to flow from the upgradient groundwater to the downgradient groundwater is referred to as the corrected ^{14}C "travel time" or as the corrected ^{14}C "age" of the downgradient groundwater.

The water-rock reaction model setup was developed by both the major-ion water chemistry collected during this study and by the mineralogy of the geologic units present in the study area. The setup included the constraints: carbon, chloride, sulfur, calcium, magnesium, sodium, potassium, and silica with $\delta^{18}O$ used to determine the mixing ratio in mixing scenarios. It also included the phases CO_2 gas, calcite, dolomite, gypsum, NaCl, albite, potassium feldspar, biotite, anorthite, plagioclase-anorthite 45 percent, SiO_2, calcium montmorillonite, sodium montmorillonite, potassium montmorillonite, felsic montmorillonite, and calcium-magnesium-sodium exchange. Dolomite, gypsum, NaCl, albite, potassium feldspar, biotite, anorthite, and plagioclase-anorthite 45 percent were only allowed to dissolve, whereas calcium montmorillonite, sodium montmorillonite, potassium montmorillonite, and felsic montmorillonite were only allowed to precipitate. Carbon dioxide gas, calcite, SiO_2, and calcium-magnesium-sodium exchange were allowed to either dissolve, precipitate or degas. Carbon isotopes for calcite and dolomite were set to 0‰ for $\delta^{13}C$ and 0 percent modern carbon (pmC) for ^{14}C, whereas $\delta^{13}C$ was set to -12‰ for CO_2 gas (Quade et al. 1989) and ^{14}C was set to 100 pmC. The soil gas $\delta^{13}C$ has not been measured in the Las Vegas Valley but the elevation and plant community in the lowest elevation in Quade et al. (1989) is similar to the Las Vegas Valley. For a given scenario, a water-rock reaction model

was considered valid when the amount of any phase change was ≤10 mmol/L and the computed $\delta^{13}C$ of the mixture was ≤1.0‰ of the measured $\delta^{13}C$ of the downgradient groundwater. *NETPATH* used $\delta^{18}O$ to calculate the mixing ratios between the different mixing components (i.e., end-member wells). Because only 19 wells were sampled for isotopic and groundwater age tracers in the study area, some wells were used to "represent" assumed water chemistry and isotopic signatures in other areas and along other flow paths where unsampled wells, or no wells exist. This technique of using data from a well in one area to "represent" data from another area where the groundwater is from the same aquifer at similar depths is a common practice in correcting groundwater ^{14}C ages for water-rock reactions (e.g., Kwicklis et al. [2021]).

2.3 Lumped Parameter Models

Lumped parameter models (LPMs) were developed for each sampled well using the USGS program *TracerLPM* (Jurgens et al. 2012). The LPMs test the age distribution sensitivity as a function of the different travel time distributions and choice of tracer used in the calibration. The resulting age distributions provide additional guidance on the mixing fractions of modern (<70 years) and older water (>1,000 years) given by the geochemical analysis. The LPM results were then compared with the Phase 6 numerical model output at each sampled well in the NERT domain. For steady-state conditions, a tracer concentration in a well is calculated as the convolution:

$$C_{out}(t) = \int_{-\infty}^{t} C_{in}(t')\, e^{-\lambda(t-t')} g(t-t')dt', \quad (1)$$

where C_{out} is the outlet tracer concentration, C_{in} is the concentration of the tracer at the inlet, t is the sampling date, t' is the date at which the water parcel entered the system, λ is a decay constant, and $t-t'$ is the age of the water parcel. Lastly, $g(t)$ is the assumed travel time distribution (TTD) that mathematically describes different groundwater flow paths. *TracerLPM* solves closed-form analytical equations by using a time series of regional atmospheric inputs for each tracer and calibrating $g(t)$ to match observed tracer observations in the well.

We optimized the age distribution using observed tracer data and varying the TTD form. Specifically, we considered age distributions based on the piston flow model (PFM), the exponential mixing model (EMM), and the dispersion model (DM). A brief overview of each TTD is provided here, but a full description can be found in Jurgens et al. (2012). The PFM is represented by a Dirac delta function and assumes a tracer travels through the subsurface with no dispersion (i.e., no mixing). It is the simplest TTD and is applicable in groundwater systems with fast advective velocity, short travel distances, or short well screens. The EMM portrays groundwater age logarithmically stratified with depth. It assumes a homogenous aquifer of constant thickness and uniform recharge. Longitudinal and transverse dispersion are not simulated along flow paths, but age mixing is assumed to occur within a well. The DM is based on the one-dimensional solution to the advection-dispersion equation and relies on defining a dispersion parameter (DP), or the inverse of the Peclet number. The DP is equal to the dispersion coefficient divided by the velocity and distance of the well from the input. In practice, the DP is a measure of the relative importance of dispersion to advection and it defines the relative width and height of the TTD. High values of the DP will push the distribution toward a larger fraction of younger water, whereas lower

values will push the distribution closer to the mean age, or a PFM. Figure 7a provides examples based on a mean age of 50 years. Ideally, the number of observations should be one more than the number of unknown parameters (p) in the TTD. For example, both PFM and EMM have only one unknown, the mean (p=1), whereas for the DM, p=2 (mean, DP). However, the challenge is to add additional observations and still simulate their concentrations with significance. Significance is considered to be established if the relative predictive error is <5 percent. Therefore, maintaining low predictive error is a cutoff for adding secondary or tertiary observations.

We also used binary mixing models (BMM) to estimate two-component mixing models for wells containing both younger and older water. For example, using an EMM-DM, the younger water is described by an EMM and the older water is described by a DM. However, for BMMs, the unknown parameters from both distributions are combined, and then one more degree of freedom is added for the mixing fraction. For example, the unknowns for a PFM-PFM and EMM-EMM are the mean of the younger water, the mean of the older water plus the mixing fraction. For a DM-DM, the number of unknowns increases to five. Given the large degree of freedom for DM-DMs, only PFM-PFMs were considered in our analysis. Figure 7b provides examples of different BMMs with the same age statistics.

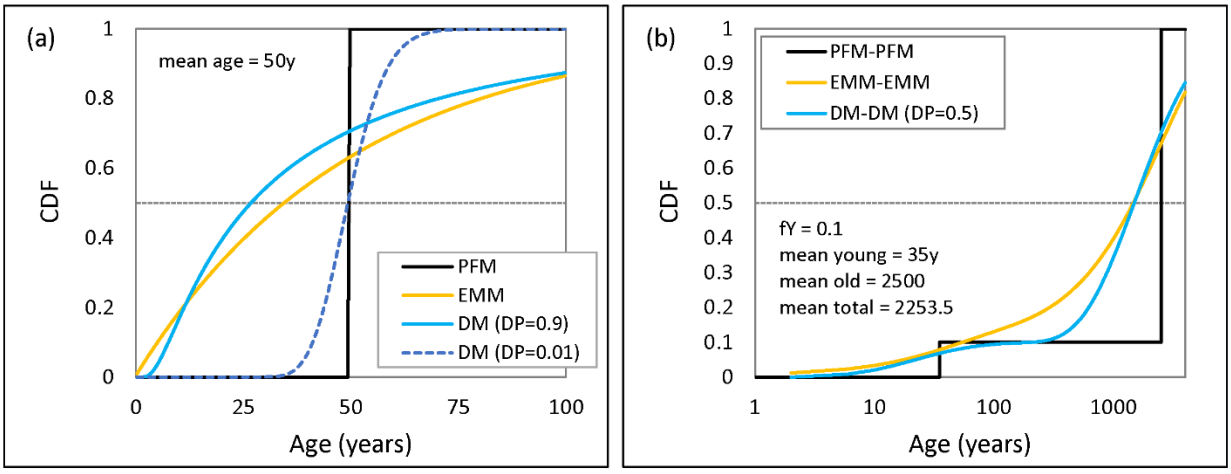

Figure 7. Examples of lumped parameter models using different travel time distributions. (a) Examples of PFM, EMM, and DM with different DPs for the same mean age of 50 years and (b) BMMs assuming PFM-PFM, EMM-EMM, and DM-DM for a 10 percent fraction of young water (fY) with the mean age of young water equal to 35 years, the mean age of old water equal to 2,500 years, and the mean age of total water equal to 2,253.5 years. Age distributions are plotted as a cumulative distribution function (CDF).

To optimize the age distribution to observed tracer concentrations, recharge concentration input history was specified by region. These atmospheric inputs were provided by *TracerLPM*. For the Las Vegas Wash, ^{3}H (tritium units [TU]) uses atmospheric data collected in California. SF_6 (pptv) and CFCs (pptv) were first corrected for recharge temperature, recharge elevation, and excess air using observed dissolved gas concentrations collected simultaneously with SF_6 and CFCs from each sampled well. Atmospheric inputs for

SF_6 and CFCs then rely on data collected in the northern hemisphere. Atmospheric inputs for ^{14}C are defined for the northern hemisphere while groundwater samples rely on the *NETPATH*-corrected ^{14}C (pmC). Radioactive decay assumes half-lives of 12.32 years for ^{3}H and 5,730 years for ^{14}C. No adjustment to travel time ages was made for the unsaturated zone.

For wells containing no evidence of old water (i.e., uncorrected ^{14}C >80 pmC), the following steps were performed to calibrate LPMs. First, individual tracers were assessed to see if various LPMs could mimic concentrations with a reasonable fit using *TracerTracerFits* subroutine in the *TracerLPM* program. Optimization solves for mean age with bounds set at 1 and 100 years. If the upper bound was exceeded, then it was raised to accommodate the optimization. For DMs, the optimization also simultaneously solved for DP, with DP bounds set at 0.01 and 0.9. These bounds were not expanded if iteration was necessary to converge on a significant solution. Solutions for which tracer concentrations were estimated with a relative error <5 percent were assumed to be a good fit and significant. Second, to limit the number of multi-tracer optimization scenarios, the *TracerTracerGraphs* subroutine in the *TracerLPM* program was used to establish which tracers and models were reasonable through a graphical interpretation. Reasonable models were then optimized using the *TracerTracerFits* routine to solve for multiple tracers simultaneously using the same criteria described for a single tracer optimization.

For wells containing both young and old water (uncorrected ^{14}C between 40 pmC and 75 pmC), PFM-PFMs were developed. To simplify the analysis, the average age for the young fraction was initiated based on the average PFM for ^{3}H (or SF_6 or CFCs if no ^{3}H was observed). Then, the average age for the corrected ^{14}C and the fraction of young water (fY) was assumed based on the geochemical analysis. Optimization was done in two parts. First, the routine adjusted the mean age of young water (bounds set to 1 and 100 years) and the fraction of young water (fY, bounds set to 0.01 and 0.99) to best match a modern tracer. These values were then held static, and the mean age of the old water was manually adjusted to reduce the error in the ^{14}C to <5 percent. The optimization bounds for the mean age of old water was set to 1,000 to 30,000 years.

2.4 Sensitivity Analysis

Using the Phase 6 model, a total of 33 steady-state simulations were run with backward particle tracking performed for each of the 19 wells sampled for age tracers. This includes the calibrated baseline simulation and 32 additional runs in which parameters were adjusted up and down from their calibrated values. Simulations mimic the sensitivity analysis conducted for the Phase 6 model based on flow and transport model objectives (Ramboll 2019). Specifically, 16 parameter groups were independently adjusted from their baseline value. The parameter groups are based on three zones defining GBF and five zones defining porosity (Por) (Table 2; also see Figure 4). Four lithologic zones defined horizontal hydraulic conductivity (HK)and four zones defined vertical (VK) hydraulic conductivity (Table 3; also see Figure 4). Model values generally represent ±25 percent of the baseline value. Exceptions include the southern GBF (zone 1) with a minimum flow 20 percent below baseline due to difficulty in converging at lower flows and ±50 percent adjustments for porosity.

Particle tracking captures advective flow only and accounts for flow across each of the six faces of a finite-difference cell (top, bottom, each side). Backward particle tracking uses the reverse sign of all the velocity components used for forward particle tracking and in theory should produce the same results. However, differences can potentially occur as a function of deformed vertical grids in which cell thickness are not perfectly horizontal. To combat this challenge, we use a large number of particles in the horizontal and vertical directions for a given well location (total 1,000 particles). Python codes were developed for batch processing to (a) run MODFLOW-NWT for a given set of parameters; (b) create MODPATH 7 files for backward particle tracking with particles aligned in each well cell evenly distributed in the x, y, and z dimensions (10x10x10), for a total of 1,000 particles; (c) assess relative volumetric contribution for each endpoint of 1,000 flow paths as either the injection well representing GBF, areal recharge, or stream leakage from the Las Vegas Wash; and (d) produce cumulative distribution functions for each of the 19 sampled wells using the volume weighted ages for each flow path from the 1,000 particles. These age distributions were then compared to significant LPM models developed using observed tracer concentrations.

Table 2. Parameter groups for the groundwater basin inflow (GBF) and porosity (Por) used in the sensitivity analysis.

	Zone	Description	Units	Baseline	High	Low
GBF	1	Southern	ft^3/d	447,991	559,989	335,993
	2	Western	ft^3/d	359,620	449,525	269,715
	3	Northern	ft^3/d	34,212	42,765	25,659
Por	1	Qal	unitless	0.1	0.15	0.05
	2	UMCf-fg	unitless	0.2	0.3	0.1
	3	paleochannels & wash gravels	unitless	0.1	0.15	0.05
	4	UMCf-cg	unitless	0.15	0.225	0.075
	5	UMCf-fg/xMCf	unitless	0.21	0.315	0.105

Table 3. Parameter groups for horizontal (HK) and vertical (VK) hydraulic conductivity used in the sensitivity analysis.

Zone	Description	MF Param. Group	HK			VK		
			Baseline	High	Low	Baseline	High	Low
1	Qal	1	45	56.25	33.75	0.40	0.5	0.30
1	Qal	10	45	56.25	33.75	45.00	56.25	33.75
1	Qal	60	45	56.25	33.75	45.00	56.25	33.75
1	Qal	23	21	26.25	15.75	1.00	1.25	0.75
2	Paleo	3	300	375	225.00	30.00	37.50	22.50
2	middle LVW	4	550	687.5	412.50	55.00	68.75	41.25
2	Paleo	6	200	250	150.00	20.00	25.00	15.00
2	Paleo	14	175	218.75	131.25	17.50	21.88	13.13
2	LVW gravels	15	100	125	75.00	10.00	12.50	7.50
2	LVW gravels	31	600	750	450.00	60.00	75.00	45.00
2	north LVW	62	700	875	525.00	70.00	87.50	52.50
3	UMCf-fg	2	0.72	0.90	0.54	0.07	0.09	0.05
3	UMCf-fg	16	0.72	0.90	0.54	0.03	0.04	0.02
3	UMCf-fg (layer 1)	24	1.70	2.13	1.28	0.02	0.02	0.01
3	Horse Springs	32	0.66	0.82	0.49	1.00	1.25	0.75
3	below LVW	54	0.72	0.90	0.54	0.72	0.90	0.54
3	below LVW	61	0.72	0.90	0.54	1.00	1.25	0.75
4	UMCf-cg	50	30	37.5	22.50	3.00	3.75	2.25
4	xMCf/UMCf-cg	13	10	12.5	7.50	1.00	1.25	0.75
4	xMCf	26	6	7.5	4.50	0.60	0.75	0.45
4	UMCf-cg	36	1	1.25	0.75	0.10	0.13	0.08
4	UMCf-cg	37	1.2	1.5	0.90	0.12	0.15	0.09
4	UMCf-cg	38	1.2	1.5	0.90	0.12	0.15	0.09
4	UMCf-cg	44	10	12.5	7.50	1.00	1.25	0.75
4	UMCf-cg	45	30	37.5	22.50	0.30	0.38	0.23
4	UMCf-cg	46	1.2	1.5	0.90	0.01	0.02	0.01
4	xMCf/UMCf-cg	51	10	12.5	7.50	1.00	1.25	0.75
4	UMCf-cg	52	30	37.5	22.50	0.00	0.00	0.00
4	xMCf	55	6	7.5	4.50	6.00	7.50	4.50
4	xMCF/UMCf-cg	59	10	12.5	7.50	1.00	1.25	0.75

MF Param. Group = MODFLOW parameter groups used in Groundwater Vista; LVW = Las Vegas Wash; Paleo = Paleochannel; Qal = Quaternary alluvium.

2.5 Las Vegas Wash Analysis

Backward particle tracking was used to assess the simulated age of groundwater discharging to surface water within the Las Vegas Wash. Using the baseline steady-state model, 1,836 model grid cells assigned to the SFR package were identified where the flow budget indicated that the stream was gaining (i.e., the aquifer discharges to the stream). These cells were then divided into six groups corresponding to the five stream reaches defined in Ramboll (2019) that fall within the model domain as well as the Duck Creek tributary, which is considered part of reach 1 in that report (Figure 5). The SFR segments were kept intact such that if a USGS gage fell inside a SFR segment, all particles assigned to cells in that segment were grouped into the reach that held the majority of that segment.

Each cell used in the particle tracking analysis was assigned ten particles evenly distributed near the bottom of each cell for a total of 18,360 particles. Unlike in the particle tracking done for the sensitivity analysis, the weak source/sink option was set to "pass through," which allowed particles to stop at these sources and resulted in all particles having an age of zero days. As in the sensitivity analysis described in Section 2.4, recharge was assessed for each particle's endpoint as either the interbasin flow rate, areal recharge, or stream leakage from the Las Vegas Wash. Flow paths were then grouped into the six reaches defining the Las Vegas Wash and plotted as volume weighted CDF.

The results of the sensitivity analysis described in Section 2.4, along with the geochemical sampling and LPM analysis results, were used to create a set of optimized model parameters intended to simulate observed groundwater ages in sampled wells more closely. Section 3.4.4 describes this set of optimized parameters and the analysis used to derive them. These parameters were then simultaneously assigned to the Phase 6 model, and the flow model was run again. As in the baseline analysis, the simulated flow budget was assessed to identify gaining SFR cells. In the optimized model, fewer SFR cells were identified as gaining (a total of 1,787 cells) compared to the baseline model. Cells were divided into the same reaches as in the baseline model, and again 10 particles were assigned per cell for a total of 17,870 particles. Simulated ages were compared to the baseline scenario and plotted by reach as volume weighted CDF.

3.0 RESULTS

3.1 Well Selection

Using a combination of particle tracking and on-site logistics, a total of 25 wells were identified for sampling (Figure 8), with 19 wells containing adequate flow rates to sample age tracers. These wells follow the principal groundwater flow direction from the southern boundary (near the NERT site OU-1) to the Las Vegas Wash. Selection attempted to capture both shallower and deeper flow paths to parse out relative mixing between the two and collect samples where shallow and deeper wells were in close proximity to one another (Figure 9). For example, wells TR-8 and TR-7 represent those sampled closest to the southern boundary. They source water from a coarse-grained unit of the Upper Muddy Creek Formation (UMCf-cg1, -cg2) and they are completed at depths below ground surface of 94 feet and 291 feet, respectively. These depths represent model layer 2 and model layer 10. Likewise, M-207, M-212, and M-155 are screened 25-45 feet (layer 2), 60-70 feet (layer 3), and 200-220 feet (layer 10) below ground surface, respectively. Well M-212 had a slow yield

(<75 mL/min) and could not be sampled for age tracers, but wells M-207 and M-155 had a sufficient flow rate to allow sampling of age tracers. Multiple wells were sampled in the vicinity of the Las Vegas Wash to capture the mixing behavior of groundwater prior to exiting into the surface water body. Moving west to east in the direction of surface water flow, these include PC-157A and PC-157B, NERT5.49S1, MW-201A, NERT4.93S1, MW-224A, NERT4.71S1, and MW-25. These wells are primarily shallow (layer 1) with a few located slightly deeper near the eastern edge of the model (layer 2-3). The physical details of each well are included in Section 3.3.

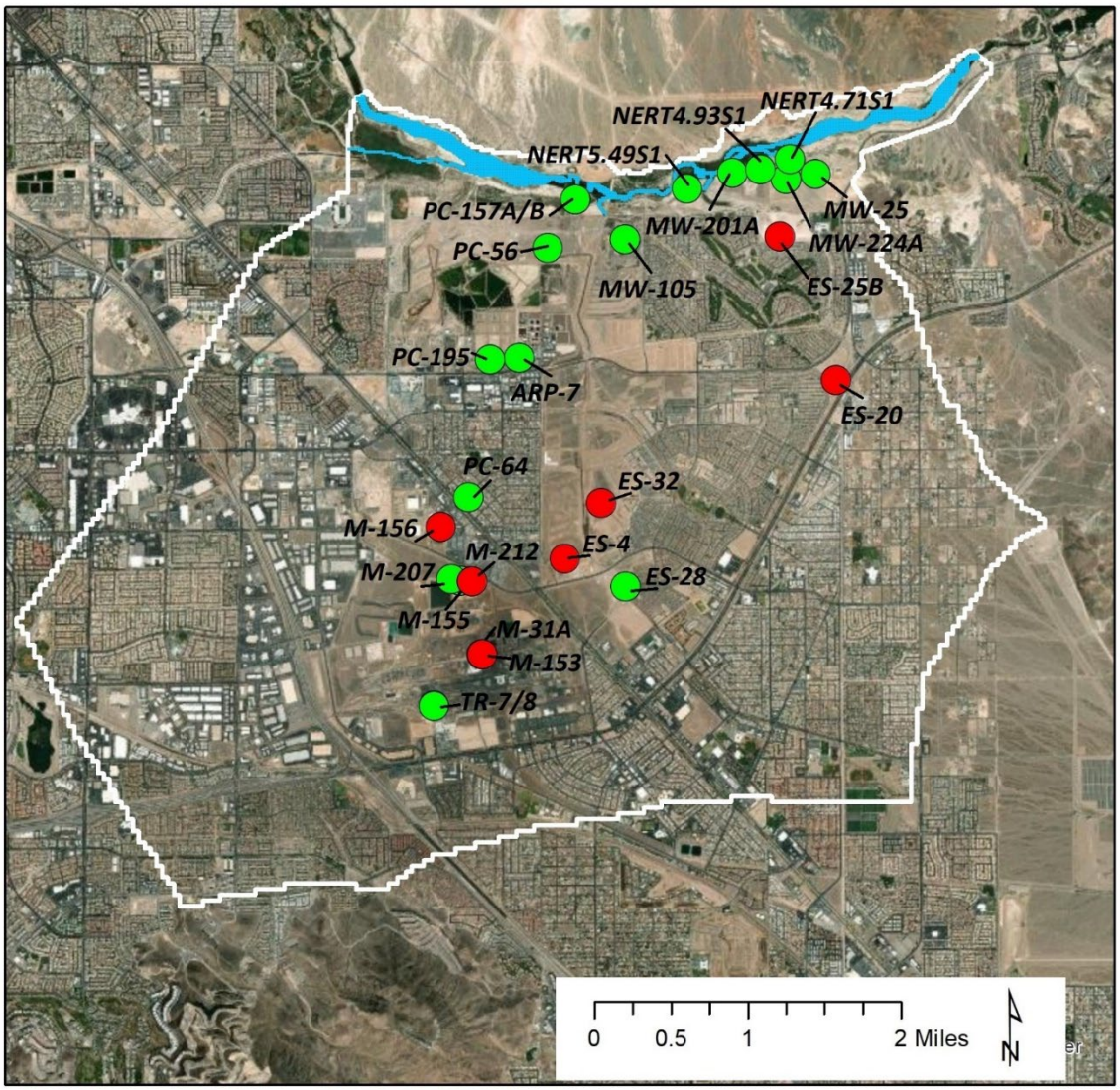

Figure 8. Selected wells for geochemical and age tracer sampling in the Phase 6 model domain (white boundary). Included is the Las Vegas Wash (light-blue area along northern edge of model domain), wells selected but not sampled for age tracers (red circles), and wells selected and sampled for age tracers (green circles). Note that M-31A was sampled for age tracers but is hidden by the M-153 symbol.

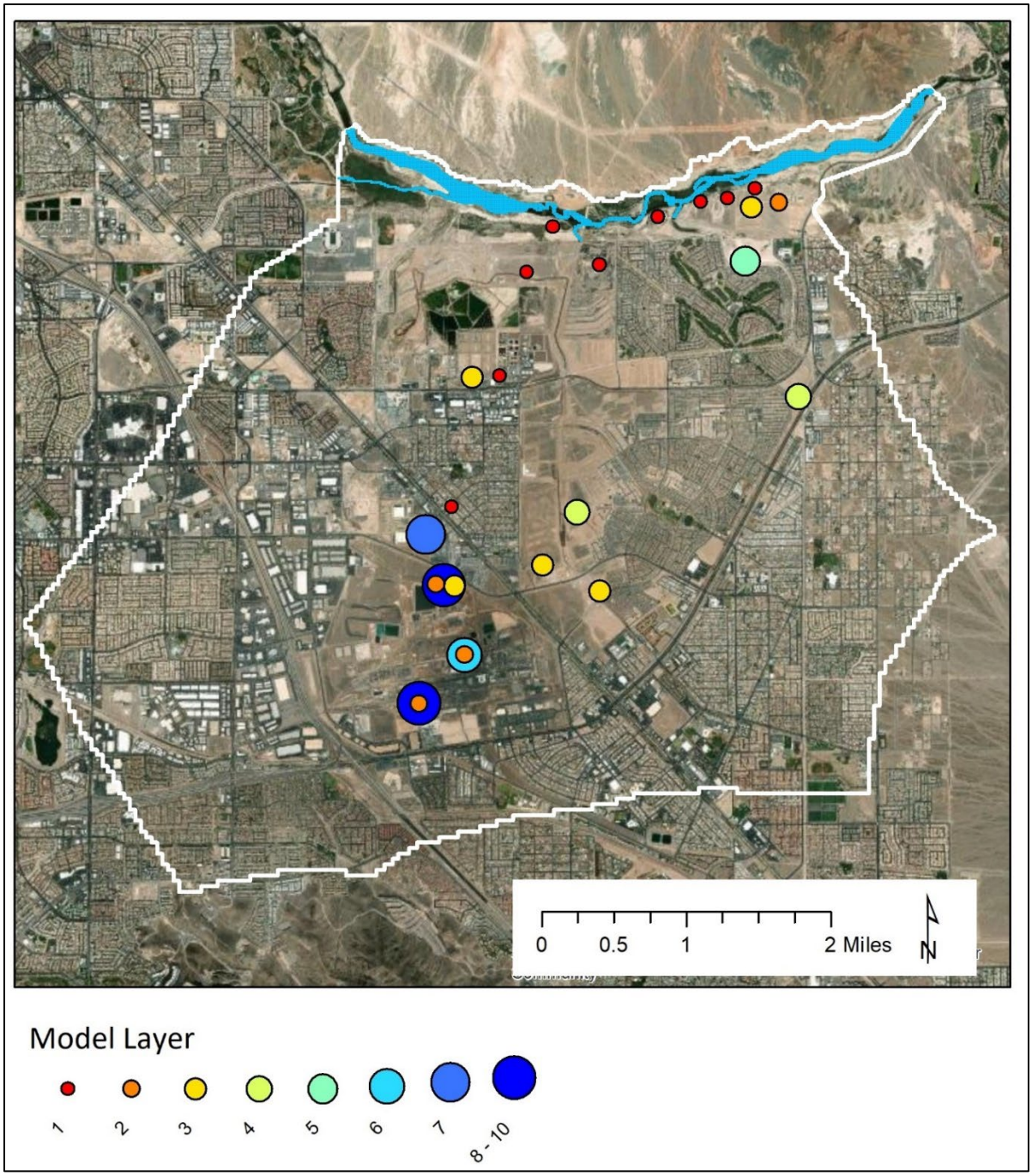

Figure 9. Model layers containing the screened interval of selected wells for geochemical and age tracer sampling. The Phase 6 model domain (white boundary) is provided. The Las Vegas Wash (light-blue area at the northern edge of the model domain) is included. The model layers in which wells are screened are identified by symbol size (increasing with depth) and are color coded. Layer 1 is the shallowest model layer and layer 10 is the deepest model layer.

3.2 Groundwater Sampling and Analysis

3.2.1 Groundwater Samples

Analytical results for groundwater samples are provided in Appendix A. These results are described in detail below.

3.2.1.1 Stable Isotopes of Water

Twenty-one samples were collected and analyzed for δ^2H and $\delta^{18}O$. The results ranged from -96 to -87‰ for δ^2H and from -12.7 to -9.4‰ for $\delta^{18}O$. Figure 10 shows the isotopic results with the Global Meteoric Water Line (GMWL, solid black line [Craig 1961]) for reference. The GMWL defines the average relationship between ^{18}O and ^{2}H in worldwide fresh surface waters (Clark and Fritz 1997) and is a straight line, $\delta^2H = 8\ \delta^{18}O + 10‰$, with a slope of 8 and a y-intercept of 10‰. The Local Meteoric Water line (LMWL) is the local relationship between ^{18}O and ^{2}H. The LMWL differs from the GMWL because of variations in climatic and geographic settings (Clark and Fritz 1997). The LMWL for the Las Vegas Valley was developed from monthly precipitation samples collected at DRI from 1997-1999 and 2016-2017 (Pohlmann and Heintz 2017) is also shown in Figure 10 as a dashed black line. The LMWL equation is $\delta^2H = 7.3\ \delta^{18}O - 4.6‰$. Water samples that plot to the right of the LMWL are evaporated from the original source water. An evaporation trend line (dotted black line in Figure 10), with a slope less than the LMWL, can be drawn through the groundwater points and extended back to the LMWL to determine the average isotopic composition of source water at the time of groundwater recharge. The evaporation trend line equation is $\delta^2H = 2.9\ \delta^{18}O - 60.4‰$ and intercepts the LMWL at -97.5‰ δ^2H and -12.8‰ $\delta^{18}O$.

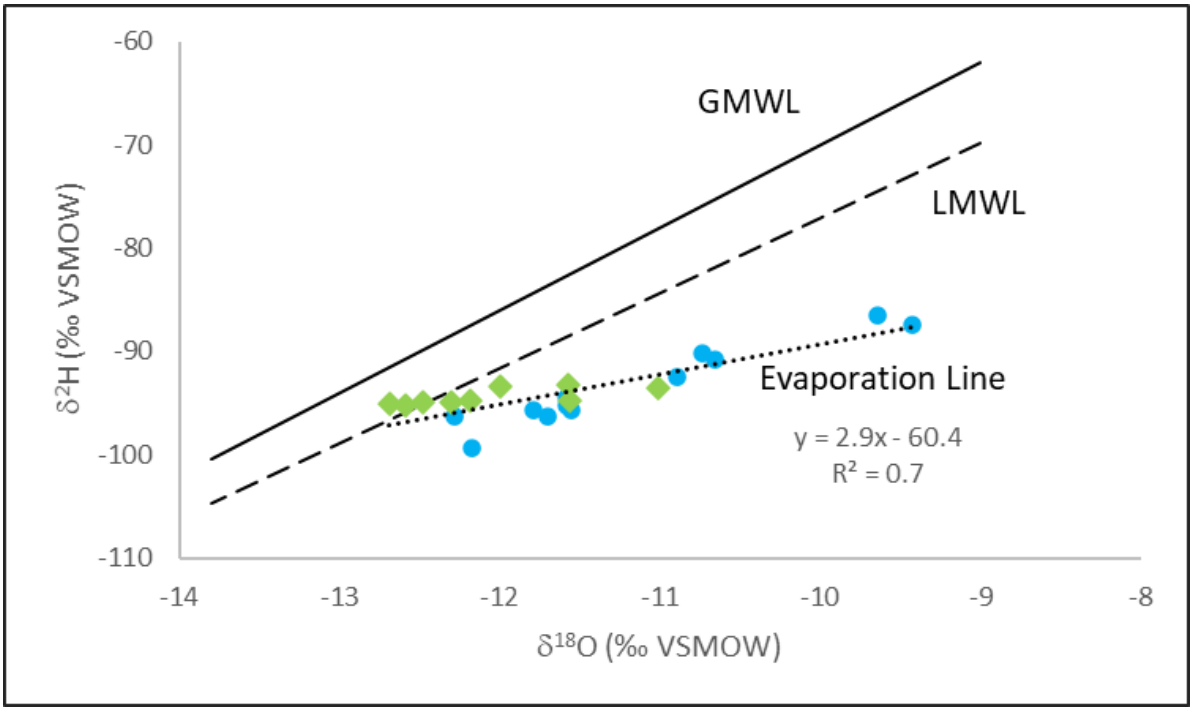

Figure 10. The δ^2H versus $\delta^{18}O$ plot of groundwater samples from the NERT site. The GMWL (solid), LMWL (dashed), and evaporation trend line (dotted) are shown along with the evaporation trend line equation and correlation coefficient. The evaporation trend line equation intercepts the LMWL at -97.5‰ δ^2H and -12.8‰ $\delta^{18}O$. Blue dots are wells in the alluvium and green diamonds are wells in the Muddy Creek Formation.

3.2.1.2 Cation and Anions

Nineteen samples were collected and analyzed for pH, electrical conductivity (EC), major cations (Ca, Mg, Na, K), major anions (HCO_3, Cl, SO_4, NO_3), and SiO_2. Major-ion chemistry is used to help develop water-rock reaction modeling. The results for pH ranged from 7.37 to 8.13, which is typical for most groundwaters (Hem 1989). Electrical conductivity ranged from 918 to 10,400 µS/cm. Calculated total dissolved solids (TDS) ranged from 525 to 7,285 mg/L. A linear regression of TDS to EC produced a slope of 0.77. Anion-cation charge balance errors were less than 5 percent for all samples except for wells ES-28 (-6.1 percent), MW-25 (-7.7 percent), and PC-195 (-9.4 percent).

Assuming Cl is predominantly from halite dissolution (NaCl), then Na is from halite dissolution, albite dissolution, or ion exchange. For halite dissolution, samples would plot along a 1:1 molar line on a Na versus Cl plot (Figure 11). Samples below the line (Na < Cl) suggest evaporative concentration in the soils during recharge with ion exchange for Na in solution for Ca on clay surfaces (which is consistent with samples with the highest TDS, wells ARP-7 and MW-105). High Cl may also be an indication of groundwater contamination. Samples above the line (Na > Cl) suggest dissolution of albite or ion exchange of Ca in solution for Na on clay surfaces (wells PC-64, ES-28, and M-31A).

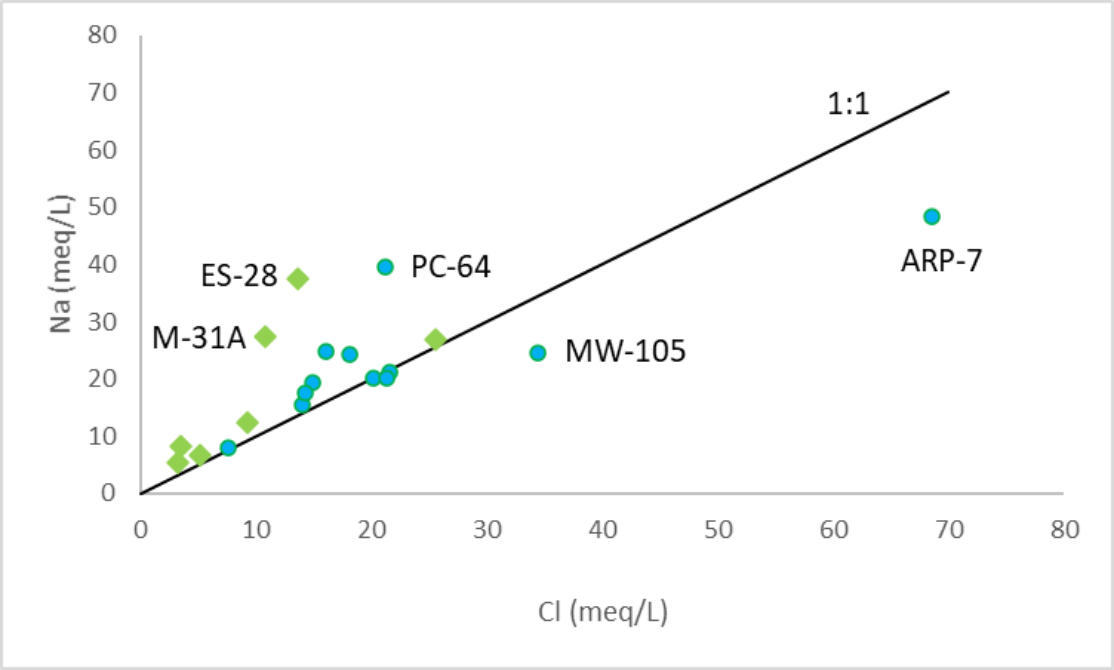

Figure 11. Na versus Cl plot of groundwater samples from the NERT site. A 1:1 molar line is shown. Most samples plot along the 1:1 line except for ARP-7 and MW-105 (which are below the line) and PC-64, ES-28, and M-31 (which are substantially above the line). Blue dots are wells in the alluvium and green diamonds are wells in the Muddy Creek Formation.

Dissolved Ca can be derived from dissolution of carbonate minerals and dissolution of gypsum ($CaSO_4 \cdot 2H_2O$. Assuming that most SO_4 is from the dissolution of gypsum ($CaSO_4 \cdot 2H_2O$), then Ca and SO_4 concentrations should be approximately equal, and samples would plot along a 1:1 molar line on a Ca versus SO_4 plot (Figure 12). Most samples were below the 1:1 molar line, suggesting the removal of Ca by calcite precipitation ($CaCO_3$) and/or ion exchange of Ca in solution for Na on clay surfaces.

A comparison of HCO_3 to SiO_2 concentrations indicates the predominance of either carbonate or silicate mineral weathering in the aquifer. Hounslow (1995) suggested that $HCO_3/SiO_2 < 5$ indicates silicate mineral weathering, whereas $HCO_3/SiO_2 > 10$ indicates carbonate mineral weathering. Most of the NERT groundwater samples collected have $HCO_3/SiO_2 < 5$ (Figure 13), suggesting that mineral weathering in the aquifer is predominately from silicate minerals, which are derived from volcanic rock weathering, and the bicarbonate in the aquifer originates mostly from soil gas CO_2 dissolution during groundwater recharge.

Non-halite Na (Na+K-Cl) is from either albite dissolution or ion exchange and K is from the weathering of biotite and K-feldspar. When comparing non-halite Na to SiO_2, most of the NERT groundwater samples have $Na+K+Cl > SiO_2$, except for ARP-7 and MW-105 (Figure 14), which suggests that the non-halite Na is predominantly from ion exchange.

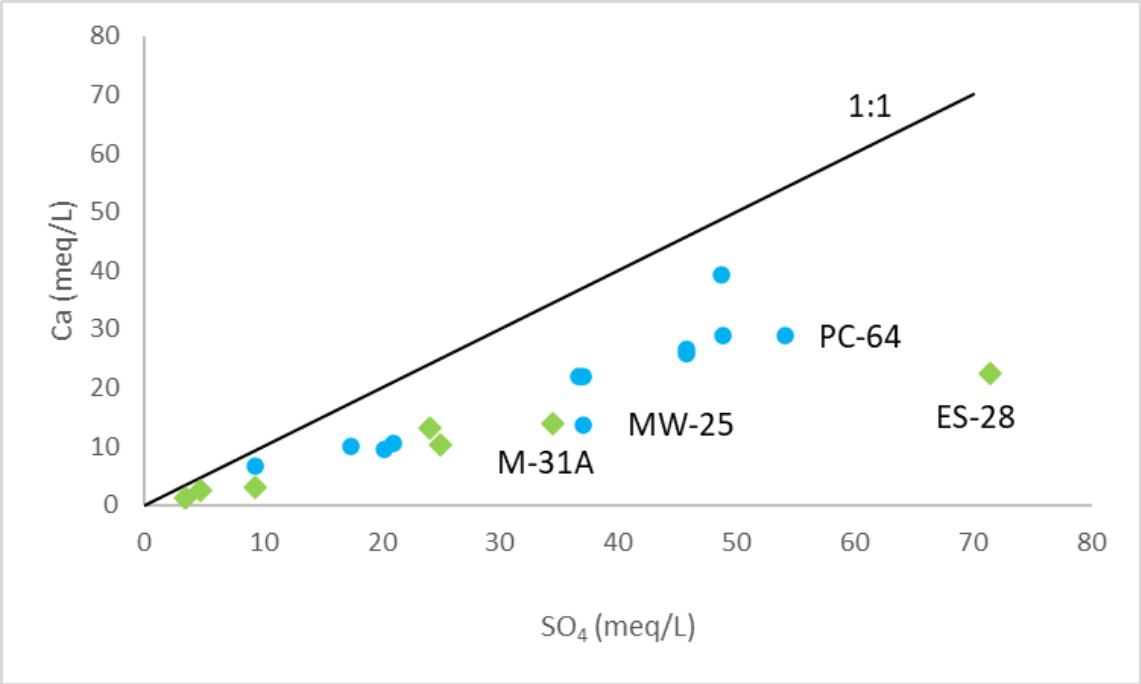

Figure 12. Ca versus SO_4 plot of groundwater samples from the NERT site. A 1:1 molar line is shown. Most samples plot below the 1:1 line. Blue dots are wells in the alluvium and green diamonds are wells in the Muddy Creek Formation.

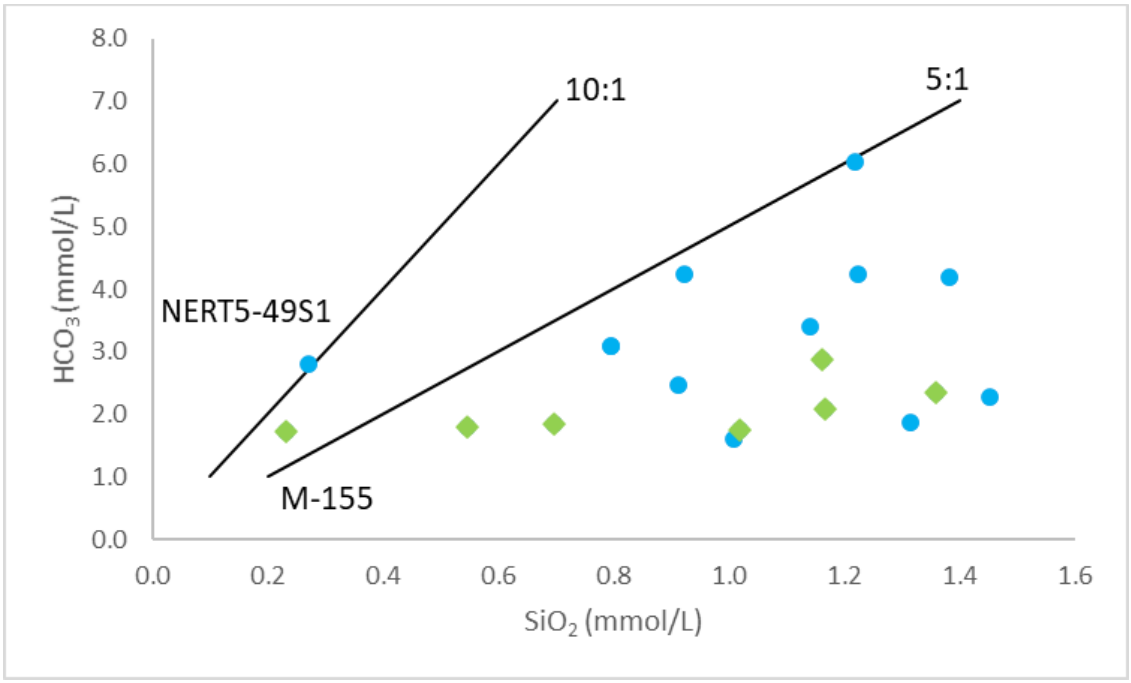

Figure 13. HCO_3 versus SiO_2 plot of groundwater samples from the NERT site. Both 5:1 and 10:1 molar lines are shown. Most samples plot below the 5:1 line. Blue dots are wells in the alluvium and green diamonds are wells in the Muddy Creek Formation.

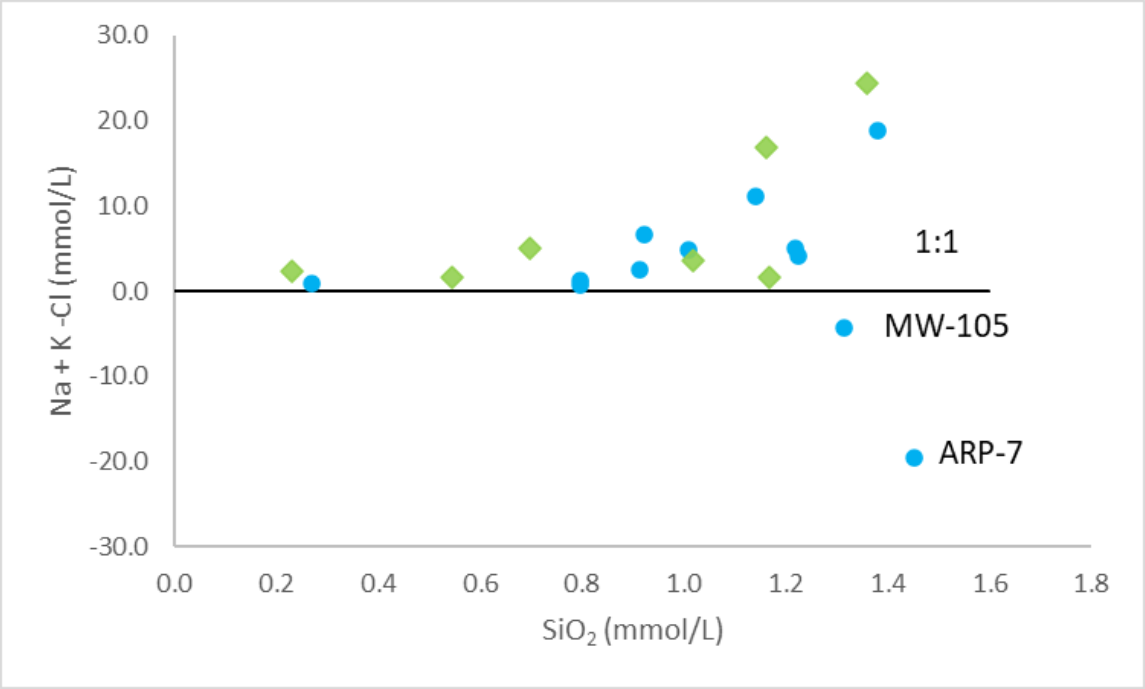

Figure 14. Na + K - Cl versus SiO_2 plot of groundwater samples from the NERT site. A 1:1 molar line is shown. Most samples plot above the line. Blue dots are wells in the alluvium and green diamonds are wells in the Muddy Creek Formation.

3.2.1.3 Tritium

Twenty samples were collected and analyzed for ^3H. The presence of ^3H in groundwater indicates that the groundwater contains a component of modern groundwater recharge where "modern" is less than 50 years (Clark 2015). Tritium is produced naturally in the atmosphere and can vary between approximately 5 and 20 TU, but there was a large spike in ^3H in the 1950s and 1960s because of atmospheric testing of thermonuclear weapons. The half-life of ^3H is 12.3 years, so the spike in atmospheric ^3H has mostly returned to background levels (Clark 2015).

At the NERT site, ^3H was found in 16 of the 20 wells sampled. Tritium concentration ranged from below detection to 5.92 TU (Table 4). Tritium was found in all the wells completed in the Quaternary alluvium plus four of the wells completed in the upper portion of the Muddy Creek Formation. The presence of ^3H indicates a component of modern recharge in groundwater in these wells. Three of the deeper wells completed in the Muddy Creek Formation have ^3H concentrations below detection.

Table 4. Tritium concentrations in groundwater at the NERT site.

Well #	TD (ft)	Water Zone	Lithology	^{3}H (TU)
PC-157A	24	Shallow	Qal	5.91
PC-157B	40	Shallow	Qal	4.82
MW224A	76	Shallow	Qal	4.20
NERT4.71S1	55	Shallow	Qal	5.39
MW-105	27	Shallow	Qal	4.17
NERT4.93S1	40	Shallow	Qal	5.67
PC-56	55	Shallow	Qal	5.89
MW201A	49	Shallow	Qal	5.41
NERT5.49S1	40	Shallow	Qal	6.72*
MW-25	53	Shallow	Qal	0.09
ARP-7	39	Shallow	Qal	5.02
PC-64	20	Shallow	Qal	4.62
PC-195	75	Shallow	UMCf-fg1	BD
M-207	45	Shallow	UMCf-fg1	3.79
M-155	220	Middle	UMCf-fg1	BD
ES-28	85	Shallow	UMCf-fg1	5.92
M-31A	55	Shallow	UMCf-fg1	3.43
TR-8	94	Shallow	UMCf-cg1	1.21
TR-7	291	Middle	UMCf-cg2	BD

BD = below detection.
* = sample reanalyzed and received March 2023. Not used in geochemical and age tracer analysis.

3.2.1.4 Carbon-14

Twenty samples were collected and analyzed for ^{14}C and δ^{13}C. Carbon-14 is used to estimate the radiocarbon age of DIC in water by measuring the decrease in ^{14}C by radioactive decay from the time groundwater entered the aquifer. There are other processes that can change the ^{14}C content besides radioactive decay that must be accounted for when estimating groundwater age with ^{14}C. The most important of these processes is isotopic exchange between DIC and solid carbonate in the aquifer (Han et al. 2014), which can be modeled based on the curved, exponential relationship ^{14}C versus δ^{13}C. Figure 15 shows this relationship for the groundwater samples collected at the NERT site, with groundwater samples in the alluvium represented by blue dots and samples from the Muddy Creek Formation represented by green diamonds. Alluvial samples have higher ^{14}C content (pmC) and isotopically lighter (more negative) δ^{13}C values, whereas Muddy Creek Formation samples have less pmC and isotopically heavier (less negative) δ^{13}C values, which suggests that groundwater in the underlying Muddy Creek Formation is older than groundwater in the alluvium and that the ^{14}C concentrations have been diluted by water-rock reaction with carbonate minerals.

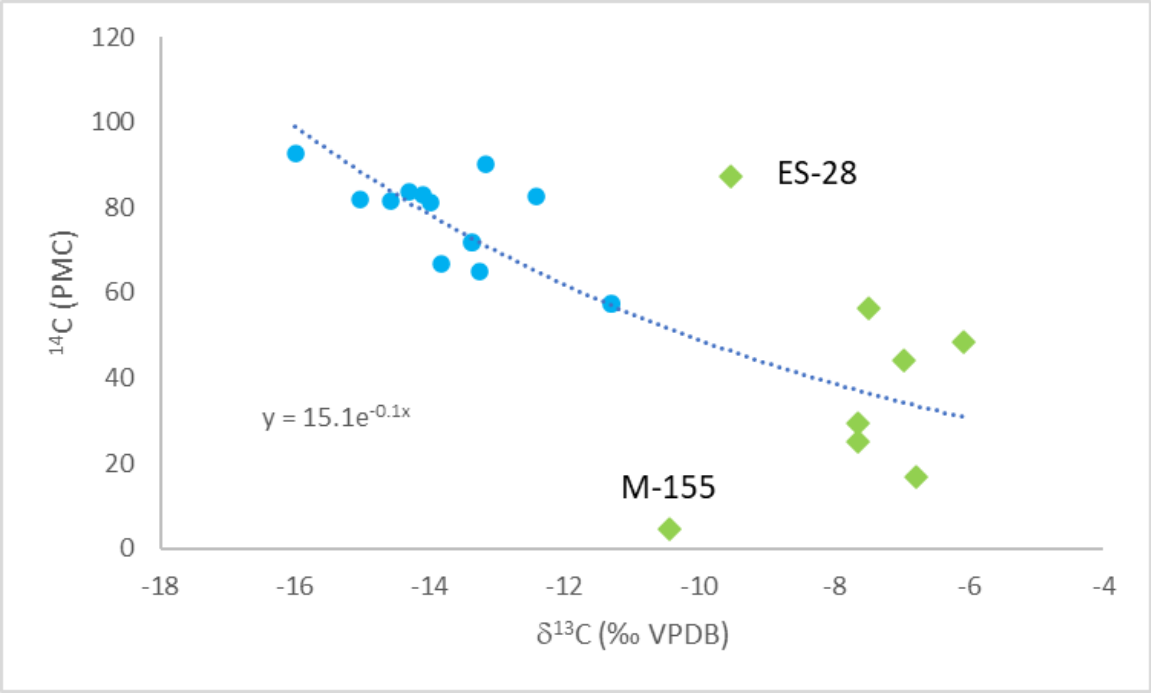

Figure 15 The ^{14}C versus δ^{13}C plot of groundwater samples from the NERT site. Samples are divided into alluvial wells (blue dots) and Muddy Springs Formation wells (green diamonds). A best-fit exponential line is shown for all samples except for ES-28 and M-155.

3.2.1.5 Sulfur Hexafluoride and Chlorofluorocarbons

Twenty samples were collected and analyzed for SF_6 and chlorofluorocarbons (CFCs=CFC-11, CFC-12, CFC-113). Significant production of SF_6, a trace atmospheric gas, began in the 1960s with increasing atmospheric concentrations over time. Sulfur hexafluoride can be used to date groundwaters that were recharged post 1990s. Chlorofluorocarbons are synthetic halogenated alkanes that were used as refrigerants and solvents and are good tracers for groundwater that has been recharged since the 1940s. Different types of CFCs were emitted at different rates and can be used to help constrain the recharge age data, assuming there has been no contamination of CFCs at the well site during well construction and/or during groundwater sampling. Table 5 shows the results of the SF_6 and CFC analyses. All the alluvial groundwater samples (Qal) are young, ranging from approximately 47 years to modern, whereas samples from the Muddy Creek Formation are generally older in age, ranging from 30 to 50 years in age. Well M-31A with a relatively shallow depth (55 ft) completed in the Muddy Creek Formation has a modern age. Wells M-155 and TR-7 have a mixture of younger and older water.

Table 5. The SF_6 and CFC piston flow model ages obtained from the U.S. Geological Survey.

Well	TD (ft)	Water Zone	Lithology	Approximate Years		Comments
				SF_6	CFC	
LVWPS-MW224A	76	Shallow	Qal	12	-	around 2010
MW-25	53	Shallow	Qal	12	-	around 2010
LVWPS-MW201A	49	Shallow	Qal	0	0	modern
NERT4.71S1	55	Shallow	Qal	0	0	modern
NERT5.49S1	40	Shallow	Qal	-	-	uncertain
PC-157A	24	Shallow	Qal	-	47	mid to late 1970s
PC-157B	40	Shallow	Qal	-	47	mid to late 1970s
NERT4.93S1	40	Shallow	Qal	7	7	mid 2010s
LVWPS-MW105	27	Shallow	Qal	30	30	mid to early 1990s
PC-56	55	Shallow	Qal/xMCf/UMCf	7	7	mid 2010s
PC-64	20	Shallow	Qal	20	-	early 2000s
ARP-7	39	Shallow	Qal	-	-	uncertain
M-207	45	Shallow	Qal/UMCf	30	30	around 1990
ES-28	85	Shallow	UMCf	30	30	around 1990
PC-195	75	Shallow	UMCf	50	50	1970 or older
M-31A	55	Shallow	UMCf	0	0	close to modern
M-155	220	Middle	UMCf-fg1	-	-	mixing young (modern) and old water
TR-8	94	Shallow	UMCf-cg1	40	40	around 1980
TR-7	291	Middle	UMCf-cg2	-	-	mixing young (modern) and old water

3.2.2 Geochemical Modeling

3.2.2.1 Quaternary Alluvium

Wells completed in Quaternary alluvium can be divided into two groups based on ^{14}C content. For wells with < 80 pmC, water-rock reaction models were run to correct ^{14}C ages for changes caused by interaction with carbonate containing phases. For wells with more than 80 pmC, a simple recharge correction model in *NETPATH* was used to calculate the minimum corrected ^{14}C age (Vogel and Ehhalt 1963; Plummer et al. 1994).

Water-rock reaction models were run for four wells completed in Quaternary alluvium, including PC-64, MW-25, MW-105, and MW-224A. Modeled scenarios for each of these four wells are described individually below.

- PC-64 is a shallow well (TD = 20 ft) completed in Quaternary alluvium in OU-2 directly downgradient of OU-1. PC-64 has a large amount of perchlorate (260 mg/L), indicating that the elevated Cl in PC-64 is likely from contamination and not water-rock reactions. Cl was removed as a constraint in water-rock reaction models. Isotopically, PC-64 is identical to shallow (TD = 55 ft), upgradient

M-31A, so a direct flow path with no mixing with other wells was modeled. In this scenario, two valid water-rock reaction models produced two slightly different corrected ^{14}C ages for groundwater in the vicinity of PC-64. The average corrected age of groundwater in the vicinity of PC-64 was 3,200 years.

- MW-25 is a shallow well (TD = 53 ft) completed in Quaternary alluvium in eastern OU-3 near Las Vegas Wash. MW-25 is isotopically lighter than most of the other shallow wells in the Quaternary alluvium, indicating an upgradient source of isotopically lighter groundwater. In this scenario, TR-7 was used to represent an isotopically light, older upgradient groundwater from OU-2 because no wells were sampled directly upgradient of MW-25. Particle tracking modeling shows the source of MW-25 to be upgradient along a south-to-north flow path from the model boundary. Additionally, MW-25 has a high sulfate concentration that is consistent with the elevated sulfate in upgradient groundwater in OU-2 and similar to that found at ES-28. ES-28 is also isotopically heavier than MW-25, which is required to obtain valid water-rock reaction models when mixing isotopically distinct end-members. In this scenario, 12 valid water-rock reaction models produced different corrected ^{14}C ages for groundwater in the vicinity of MW-25. These corrected ages ranged from 2,900 to 3,400 years with an average of 3,100 years. Water-rock reaction modeling results suggest that groundwater in the vicinity of MW-25 is predominantly older groundwater from upgradient (76 percent) mixed with younger, sulfate rich groundwater (24 percent).
- MW-105 is a shallow well (TD = 27 ft) completed in Quaternary alluvium centrally located in OU-3, upgradient of the Las Vegas Wash. Similar to MW-25 and MW-224A, particle track modeling shows the source of MW-105 to be upgradient along a south-to-north flow path from the model boundary of OU-2. A combination of isotopically light, upgradient groundwater mixed with an upgradient, high-sulfate groundwater and an isotopically heavy, recent recharge groundwater is needed to produce the water chemistry observed at MW-105. Wells TR-7, ES-28, and PC-157A were chosen to represent three end-member mixing components along the groundwater flow path from MW-105. Specifically, TR-7 was used to represent an isotopically light upgradient groundwater from OU-2; ES-28 was used to represent high-sulfate, upgradient groundwater from OU-2; and PC-157A was used to represent isotopically heavy, recent groundwater recharge. Additionally, because of the large chloride concentration in MW-105 and the presence of perchlorate (5.8 mg/L), chloride was not used as a modeling constraint. In this scenario, 15 valid models with different corrected ^{14}C ages were produced. Corrected ages ranged from 1,600 to 1,900 years with an average of 1,700 years. Water-rock reaction modeling results suggest that the groundwater in the vicinity of MW-105 is predominantly upgradient groundwater from OU-2 with significant input from recent groundwater recharge.
- MW-224A is similar to MW-25. It is a shallow well (TD = 76 ft) completed in Quaternary alluvium in eastern OU-3 near Las Vegas Wash and just east of MW-25. MW-224A is not as isotopically light as MW-25, which suggests that a recent recharge component is needed to produce the isotopic signature in groundwater in the vicinity of MW-224A in addition to the older, deeper,

upgradient groundwater and a component with high sulfate. The same as the mixing model for MW-105, wells TR-7, ES-28, and PC-157A were chosen to represent three end-member mixing components. Particle track modeling shows the source of MW-224A to be upgradient along a south-to-north flow path from the model boundary. The results from this scenario included four valid water-rock reaction models with different corrected ^{14}C groundwater ages. Corrected ages ranged from 1,200 to 1,500 years with an average of 1,400 years. Water-rock reaction modeling results suggest that the groundwater in the vicinity of MW-224A is predominantly upgradient groundwater from OU-2 with significant input from recent groundwater recharge.

For shallow wells at the NERT site with $^{14}C > 80$ pmC, no water-rock reaction modeling was attempted to correct laboratory ^{14}C ages. Rather, for shallow wells with $^{14}C > 80$ pmC, the ^{14}C content can be explained by the shallow water table being in contact with the soil zone CO_2 reservoir. In this situation, the soil gas CO_2 reservoir ^{14}C content is controlled by plant respiration and decay of organic matter in the soil zone, which should be approximately 100 pmC (or higher depending on the time of groundwater recharge since 1950). Uncorrected ^{14}C ages are based on approximately 100 pmC for the initial ^{14}C activity, referred to as A_0 (100 percent modern is defined as 95 percent of the radiocarbon concentration [in AD 1950] of NBS Oxalic Acid I [SRM 4990B, OX-I] normalized to $\delta^{13}C_{VPDB}$=-19‰ [e.g., https://www2.whoi.edu/site/nosams/client-services/radiocarbon-data-calculations/]).

NETPATH presents multiple models for estimating the initial ^{14}C activity at the time of recharge (A_0), which is used to calculate groundwater ages. Of these models, the Vogel model assumes that groundwater starts at 85 pmC (Vogel and Ehhalt 1963; Plummer et al. 1994). To correct ^{14}C ages in shallow groundwater at the NERT site, the Vogel model's A_0 value of 85 pmC was used to estimate a minimum ^{14}C age, whereas 100 pmC was used to estimate a maximum age. An average age was calculated using the minimum and maximum ages. For shallow wells with $^{14}C > 85$ pmC, an A_0 value of 100 pmC was used to estimate an ^{14}C age for water at a given well.

3.2.2.2 Muddy Creek Formation

Groundwater samples were collected from seven wells completed in the Muddy Creek Formation. The most upgradient wells sampled were TR-7 and TR-8 in OU-1, and ES-28 in OU-2. Water-rock reaction models were run to correct the ^{14}C ages of downgradient wells M-31A, M-155, M-207, and PC-195.

- TR-7, TR-8, and ES-28: Because these three wells are upgradient of all other wells, close to the southern model boundary, and upgradient water chemistry and age-tracer data are not available, water-rock reaction modeling to correct ^{14}C ages was not attempted. For these three wells, the ^{14}C content in pmC measured by the laboratory was used to calculate the average ^{14}C age of the groundwater rounded to the nearest thousand years.
- M-31A is screened shallower than TR-7 and TR-8. Because there are upward gradients in the Muddy Creek Formation, it is possible that a groundwater component similar to that of TR-7 and TR-8 flows upward in the vicinity of M-31A. The

dissolved atmospheric gases SF_6 and CFCs were measured in TR-7, TR-8, and M-31A, which indicates that there is also a component of recent groundwater recharge in the Muddy Creek Formation in this area of the NERT site. The chemical and isotopic compositions of TR-8 along with an isotopically heavy recent groundwater recharge composition were used to model the water-rock reactions and carbon isotopic changes along a groundwater flow path from the vicinity of TR-7 and TR-8 to correct the ^{14}C age of M-31A. The chemical and isotopic composition of well PC-157A, the isotopically heaviest shallow groundwater sample from the Quaternary alluvium in the NERT study area near Las Vegas Wash, was used to represent the recent groundwater recharge component of the proposed groundwater mixture. This scenario did not produce any valid water-rock reaction models because of the large amount of sulfate in M-31A. Water-rock reaction modeling required more than 11 mmol/L of gypsum to be dissolved to produce the groundwater chemical composition at M-31A, which is greater than the criterion that valid water-rock reaction models have ≤10 mmol/L of any phase change.

    - To produce the chemical and isotopic composition of groundwater at M-31A, a groundwater mixing component with higher concentrations of sulfate was needed so that less gypsum dissolved in this modeling scenario. An upgradient groundwater composition with higher sulfate concentrations is found at nearby well ES-28. In this scenario, the groundwater chemical and isotopic composition of ES-28 was used to represent a high-sulfate groundwater mixing component assumed to be in the vicinity of M-31A. In this scenario, PC-157A was not used to represent the recent groundwater recharge component because ES-28 is isotopically heavier than TR-8 and M-31A. This scenario produced eight valid water-rock reactions (note: a small amount of gypsum [1.22 mmol/L] was required to precipitate for these models to be valid) with different corrected ages for groundwater in the vicinity of M-31A. These corrected ages ranged from 80 to 2,000 years with an average of 1,200 years. The water-rock reaction modeling results suggests that the groundwater at M-31A is a mixture of older (56 percent) and younger groundwater (44 percent).

- M-155 is completed deep within the Muddy Creek (Total Depth = 220 ft) and is downgradient of TR-7, TR-8, and M-31A. In this scenario, the deep upgradient well TR-7 was mixed with a recent groundwater recharge component, PC-157A. This scenario produced three valid water-rock reaction models (note: a small amount of gypsum [0.86 mmol/L] and NaCl [2.25 mmol/L] was required to precipitate for these models to be valid) with different corrected ages for groundwater in the vicinity of M-155. These corrected ages ranged from 19,000 to 23,000 years with an average of 21,000 years. The water-rock modeling results suggests that the groundwater at M-155 is mostly old groundwater (97 percent) with a very small component of younger groundwater (3 percent).
- M-207 is close to M-155 and much shallower (TD = 45 ft), but it is still completed in the Muddy Creek Formation. M-207 has elevated perchlorate concentrations (240 mg/L on May 20, 2020), indicating contamination from process fluids. Many different water-rock reaction mixing scenarios were modeled, but too much NaCl had

to dissolve in all scenarios to balance the chloride present in M-207. Because of the presence of elevated perchlorate concentrations, the chloride in this groundwater sample is most likely not from the dissolution of a chloride-containing mineral phase such as NaCl. Chloride was removed as a constraint and water-rock reaction modeling scenarios were run again. This scenario produced three valid water-rock reaction models with different corrected ages for groundwater in the vicinity of M-207. These corrected ages ranged from 2,600 to 2,900 years with an average of 2,700 years. The water-rock reaction modeling results suggest that the water at M-207 is a mixture of 36-57 percent deeper water from the Muddy Creek Formation, 32-57 percent shallower upgradient groundwater, and 7-11 percent recent groundwater recharge.

- PC-195 is located near the northern boundary of OU-2 (just north of the Athens Road Well Field), 75 ft deep, and completed in the fine-grained Muddy Creek Formation. In this scenario, the deep upgradient well TR-7 completed in the coarse-grained #2 unit of the Muddy Creek Formation was mixed with the shallow upgradient well TR-8 completed in the coarse-grained #1 unit of the Muddy Creek Formation and with a recent groundwater recharge component, PC-157A. This scenario produced four valid water-rock reaction models with different corrected ages for groundwater in the vicinity of PC-195. These corrected ages ranged from 5,000 to 5,400 years with an average of 5,100 years. The water-rock reaction modeling suggests that the groundwater at PC-195 is mostly old groundwater (98 percent) with a very small component of younger groundwater (2 percent).

3.2.3 Synthesis of Age Tracer Results

3.2.3.1 Wells Completed in the Quaternary Alluvium

Shallow wells completed in the Quaternary alluvium with young groundwater ages indicative of recharge in modern times include PC-157A, PC-157B, NERT4.71S1, NERT4.93S1, PC-56, MW-201A, NERT5.49S1, and ARP-7. These wells are characterized by having >80 pmC ^{14}C, which is equivalent to <1,000 years (indistinguishable from modern water); ^{3}H above 4.5 TU, indicating recharge since approximately 1960; and measurable concentrations of modern atmospheric, anthropogenic gases CFCs and SF_6 (Tables 4 and 5, and Appendix A). The lack of older water in these wells suggests recharge occurred recently, groundwater flow paths are short and shallow, and/or groundwater velocities are fast.

Four wells completed in the Quaternary alluvium (MW-224A, MW-105, MW-25, and PC-64) have uncorrected ^{14}C content between 60 and 75 pmC, ^{3}H less than 4.5 TU, and measurable concentrations of CFCs and SF_6, which indicates that they are a mixture of younger and older groundwater. MW-224A has an average corrected ^{14}C age of 1,400 years, 4.2 TU, and an SF_6 age of >10 years. CFCs for this sample could not be analyzed. MW-105 has an average corrected ^{14}C age of 1,700 years, 4.2 TU, and SF_6 and CFC ages ranging between approximately 20 and 40 years. MW-25 has an average corrected ^{14}C age of 3,100 years, 0.09 TU, and very different ages for SF_6 (<10 years) and CFCs (<80 years). Water-rock reaction models developed to correct ^{14}C ages for these three wells indicate that groundwater in the vicinity of these wells is a mixture of upgradient older groundwater from the Muddy Creek Formation and recent groundwater recharge.

3.2.3.2 Wells Completed in the Upper Muddy Creek Formation

Seven wells were sampled in the Upper Muddy Creek Formation. Each is described individually below.

- PC-195 is downgradient of OU-1 completed in the fine-grained Upper Muddy Creek Formation. The average corrected ^{14}C age is 5,100 years and ^{3}H is below detection, both indicating that this well is composed of old groundwater. However, CFCs (<60 years) and SF_6 (<50 years) indicate that there is a component of recent groundwater recharge in this well. Water-rock reaction modeling showed that the recent recharge component is small, approximately two percent.
- M-207 is located in OU-1 just north of the WC-West Pond and is completed in the fine-grained Muddy Creek Formation. The average corrected ^{14}C age is 2,700 years and ^{3}H is 3.8 TU. Tritium, CFCs, and SF_6 all indicate that M-207 is a mixture of older and younger groundwater. Water-rock reaction modeling is consistent with age-tracer data, indicating that groundwater in the vicinity of M-207 is a mixture of older groundwater in the Muddy Creek Formation (36 to 57 percent), younger groundwater in the Muddy Creek Formation (32 to 57 percent) and a recent recharge component (7 to 11 percent). The elevated perchlorate concentration (240 mg/L) indicates that the water in the vicinity of M-207 also has a component of contamination fluids.
- M-155 is in OU-1 and completed deep in the fine-grained Muddy Creek Formation (TD = 220 ft). The groundwater in this well is very old with an average corrected ^{14}C age of 21,000 years with ^{3}H below detection. Chlorofluorocarbons and SF_6 were found in this well, but the SF_6 concentration were above the dateable range, whereas the CFC age was >40 years. The elevated SF_6 concentration and presence of CFCs are inconsistent with the old ^{14}C age, and the lack of ^{3}H possibly indicates atmospheric contamination during groundwater sampling. Water-rock reaction modeling indicates that the water in M-155 is mostly composed of deep, older, upgradient groundwater (97 percent) with possibly a very small component of recent groundwater recharge (3 percent).
- M-31A is in OU-1 with a relatively shallow completion (TD = 55 ft) in the fine-grained Muddy Creek Formation. The water in this well is a mixture of young and old groundwater with an average corrected ^{14}C age of 1,200 years and a ^{3}H activity of 3.4 TU, with SF_6 (<10 years) and CFC (>30 years) present. Water-rock reaction modeling indicates that the water in this well is a mixture of deeper groundwater (56 percent) and recent groundwater recharge (44 percent).
- ES-28 is located in the upgradient portion of OU-2 completed in the fine-grained Muddy Creek Formation. The uncorrected ^{14}C age is <1,000 years, with a significant ^{3}H activity of 5.9 TU and young CFC (>30 years) and SF_6 (>20 years) ages. Water-rock reaction models to correct ^{14}C ages were not required because of the high ^{14}C content (87 pmC).
- TR-8 is from the upper coarse-grained unit of the Muddy Creek Formation with a total depth of 94 feet. The uncorrected ^{14}C age is 6,000 years with a small amount of ^{3}H (1.2 TU). The CFC and SF_6 ages are <40 years. Water-rock reaction models could

not be run because water chemistry and isotopic data for groundwater upgradient from TR-8 are not available. The groundwater age tracers suggest that groundwater in the vicinity of TR-8 is a mixture of younger and older groundwater.

- TR-7 is from the lower coarse-grained unit of the Muddy Creek Formation with a total depth of 291 feet. The uncorrected ^{14}C age is 14,000 years and ^{3}H is below detection. The CFC and SF_6 ages are >40 years and >20 years, respectively. Water-rock reaction models could not be run because water chemistry and isotopic data for groundwater upgradient from TR-7 are not available. The presence of SF_6 and CFCs is inconsistent with the old ^{14}C age and the lack of ^{3}H, possibly indicating atmospheric contamination during groundwater sampling. The groundwater age tracers suggest that groundwater in the vicinity of TR-7 is old groundwater.

3.3 Lumped Parameter Models

The LPMs were developed for each of the 19 wells with age tracer data collected. A summary of the tracer results is provided in Table 6 with detailed LPM analysis for individual wells provided in subsequent sections below. Detailed analyses are catalogued into the two lithologic units of Quaternary alluvium (Qal) and the Upper Muddy Creek Formation (UMCf). Within these lithologic units, results are presented for wells with and without an old water fraction and moving along principal flow paths . Refer to Section 2.3 for the methods and criteria for LPM development and significance. Where relevant, multi-tracer calibration is highlighted with the subroutine *TracerTracerGraph* output. Bimodal plots (i.e., concentration X versus concentration Y) contain the observed sample (a single point) and estimated values for different TTD interpolated across various ages (line plots) with ages identified. An observed sample situated close to a given TTD line plot indicates that the TTD can estimate the observed concentrations X and Y simultaneously. Single LPM results insinuate false accuracy with highly specific ages in their output. They do not reflect the inherent uncertainty in tracer-based approaches. To address this uncertainty, we explore age distribution ranges based on different TTDs and different tracers for calibration. In addition, false accuracy is removed by looking at ranges in means (and medians) and a reduction of detailed age distributions into the fraction of young water (<70 years old).

3.3.1 Quaternary Alluvium (Qal)

Eight wells screened in the shallow alluvium with ^{14}C>80 pmC were estimated to contain mostly modern water. The LPMs consider PFM, EMM, and DM. They do not include BMM approaches that account for older water sources that are not found in these wells.

ARP-7: The USGS identified SF_6 and CFC samples as contaminated and the analysis limits the observations to only ^{3}H. Table 7 indicates that only the PFM model is significant, with an error <5 percent.

Table 6. Summary of LPM analysis for sampled wells. Refer to Section 2.3 for LPM methodology and TTD descriptions.

Well	Unit	Total Depth (ft)	Table	Tracers Used in LPM	TTDs	Mean Age (years)				Fraction Young (fY)	
						Young (<70)		[a]Old			
						Low	High	Low	High	Low	High
ARP-7	Qal	39	7	^{3}H	PFM	64	-	-	-	1	-
[b]ES-28	UMCf-fg	85	17	SF_6, CFC-113	PFM,EM,DM	17	39	-	-	0.85	1
MW-105	Qal	27	14	^{3}H,SF_6,CFC-11,^{14}C	PFM-PFM	1	58	2,100	13,000	0.15	0.68
[b]MW-201A	Qal	49	12	CFC-11, -113	PFM,EM,DM	27	84	-	-	0.62	1
MW-224A	Qal	76	15	^{3}H, SF_6,^{14}C	PFM-PFM	1	58	2,800	2,900	0.15	0.71
M-31A	UMCf-fg	55	20	^{3}H, SF_6,CFC-113,^{14}C	PFM-PFM	1	58	2,100	9,600	0.12	0.89
[c,d]M-155	UMCf-fg	220	22	CFC-113,^{14}C	PFM-PFM	58		29,500	-	0.02	-
M-207	UMCf-fg	45	21	^{3}H, SF_6,^{14}C	PFM-PFM	1	58	4,500	5,000	0.14	0.41
NERT4.71S1	Qal	55	-	^{3}H	PFM	63	-	-	-	1	-
NERT4.93S1	Qal	40	-	CFC-11	PFM	24	-	-	-	1	-
[b]NERT5.49S1	Qal	40	11	SF_6, CFC-11,-12,-113	PFM,EM,DM	12	605	-	-	0.1	1
[b]PC-56	Qal	55	8	^{3}H, SF_6,CFC-11,-12,-113	PFM,EM,DM	4	35	-	-	0.92	1
PC-64	Qal	20	13	^{3}H, SF_6,CFC-11,^{14}C	PFM-PFM	2	58	7,500	13,500	0.17	0.55
[b]PC-157A	Qal	24	9	^{3}H, SF_6,CFC-11,-113	PFM,EM,DM	19	390	-	-	0.16	1
[b]PC-157B	Qal	40	10	^{3}H, SF_6,CFC-11,-113	PFM,EM,DM	14	239	-	-	0.26	1
[c]PC-195	UMCf-fg	75	23	SF_6,CFC-12,-113,^{14}C	PFM-PFM	2	27	5,660	6,000	0.05	0.7
[c]TR-7	UMCf-cg2	291	19	CFC-12,^{14}C	PFM-PFM	16	16	24,000	-	0.11	-
TR-8	UMCf-cg1	94	18	^{3}H,SF_6,CFC-113,^{14}C	PFM-PFM	2	28	7,500	16,500	0.04	0.35
[d]MW-25	Qal	53	16	^{3}H,^{14}C	PFM-PFM	59	59	3,100	-	0.01	-

[a]Age determined from corrected ^{14}C.

[b]fY determined from EMM or DM, not ^{14}C.

[c]No ^{3}H observed (refer to Table 4), fY uncertain.

[d]Best solution >5% error.

Table 7. Age distribution statistics for ARP-7 *TracerLPM* optimization runs.

Model Name	Age (years)		Dispersion Parameter	Tracers in Optimization	Error	Significant
	Mean	Median				
PFM	64	64	na	^{3}H	0.60%	Y
DM	8	5	0.90	^{3}H	26.99%	N

PC-56: Tritium, SF_6, and all the CFCs were obtained for age analysis. No tested LPM could reproduce ^{3}H, so this was removed from optimization trials. Sulfur hexafluoride and CFCs could be replicated independently with multiple models. *TracerTracerGraph* analysis indicated the following pairs could be optimized simultaneously: SF_6 and CFC-12, CFC-11 and CFC-12, and CFC-11 and CFC-113 (Figure 16). Attempts to combine three tracers into a single optimization did not produce significant results. Table 8 provides optimization results for individual tracers and select pairs with significant models indicating mean and median ages ranging from 5 to 35 years.

Table 8. Age distribution statistics for PC-56 *TracerLPM* optimization runs.

Model Name	Age (years)		Dispersion Parameter	Tracers in Optimization	Error				
	Mean	Median			SF_6	CFC-11	CFC-12	CFC-113	Signif.
PFM	1	1	-	SF_6	9.6%				N
	19	19	-	CFC-11		0.2%			Y
	30	30	-	CFC-12			0.0%		Y
	35	35	-	CFC-113				1.7%	Y
	5	5	-	SF_6, CFC-12	0.6%		0.2%		Y
	19	19	-	CFC-11, CFC-12	0.2%		5.8%		N
	35	35	-	CFC-11, CFC-113		4.8%		1.7%	Y
EMM	5	3	-	SF_6	0.0%				Y
	11	7	-	CFC-11		10.5%			N
	4	3	-	CFC-12			0.0%		Y
	25	17	-	CFC-113				0.0%	Y
	5	3	-	SF_6, CFC-12	0.0%		0.2%		Y
	10	6	-	CFC-11, CFC-12		10.6%	0.0%		N
	25	17	-	CFC-11, CFC-113		21.2%	0.0%		N
DM	5	3	0.90	SF_6	0.0%				Y
	19	19	0.01	CFC-11		0.0%			Y
	10	7	0.44	CFC-12			0.0%		Y
	30	21	0.43	CFC-113				0.0%	Y
	5	3	0.57	SF6, CFC-12	0.0%		0.0%		Y
	25	24	0.04	CFC-11, CFC-12		0.0%	0.3%		Y
	34	34	0.01	CFC-11, CFC-113		7.7%		0.0%	N

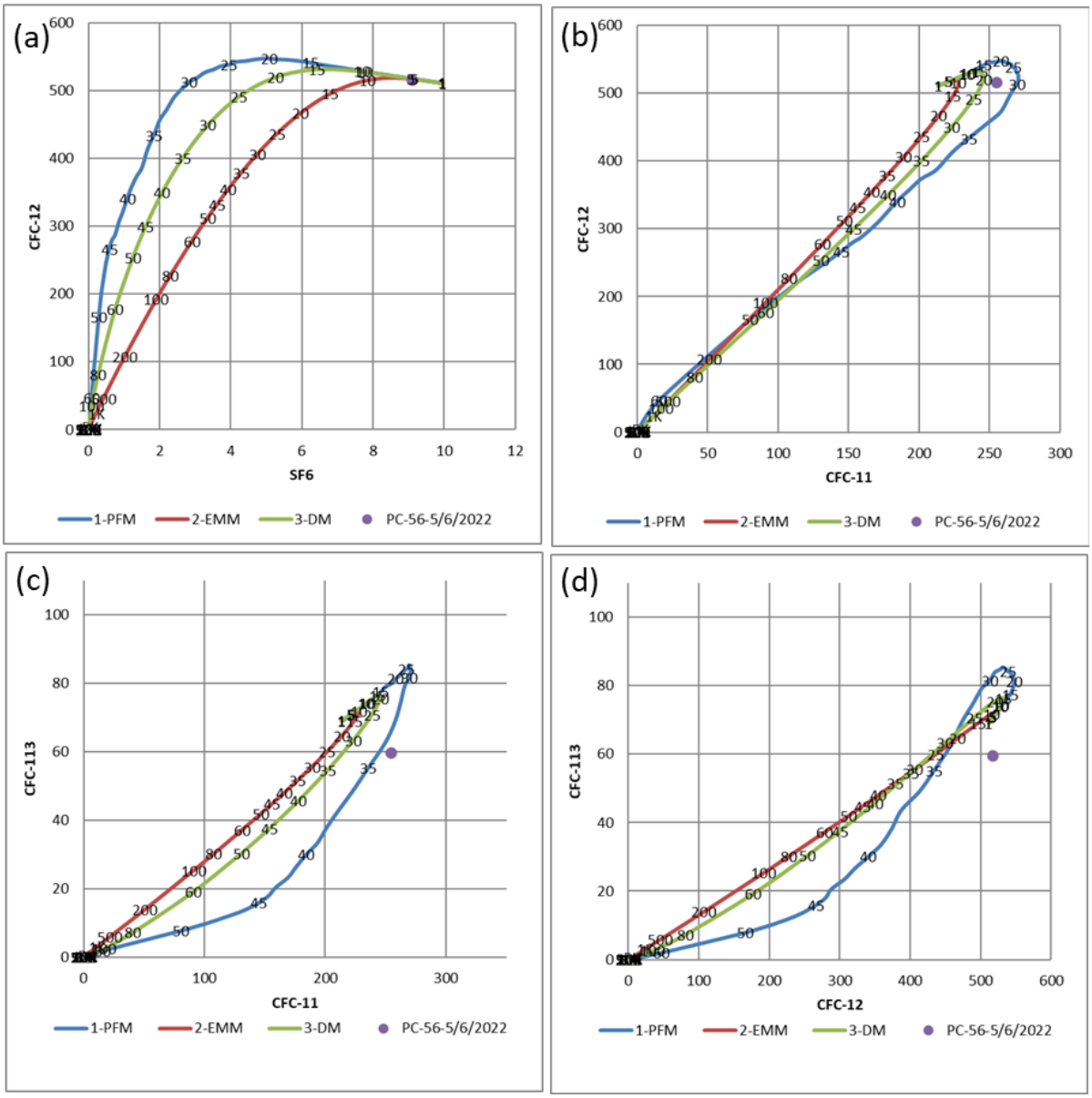

Figure 16. *TracerTracerGraph* representations for PC-56. (a) SF_6 and CFC-12, (b) CFC-11 and CFC-12, (c) CFC-11 and CFC-113, and (d) CFC-12 and CFC-113. CFC-12 and CFC-113 are illustrative of a pair that cannot be simultaneously optimized using any of the given LPMs. The observed sample concentration is shown as a purple point. Age labels in years are included. Units for SF_6 and CFCs are pptv.

PC-157A: Tritium, SF_6, and CFCs were obtained for age analysis. No LPM could replicate CFC-12 and it was discarded from optimization trials. *TracerTracerGraph* analysis indicated only the DM for ^3H and CFC-11 were appropriate for multi-tracer optimization (Figure 17a, observed sample is located near the green DM line). However, for completeness, all LPM models were tested with this pair. The results for LPMs are provided in Table 9 and indicate that EMMs pushed past the 100-year upper bound defined for mean age in the calibration, and therefore the upper age limit was increased. Several DMs hit the lower DP

bound of 0.01 but were kept. No model could estimate the ^{3}H and CFC-11 pair with error <5 percent, but the DM model was close at 6.9% with a mean age of 61 years. This result is worth noting, given the multi-tracer optimization results are more rigorous than the single tracer approach. Significant models produced mean ages from 19 to 390 years.

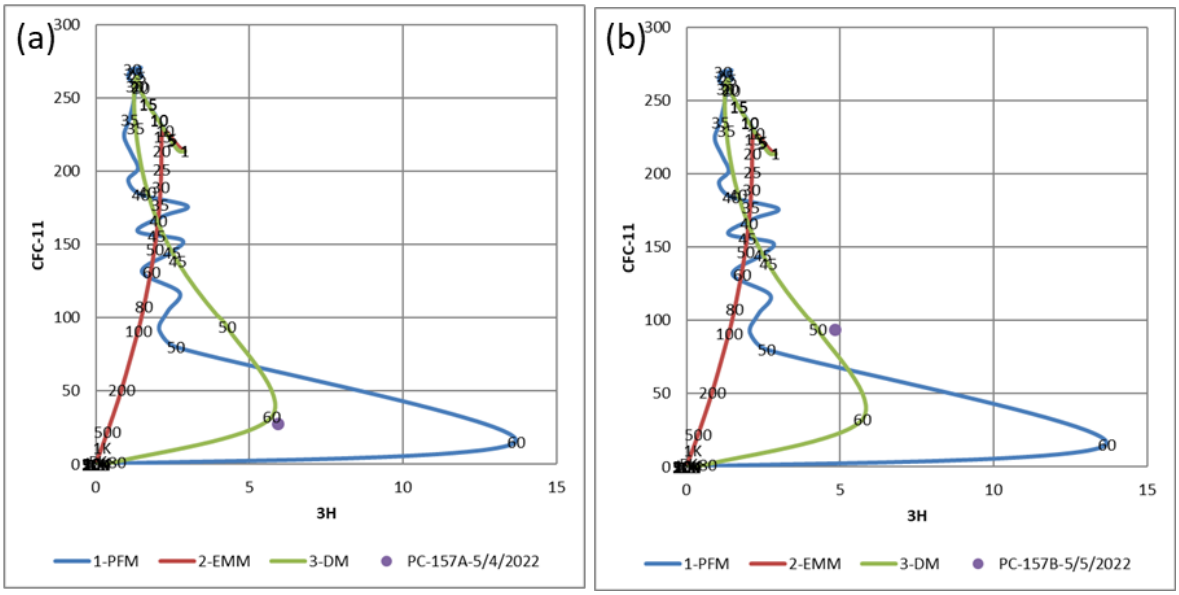

Figure 17. *TracerTracerGraph* representations for ^{3}H and CFC-11 (a) in well PC-157A and (b) in well MW-201A. The observed concentrations are indicated with purple point. Age labels in years are included. Units for ^{3}H is TU and CFC-11 is pptv.

Table 9. Age distribution statistics for PC-157A *TracerLPM* optimization runs.

Model Name	Age (years)		Dispersion Parameter	Tracers in Optimization	Error				
	Mean	Median			^{3}H	SF_6	CFC-11	CFC-113	Signif.
PFM	63	63	-	^{3}H	12.0%				N
	19	19	-	SF_6		1.6%			Y
	56	56	-	CFC-11			6.8%		N
	41	41	-	CFC-113				2.7%	Y
	57	57	-	^{3}H, CFC-11	15.2%		6.8%		N
EMM	None	-	-	^{3}H					N
	1	1	-	SF_6		80.8%			N
	390	270	-	CFC-11			0.0%		Y
	84	58	-	CFC-113				0.0%	Y
	none	-	-	^{3}H, CFC-11					N
DM	57	56	0.01	^{3}H	0.4%				Y
	27	15	0.84	SF^6		0.0%			Y
	86	78	0.09	CFC-11			0.0%		Y
	86	54	0.60	CFC-113				0.0%	Y
	61	59	0.01	^{3}H, CFC-11	6.9%		0.0%		N

PC-157B: This well is in the same location as PC-157A, but it is approximately 20 feet deeper in the alluvium. Tracers ^{3}H, SF_6, and CFCs were available. Similar to PC-157A, no LPM could mimic CFC-12 with reasonable error and this observation was discarded from optimization trials. Three pairs of tracers appear adequate for simultaneous optimization using the DM model: ^{3}H and CFC-11 (Figure 17b, observed sample is located near the green DM line), ^{3}H and CFC-113, and CFC-11 and CFC-113 (Figure 18, observed sample located near the green DM line). The optimized LPMs presented in Table 10 show that significant but independent trials produce mean ages between 14 and 236 years. Only one pair of tracers can be predicted with each estimate containing an error <5 percent. This was done using the DM (DP = 0.01) for CFC-11 and CFC-113 to produce a mean age of 50 years.

NERT5.49S1: Sulfur hexafluoride and all the CFCs were obtained for age analysis. Tracers tested independently were replicated using all tested LPM forms with an error <5 percent and reproduced a wide range in mean ages (12 to 605 years). *TracerTracerGraph* results indicate only CFC-12 and CFC-113 can be reasonably represented simultaneously (Figure 19b, observed sample located near the green DM line) with a DM (mean = 63 years). Table 11 provides the optimization results.

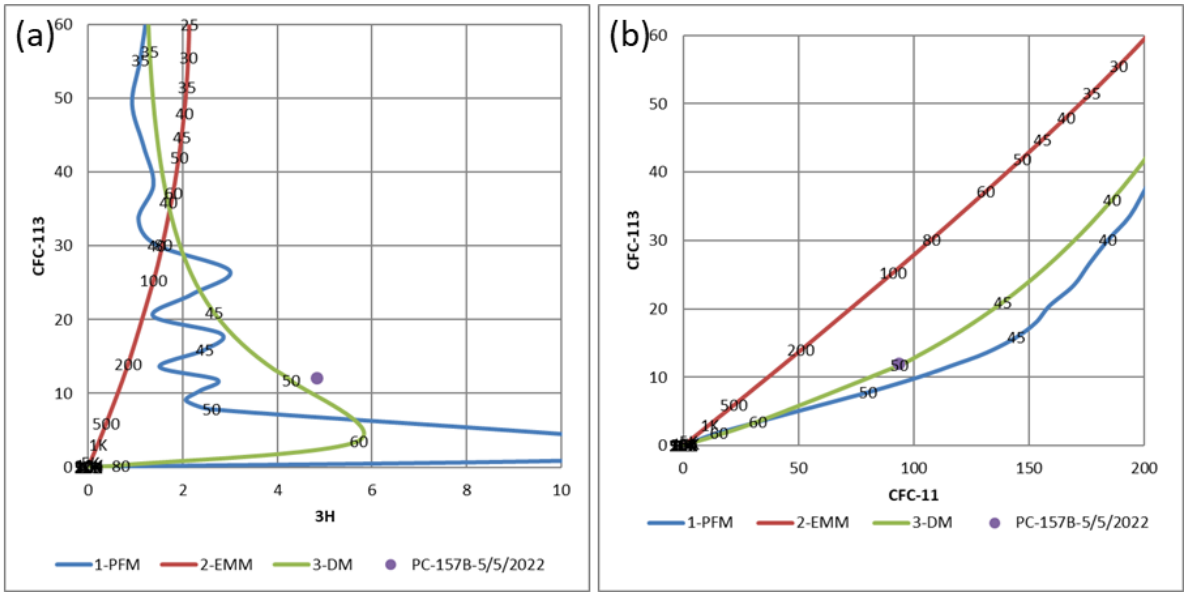

Figure 18. *TracerTracerGraph* representations for well PC-157B for (a) ^{3}H and CFC-113, and (b) CFC-11 and CFC-113. The observed concentrations are indicated with purple point. Age labels in years are included. Units for ^{3}H is TU and for CFCs is pptv.

Table 10. Age distribution statistics for PC-157B *TracerLPM* optimization runs.

Model Name	Age (years)		Dispersion Parameter	Tracers in Optimization	Error				
	Mean	Median			^3H	SF_6	CFC-11	CFC-113	Signif.
PFM	64	64	-	^3H	4.8%				Y
	14	14	-	SF_6		1.0%			Y
	49	49	-	CFC-11			5.0%		N
	47	47	-	CFC-113				5.2%	N
EM	1	0.5	-	^3H	40.0%				N
	17	11	-	SF_6		0.0%			Y
	96	66	-	CFC-11			0.0%		Y
	236	163	-	CFC-113				0.0%	Y
DM	59	56	0.05	^3H	0.0%				Y
	17	11	0.51	SF_6		0.0%			Y
	88	61	0.45	CFC-11			0.0%		Y
	59	56	0.05	CFC-113				0.0%	Y
	50	49	0.01	^3H, CFC-11	11.1%		0.0%		N
	52	50	0.02	^3H, CFC-113	11.6%			0.0%	N
	50	49	0.01	CFC-11, CFC-113			1.7%	0.0%	Y

Table 11. Age distribution statistics for NERT5.49S1 *TracerLPM* optimization runs.

Model Name	Age (years)		Dispersion Parameter	Tracers in Optimization	Error				
	Mean	Median			SF_6	CFC-11	CFC-12	CFC-113	Signif.
PFM	12	12	-	SF_6	1.0%				Y
	59	59	-	CFC-11		6.7%			N
	53	53	-	CFC-12			4.7%		Y
	49	49	-	CFC-113				3.0%	Y
EMM	13	9	-	SF_6	0.0%				Y
	605	419	-	CFC-11		0.0%			Y
	185	128	-	CFC-12			0.0%		Y
	311	215	-	CFC-113				0.0%	Y
DM	12	11	0.06	SF_6	0.0%				Y
	301	175	0.75	CFC-11		0.0%			Y
	171	97	0.80	CFC-12			0.0%		Y
	211	121	0.77	CFC-113				0.0%	Y
	63	60	0.05	CFC-12 CFC-113			0.9%	0.0%	Y

MW-201A: *TracerTracerGraph* results indicated CFC-11 and CFC-113 have the potential to be used for multi-tracer optimization using the PFM to produce mean ages close to 40 years (Figure 19a, observed sample located near the blue PFM line at approximately 40 years). No LPM was able to replicate observed CFC-12 and this tracer was discarded. Table 12 provides results for each LPM. As expected, based on the *TracerTracerGraph* results, only the PFM model maintains significant results (mean age 40 years, error <5 percent) using CFC-11 and CFC-113 simultaneously.

NERT4.93S1: Only ^{3}H, SF_6, and CFC-113 were available for analysis, with no LPM able to reproduce the observed ^{3}H and SF_6 with error <5 percent. Only the PFM can replicate CFC-113 with error <2 percent for an age of 24 years.

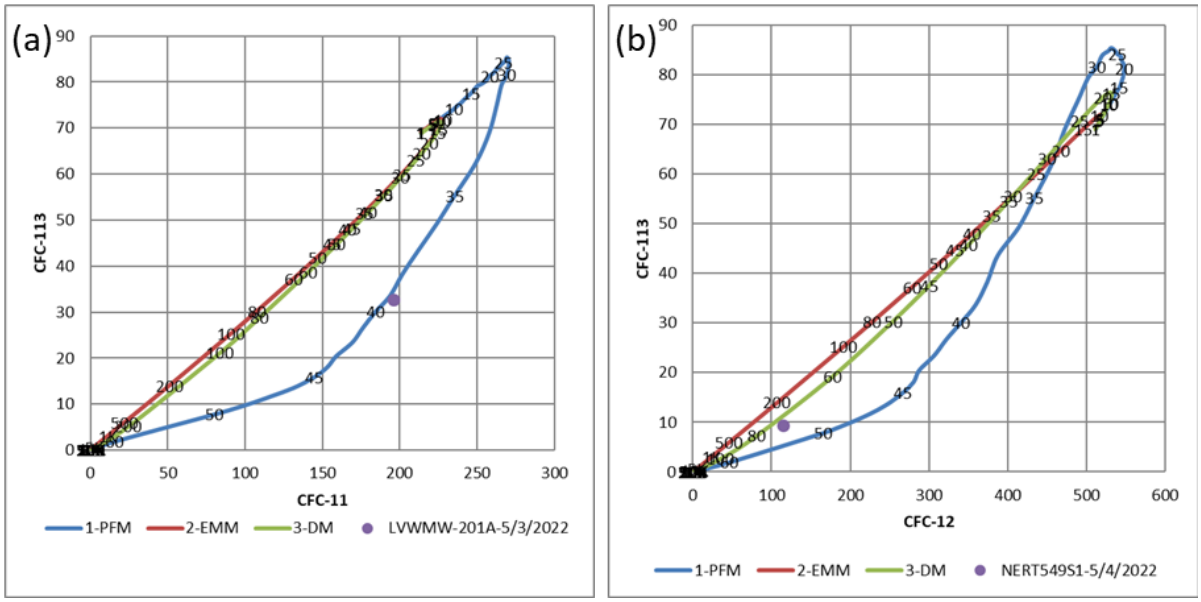

Figure 19. *TracerTracerGraph* representations using (a) CFC-11 and CFC-113 in well MW-201A, and (b) CFC-12 and CFC-113 in well NERT5.49S1. The observed sample concentration is shown as a purple point. Age labels in years are included. Units for CFCs are pptv.

Table 12. Age distribution statistics for MW-201A *TracerLPM* optimization runs.

Model Name	Age (years)		Dispersion Parameter	Tracers in Optimization	Error		
	Mean	Median			CFC-11	CFC-113	Significant
PFM	39	39	-	CFC-11	1.3%	-	Y
	40	40	-	CFC-113	-	2.7%	Y
	40	40	-	CFC-11, -113	3.4%	2.7%	Y
EMM	27	19	-	CFC-11	0.0%	-	Y
	71	49	-	CFC-113	-	0.0%	Y
	72	50	-	CFC-11, -113	40.6%	0.0%	N
DM	48	44	0.10	CFC-11	29.4%	-	N
	84	48	0.73	CFC-113	-	0.0%	Y
	48	44	0.10	CFC-11, -113	29.4%	0.0%	N

NERT4.71S1: Only ^{3}H, SF_6, and CFC-113 were available for LPM analysis. No LPM could significantly match observed SF_6 or CFC-113 concentrations. Relying only on ^{3}H limits the LPM to a PFM result of approximately 63 years with an error of 3.6 percent.

Four wells (PC-64, MW-105, MW-224A and MW-25) are screened in the shallow alluvium with uncorrected ^{14}C pmC values between 60 and 75 pmC, ^{3}H <4.5 TU, and measurable CFCs and/or SF_6. These wells are considered a mixture of modern and older water. The PFM-PFM models were developed to establish the fraction of young water (fY), the mean age of young water, and the mean age of old water. Tables 13 to 16 tabulate the results for each well with significance indicated (i.e., error <5 percent). Calibrated fractions of young water tended to be low if using ^{3}H in the solution (e.g., 15 to 17 percent) and were much higher if SF_6 or CFCs were applied (47 to 71 percent). In all cases, the mean for old water represents a minimum age to reduce error <5 percent. No significant solution was found for MW-25 but allowing for <10 percent error produced a single result.

Table 13. Binary mixing model results for PC-64. Calibration initiated with *NETPATH* output of a mean age of old water and the fraction of young water equal to 3,200 years and 44 percent, respectively. The ^{14}C error can be further reduced by increasing the mean age of old water.

Model Name	Age (years)		Fraction Young Water	Tracers in Optimization	Error		Signif.
	Young Mean	Old Mean			Other	^{14}C	
PFM-PFM	58	8,200	0.17	^{3}H,^{14}C	0.0%	4.2%	Y
	2	7,500	0.53	SF_6,^{14}C	0.0%	4.9%	Y
	25	13,500	0.55	CFC-11,^{14}C	0.0%	4.5%	Y

Table 14. Binary mixing model results for MW-105. Calibration initiated with *NETPATH* output of a mean age of old water and the fraction of young water equal to 1,700 years and 85 percent, respectively. The ^{14}C error can be further reduced by increasing the mean age of old water.

Model Name	Age (years)		Fraction Young Water	Tracers in Optimization	Error		Signif.
	Young Mean	Old Mean			Other	^{14}C	
PFM-PFM	58	3,500	0.15	^{3}H,^{14}C	0.0%	4.3%	Y
	1	2,100	0.47	SF_6,^{14}C	0.0%	4.9%	Y
	30	13,000	0.68	CFC-11,^{14}C	0.0%	4.5%	Y
	28	30,000	0.79	CFC-113,^{14}C	0.0%	8.4%	N

Table 15. Binary mixing model results for MW-224A. Calibration initiated with *NETPATH* output of a mean age of old water and fraction of young water equal to 1,400 years and 83 percent, respectively. The ^{14}C error can be further reduced by increasing the mean age of old water.

Model Name	Age (years)		Fraction Young Water	Tracers in optimization	Error		Signif.
	Young Mean	Old Mean			Other	^{14}C	
PFM-PFM	58	2,900	0.15	^{3}H,^{14}C	0.0%	4.8%	Y
	1	2,800	0.71	SF_6,^{14}C	0.0%	4.9%	Y

Table 16. Binary mixing model results for MW-25. Calibration initiated with *NETPATH* output of a mean age of old water and the fraction of young water equal to 3,100 years and 24 percent, respectively. The ^{14}C error can be further reduced by increasing the mean age of the old water.

Model Name	Age (years)		Fraction Young Water	Tracers in Optimization	Error		Signif.
	Young Mean	Old Mean			Other	^{14}C	
PFM-PFM	59	3,100	0.01	^{3}H,^{14}C	6.4%	1.6%	N
	2	30,000	0.79	SF_6,^{14}C	0.0%	10.9%	N

3.3.2 Upper Muddy Creek Formation (UMCf)

One well (ES-28) is screened in the Upper Muddy Creek Formation and contains no old water. The LPM development follows the procedure for estimating the range in distributions similar to those wells with >80 pmC in the alluvium. Samples available for analysis include ^{3}H, SF_6, and CFC-113. *TracerTracerGraph* analysis suggests the DM can simultaneously solve for SF_6 and CFC-113 (Figure 20, observed sample located near the green DM). Table 17 provides the tested LPM statistics.

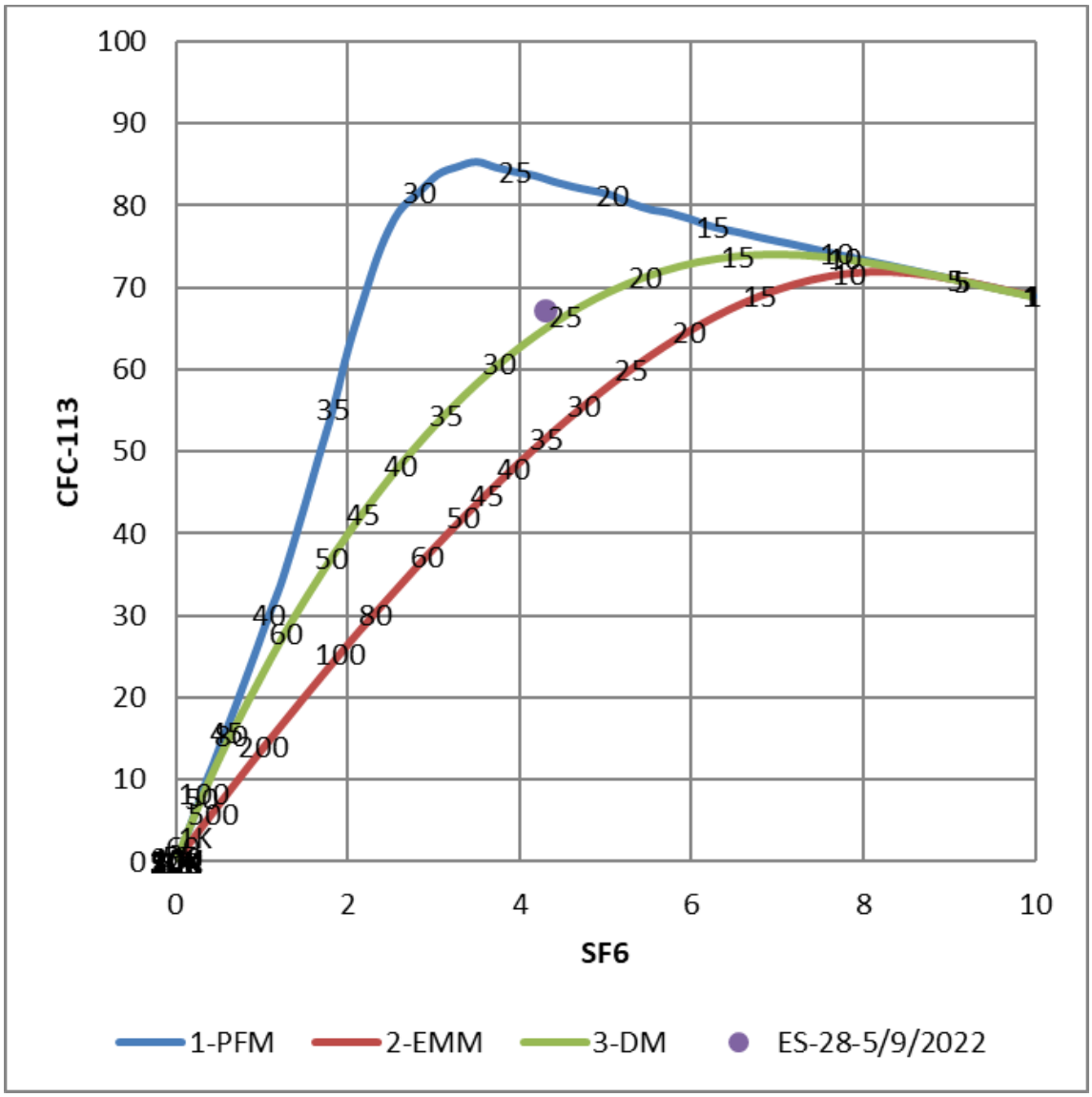

Figure 20. *TracerTracerGraph* representations for SF_6 and CFC-113 in well ES-28. The observed sample concentration is shown as a purple point. Age labels in years are included. Units for SF_6 and CFC-113 are pptv.

Table 17. Age distribution statistics for well ES-28 *TracerLPM* optimization runs.

Model Name	Age (years)		Dispersion Parameter	Tracers in Optimization	Error			
	Mean	Median			^3H	SF_6	CFC-113	Signif.
PFM	63	63	-	^3H	12.3%			N
	24	24	-	SF_6		0.4%		Y
	34	34	-	CFC-113			2.1%	Y
EM	None	-	-	^3H	-			N
	35	24	-	SF_6		0.0%		Y
	17	11	-	CFC-113			0.0%	Y
DM	1	1	0.10	^3H	49.0%			N
	39	22	0.79	SF_6		0.0%		Y
	19	12	0.54	CFC-113			0.0%	Y
	26	22	0.16	SF_6, CFC-113		0.0%	0.0%	Y

Tracer observations in six wells sampled in the Upper Muddy Creek Formation indicate a mix of younger and older water. Listed from upgradient to downgradient: TR-8, TR-7, M-31A, M-207, M-155, and PC-195. Development of LPMs relies on the BMM approach with results provided in Tables 18 to 23. Well PC-195, M-155, and TR-7 did not have observable ^3H, but they did have observable SF_6 and CFCs. For LPM development of these three wells, the presence of SF_6 and/or CFCs suggests younger water, but we acknowledge the lack of ^3H makes the presence of young water uncertain. Uncertainty in the presence of young water in well M-155 is compounded by the inability to find a significant LPM to match observed SF_6 or CFCs.

Table 18. Binary mixing model results for TR-8 using *TracerLPM*. No *NETPATH* modeling was done for this well because no upgradient groundwater chemistry was available. The initial mean age of the old water assumed 6,000 years based on the uncorrected ^{14}C observation. The ^{14}C error can be further reduced by increasing the mean age of the old water.

Model Name	Age (years)		Fraction Young Water	Tracers in Optimization	Error		Signif.
	Young Mean	Old Mean			Other	^{14}C	
PFM-PFM	58	7,500	0.04	^3H,^{14}C	0.0%	3.9%	Y
	2	7,700	0.15	SF_6,^{14}C	0.0%	4.1%	Y
	2	6,300	0.01	CFC-11,^{14}C	62.2%	5.0%	N
	2	30,000	0.38	CFC-12,^{14}C	0.0%	20.8%	N
	27	16,500	0.35	CFC-113,^{14}C	0.0%	3.9%	Y

Table 19. Binary mixing model results for TR-7 using *TracerLPM*. No *NETPATH* modeling was done for this well because no upgradient groundwater chemistry was available. The initial mean age of the old water assumed 14,000 years based on the uncorrected ^{14}C observation. The ^{14}C error can be further reduced by increasing the mean age of the old water.

Model Name	Age (years)		Fraction Young Water	Tracers in Optimization	Error		Signif.
	Young Mean	Old Mean			Other	^{14}C	
PFM-PFM	2	14,000	0.01	SF_6,^{14}C	97.6%	24.2%	N
	2	14,000	0.01	CFC-11,^{14}C	99.2%	24.2%	N
	16	24,000	0.11	CFC-12,^{14}C	0.0%	4.6%	Y
	58	23,000	0.06	CFC-113,^{14}C	99.5%	4.7%	N

Table 20. Binary mixing model results for M-31A using *TracerLPM*. Calibration initiated with *NETPATH* output of a mean age of old water and the fraction of young water equal to 2,100 years and 44 percent, respectively. The ^{14}C error can be further reduced by increasing the mean age of the old water.

Model Name	Age (years)		Fraction Young Water	Tracers in Optimization	Error		Signif.
	Young Mean	Old Mean			Other	^{14}C	
PFM-PFM	58	2,100	0.12	^{3}H,^{14}C	0.0%	4.6%	Y
	1	5,600	0.89	SF_6,^{14}C	0.0%	5.0%	Y
	28	9,600	0.73	CFC-113,^{14}C	0.0%	5.0%	Y

Table 21. Binary mixing model results for M-207 using *TracerLPM*. Calibration initiated with *NETPATH* output of a mean age of old water and the fraction of young water equal to 2,700 years and nine percent, respectively. The ^{14}C error can be further reduced by increasing the mean age of the old water.

Model Name	Age (years)		Fraction Young Water	Tracers in Optimization	Error		Signif.
	Young Mean	Old Mean			Other	^{14}C	
PFM-PFM	58	5,000	0.14	^{3}H,^{14}C	0.0%	4.7%	Y
	1	4,500	0.41	SF_6,^{14}C	0.0%	3.5%	Y
	2	30,000	0.95	CFC-12,^{14}C	0.0%	25.6%	N

Table 22. Binary mixing model results for M-155 using *TracerLPM*. Calibration initiated with *NETPATH* output of a mean age of old water and the fraction of young water equal to 21,000 years and three percent, respectively. No LPMs are significant and the lack of observable ^{3}H indicates the presence of a young water fraction in this well is highly uncertain.

Model Name	Age (years)		Fraction Young Water	Tracers in Optimization	Error		Signif.
	Young Mean	Old Mean			Other	^{14}C	
PFM-PFM	2	30,000	0.01	SF_6,^{14}C	99.6%	37.6%	N
	58	29,500	0.02	CFC-11,^{14}C	99.8%	2.8%	N
	2	30,000	0.01	CFC-12,^{14}C	89.9%	37.6%	N
	58	29,500	0.02	CFC-113,^{14}C	99.8%	2.8%	N

Table 23. Binary mixing model results for PC-195 using *TracerLPM*. Calibration initiated with *NETPATH* output of a mean age of old water and the fraction of young water equal to 5,100 years and three percent, respectively. The ^{14}C error can be further reduced by increasing the mean age of the old water. A lack of observable ^{3}H makes the presence of young water in this well uncertain.

Model Name	Age (years)		Fraction Young Water	Tracers in Optimization	Error		Signif.
	Young Mean	Old Mean			Other	^{14}C	
PFM-PFM	2	5,660	0.05	SF_6,^{14}C	0.0%	4.4%	Y
	2	5,400	0.01	CFC-11,^{14}C	80.0%	3.2%	N
	21	5,700	0.05	CFC-12,^{14}C	0.0%	4.2%	Y
	27	6,000	0.70	CFC-113,^{14}C	0.0%	4.0%	Y

3.4 Phase 6 Sensitivity Analysis

Figure 21 shows the baseline backward particle tracking results and the associated ages for the 19 wells sampled for age tracers. These ages are calculated using the baseline ground water flow model and are calculated independently of any ages determined using environmental tracers that were discussed in the previous section. Shallow flow paths derived from surface recharge, with emphasis on particles traveling through paleochannels, produced the youngest path lines (≤10 years), whereas flow paths through the alluvium outside of the paleochannels were older (≤150 years). Deeper flow sourced from the GBF inputs represent flow paths from 200 to 3,400 years. Very young water estimates (<1 month) are simulated for two wells with well water obtained exclusively from the Las Vegas Wash (NERT5.49S1 and MW-201A). As a reminder, the sensitivity analysis independently adjusted 16 parameters above and below the baseline value for a total of 32 additional simulations. Particle tracking results for the baseline scenario and the 32 simulations defining the sensitivity analysis are compared to significant LPMs derived from observed age tracers (Section 3.3). Comparison between the Phase 6 model and various LPMs is focused on matching the relative fraction of young water in each well. The presentation of individual

wells are grouped as a function of the geologic unit in which they are screened. Specifically, wells are grouped by those screened in the Quaternary alluvium and those screened in the coarse-grained (UMCf-cg1 and UMCf-cg2) and fine-grained (UMCf-fg1) units of the Upper Muddy Creek Formation.

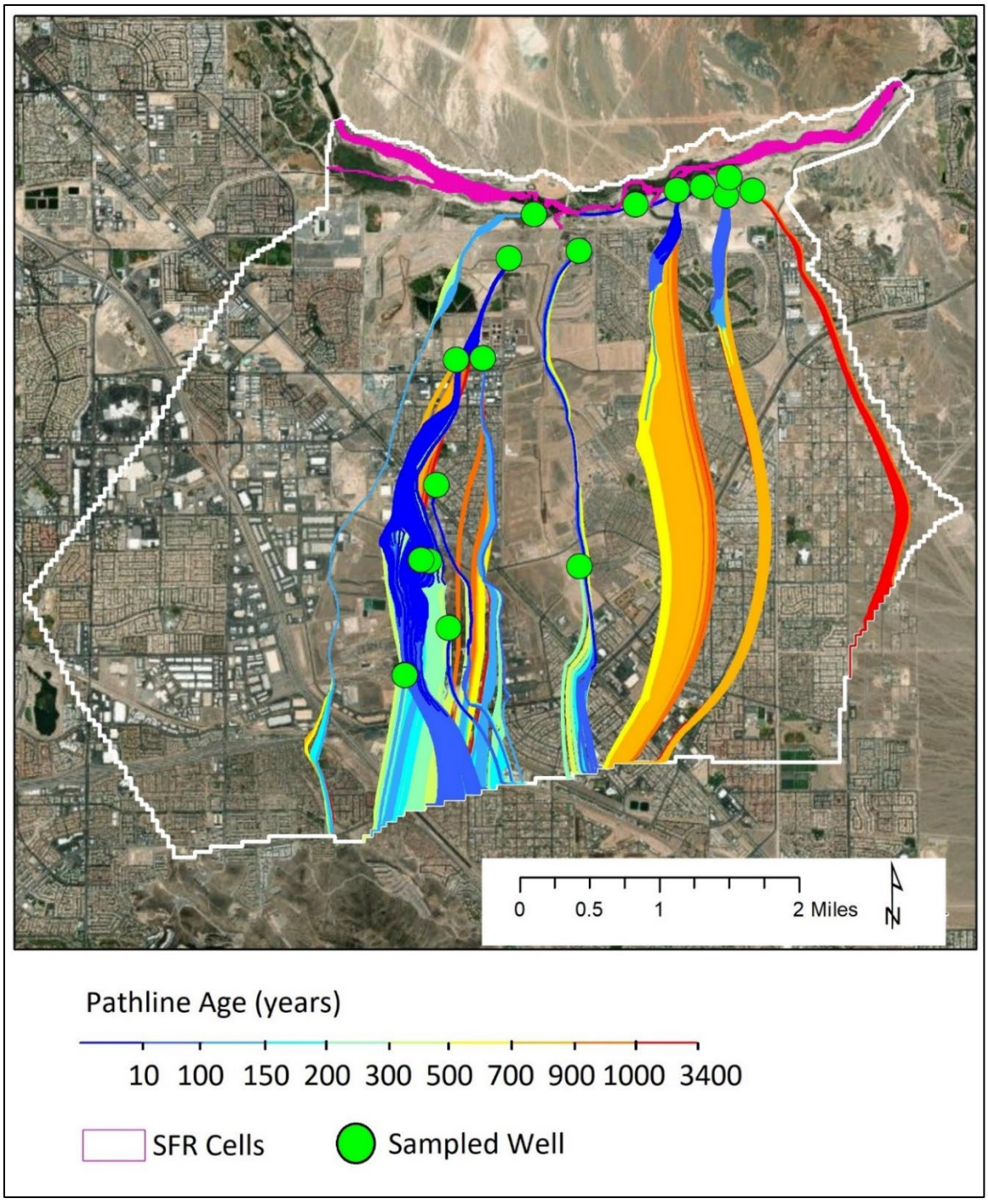

Figure 21. Pathline ages for baseline backward particle tracking from the 19 wells sampled for age tracers.

3.4.1 Age Distributions for Wells in the Quaternary Alluvium

Twelve wells are screened in the shallow water-bearing zone in the Quaternary alluvium with depths below ground surface ranging from 24 to 75 feet. All wells are screened in the top layer of the model (layer 1). Wells are presented along the primary flow directions (from the southern portion of the model domain toward the Las Vegas Wash) and from west to east (see Figure 8 for well locations with names).

PC-64: This well is located in the upper regions of OU-2 just to the north of State Route 582. Simulated water sourcing to the well is primarily from the southern IBF boundary across model layers 2 to 10. Deep flows move upward through the coarse-grained Muddy Creek into the fined-grained unit and eventually into the more conductive alluvial material in layer 1 (Figure 22). Age distributions (Figure 23) indicate the baseline simulations produce a mean age of 837 years (sensitivity range from 185 to 1,188 years) and a median age of 391 years (sensitivity range from 100 to 519 years) with the fraction of water <70 years, or modern water, equal to 0.5 percent of the well volume (sensitivity range 0 to 2 percent). In comparison, the LPMs produce a range in modern water (<70 years) of 17 to 55 percent, with the Phase 6 model most closely resembling the lowest LPM fraction defined by calibration using ^{3}H. The lack of simulated surface recharge limits the ability of the Phase 6 model to fully replicate the LPM but moving GBF-derived water more quickly through the subsurface could potentially achieve sufficient replication of the LPM. This would require simultaneously decreasing horizontal hydraulic conductivity in the alluvial material outside the paleochannels and the UMCf-fg unit, increasing horizontal hydraulic conductivity in the UMCf-fg and decreasing vertical hydraulic conductivity in the UMCf-cg. It is important that this LPM be older than most of the simulated flow paths derived from the southern GBF to account for the time accrued in the subsurface prior to entering the model domain.

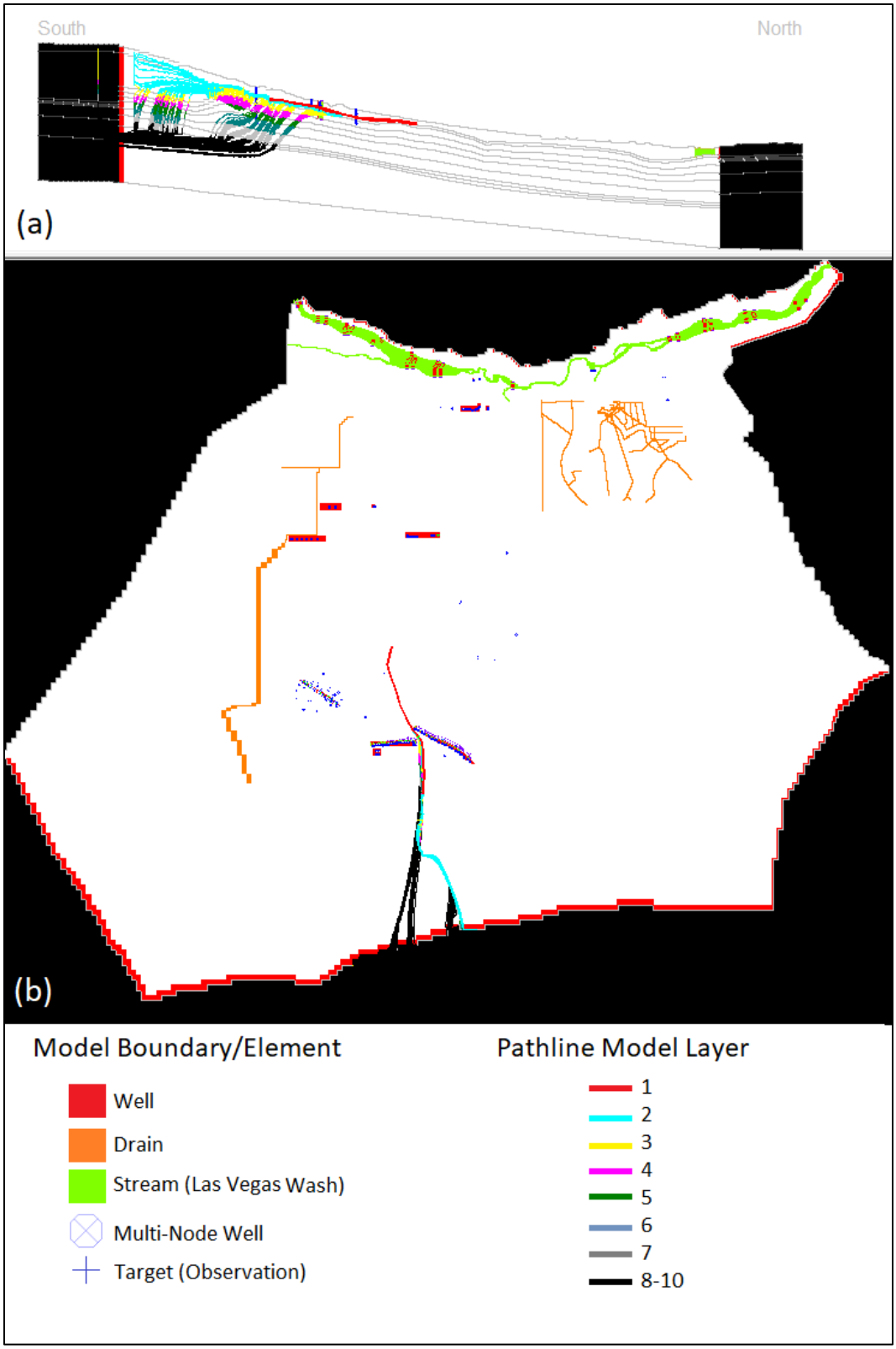

Figure 22. Backward tracking results for the baseline simulation well PC-64. Pathlines are color coded by model layer in (a) a cross section along column 148 (north-south center of model) with layers delineated in light gray and (b) an aerial view.

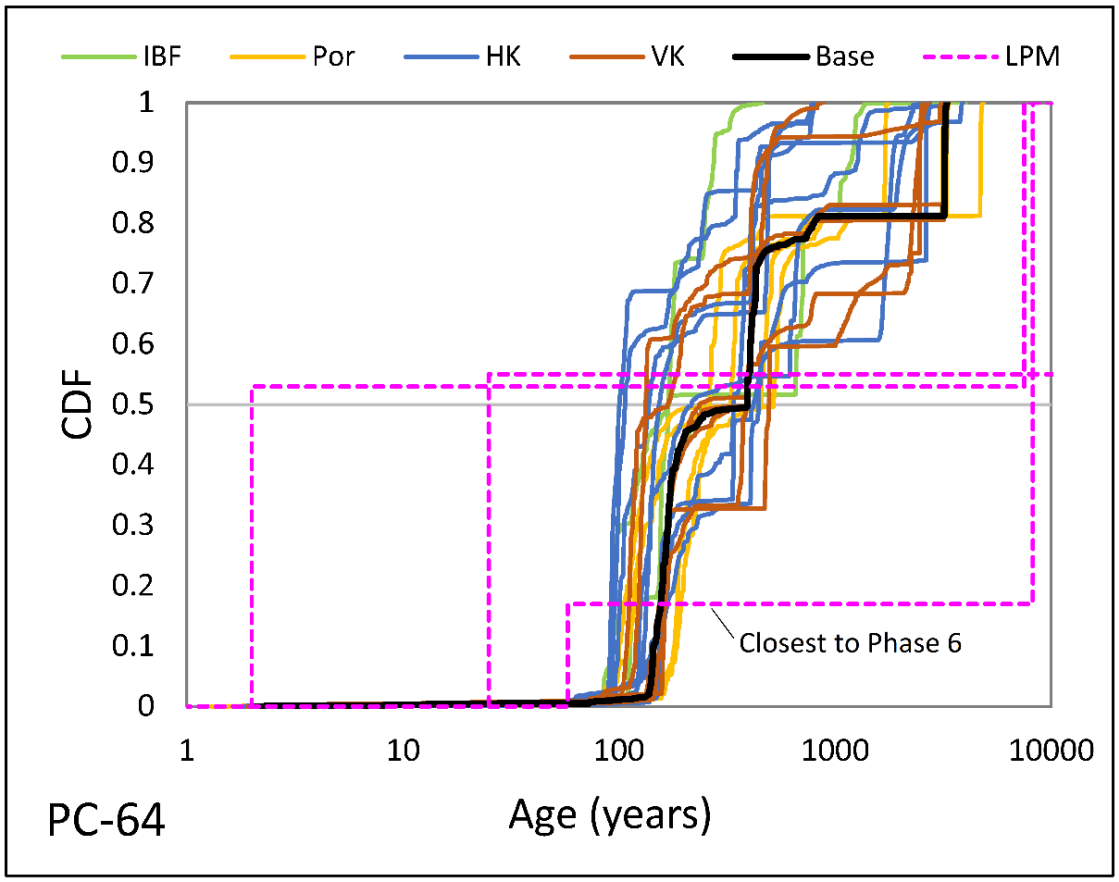

Figure 23. Age distributions for well PC-64 calculated for the sensitivity analysis using the Phase 6 model and significant LPMs. The LPMs are binary mixing models using PFM-PFM using ^{3}H to calibrate the model for the young fraction most representative of the Phase 6 output.

ARP-7: This well is located downgradient from PC-64 in the upper regions of OU-3 and positioned in one of the paleochannels. Simulated water sourcing to the well is primarily from the southern GBF boundary, with some particles originating in layer 2 (relatively shallow) and most particles sourced from layers 8 to 10 (very deep). Deep flows move upward through the coarse-grained and fine-grained Muddy Creek to emerge into the more conductive alluvial and paleochannel material in layer 1 (Figure 24). Age distributions (Figure 25) indicate a mean age of 438 years (sensitivity range from 303 to 645 years) and a median of 484 (sensitivity range from 121 to 756 years) with no/little modern water under 70 years (sensitivity range from 0 to 0.9 percent). In comparison, the single significant LPM indicates all water in the well is <70 years. No version of the Phase 6 model was able to replicate the observed tracer information because of the lack of surface recharge entering the well and an overreliance on simulated flow paths originating along the southern GBF that are not supported by the lack of old water in the well (^{14}C >80 pmC).

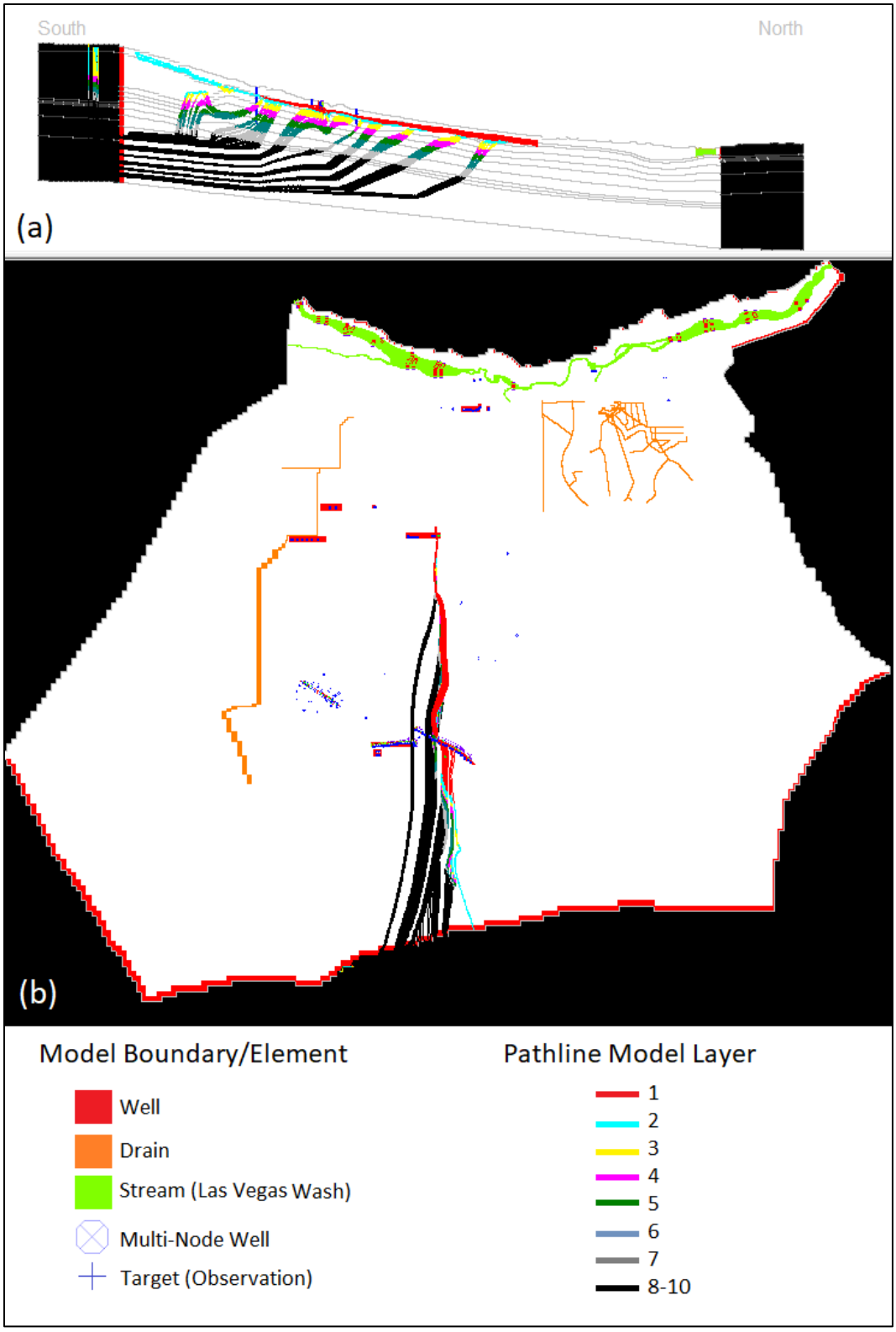

Figure 24. Backward tracking results for the baseline simulation well ARP-7. Pathlines are color coded by model layer in (a) a cross section along column 148 (north-south center of model) with layers delineated in light gray and (b) an aerial view.

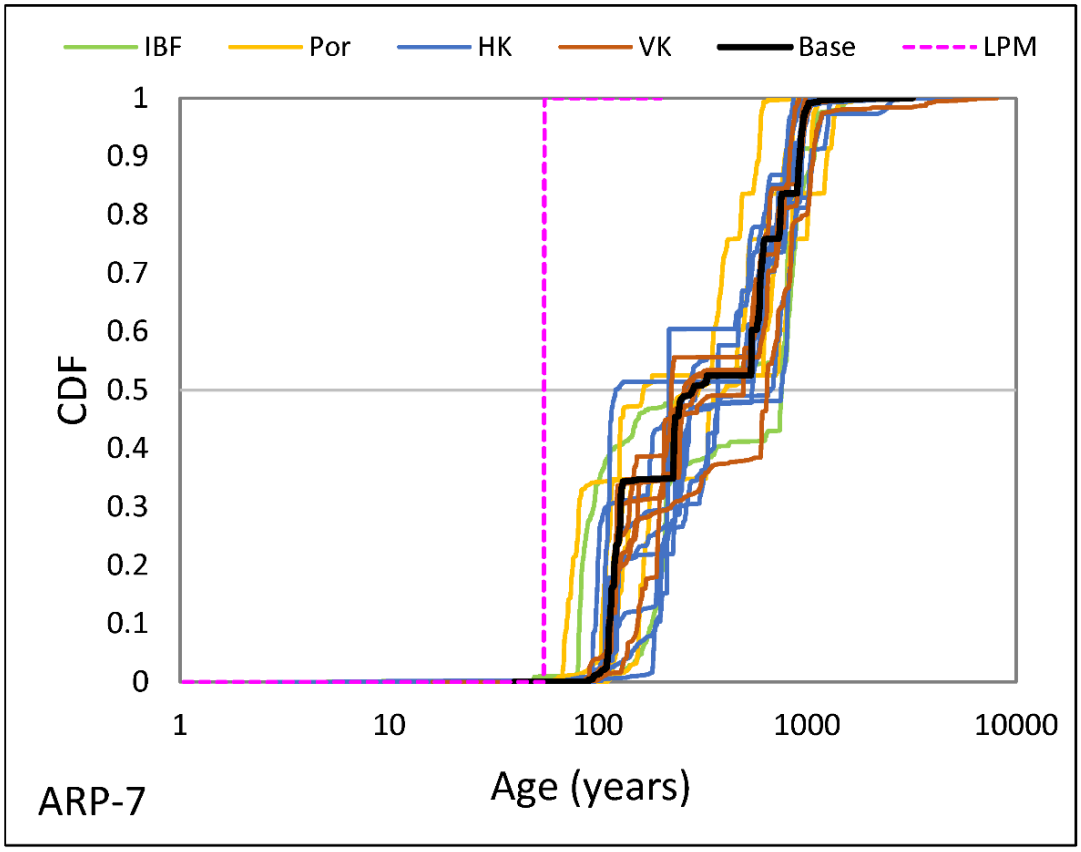

Figure 25. Age distributions for well ARP-7 calculated for the sensitivity analysis using the Phase 6 model and a single significant LPM defined as a PFM calibrated using ^{3}H with a mean age of 64 years.

PC-56: This well is located downgradient from ARP-7 in OU-3 and positioned in one of the paleochannels. Simulated water sourcing to the well is primarily from the southern GBF boundary, although the youngest water is derived from recharge in OU-1. The GBF particles originate from layer 2 (relatively shallow) through layers 8 to 10 (deep). As in the previous wells described, deep flows move upward from the coarse-grained and fine-grained Muddy Creek Formation to emerge into the more conductive alluvial and paleochannel material in layer 1 (Figure 26). Age distributions (Figure 27) indicate a mean age of 407 years (sensitivity range from 231 to 595 years) and a median of 300 years (sensitivity range from 181 to 489 years). Modern water accounts for 12 percent of well volume (sensitivity range from 4 to 22 percent) largely because of surface recharge and water moving relatively fast through alluvial units. Phase 6 simulated age distributions are most sensitive to porosity reductions in the fine-grained and coarse-grained Muddy Creek Formation, as well as increased horizontal hydraulic conductivity in these units. A large number of significant LPMs indicate the well is largely modern water (mean = 4 to 35 years; median = 3 to 35 years) and the fraction of water <70 years is 92 to 100 percent. No version of the Phase 6 model can replicate the observed tracer information because of an overreliance on simulated deep flow paths originating along the southern GBF that are not supported by the lack of old water in the well (^{14}C >80 pmC).

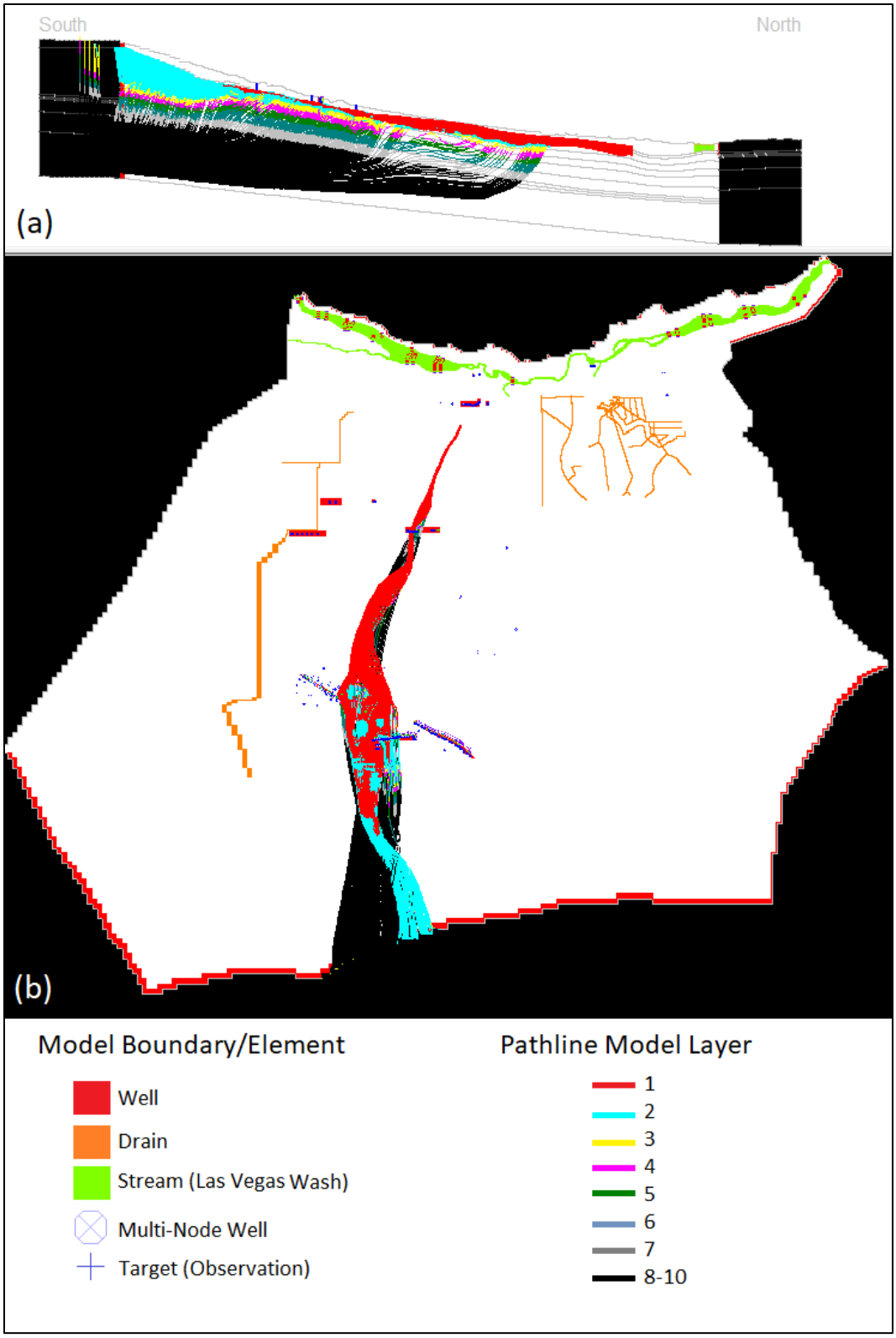

Figure 26. Backward tracking results for the baseline simulation well PC-56. Pathlines are color coded by model layer in (a) a cross section along column 148 (north-south center of the model) with layers delineated in light gray and (b) an aerial view.

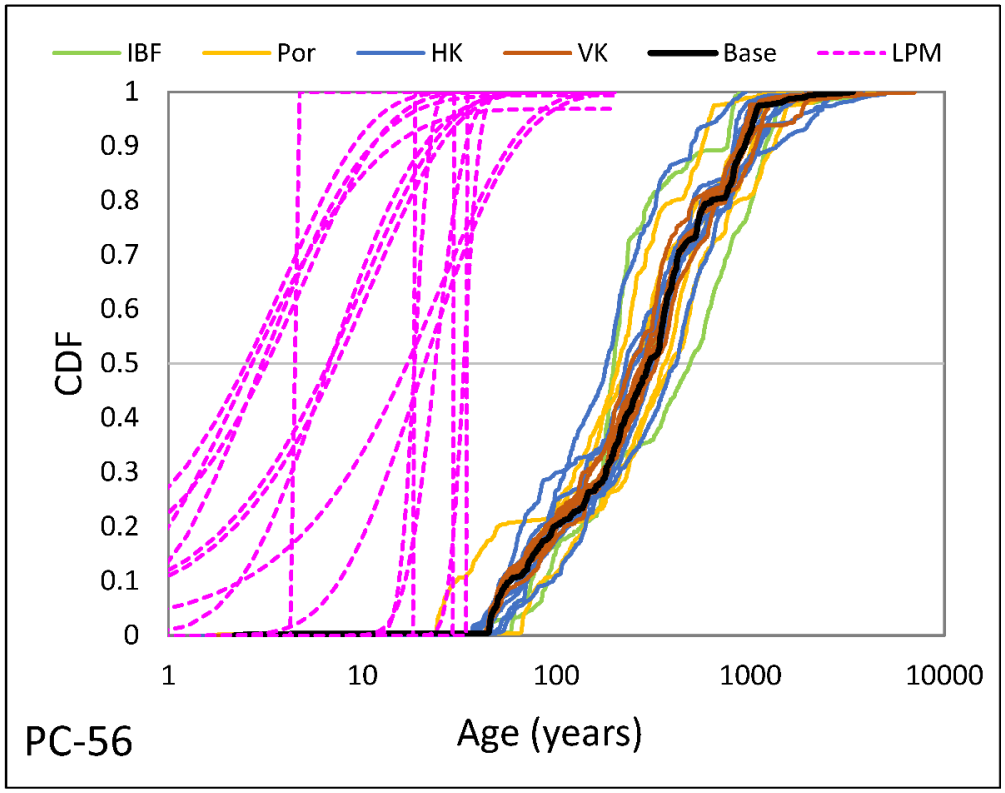

Figure 27. Age distributions for well PC-56 calculated for the sensitivity analysis using the Phase 6 model and all significant LPMs (see Table 10).

PC-157A/B: These wells are located downgradient from PC-56 in OU-3 and are proximal to the Las Vegas Wash in the gravels. Well PC-157B is screened approximately 20 feet below PC-157A. These wells are located in the same Phase 6 cell and have identical simulated flow paths (Figure 28). It is believed to receive most of its recharged water from the effluent water from the wastewater treatment plants and it may not be representative of young water recharged upgradient. Nonetheless, simulated water sourcing to the well is primarily from the southern GBF boundary, with only a small fraction of water estimated by the numerical model derived from surface recharge. Some of the flow across the southern boundary enters the model and moves vertically upward into the upper model layers, whereas other water dives downward into layers 7 to 9 before moving upward to the alluvium further south on the flow path trajectory. Subsequently, a portion of this shallow flow temporarily dives into the subsurface in OU-3 (layers 2 to 6) before moving upward into the well. Inverse pathlines of PC-157A/B reach back to OSSM groundwater extraction well field, which has some discrepancy from the conceptual model. Future work will need to check these results since they have implications on comingled plumes and remediation efforts. Age distributions (Figure 29) indicate a mean age of 180 years (sensitivity range from 122 to 237 years) and a median of 163 (sensitivity range from 8 to 225 years). Modern water accounts for none of the well volume in the baseline Phase 6 model, but a large range in young water occurs as a function of reducing flow from the southern GBF (sensitivity range from 0 to 85 percent). The young fraction can also be increased by decreasing porosity in the fine-grained and

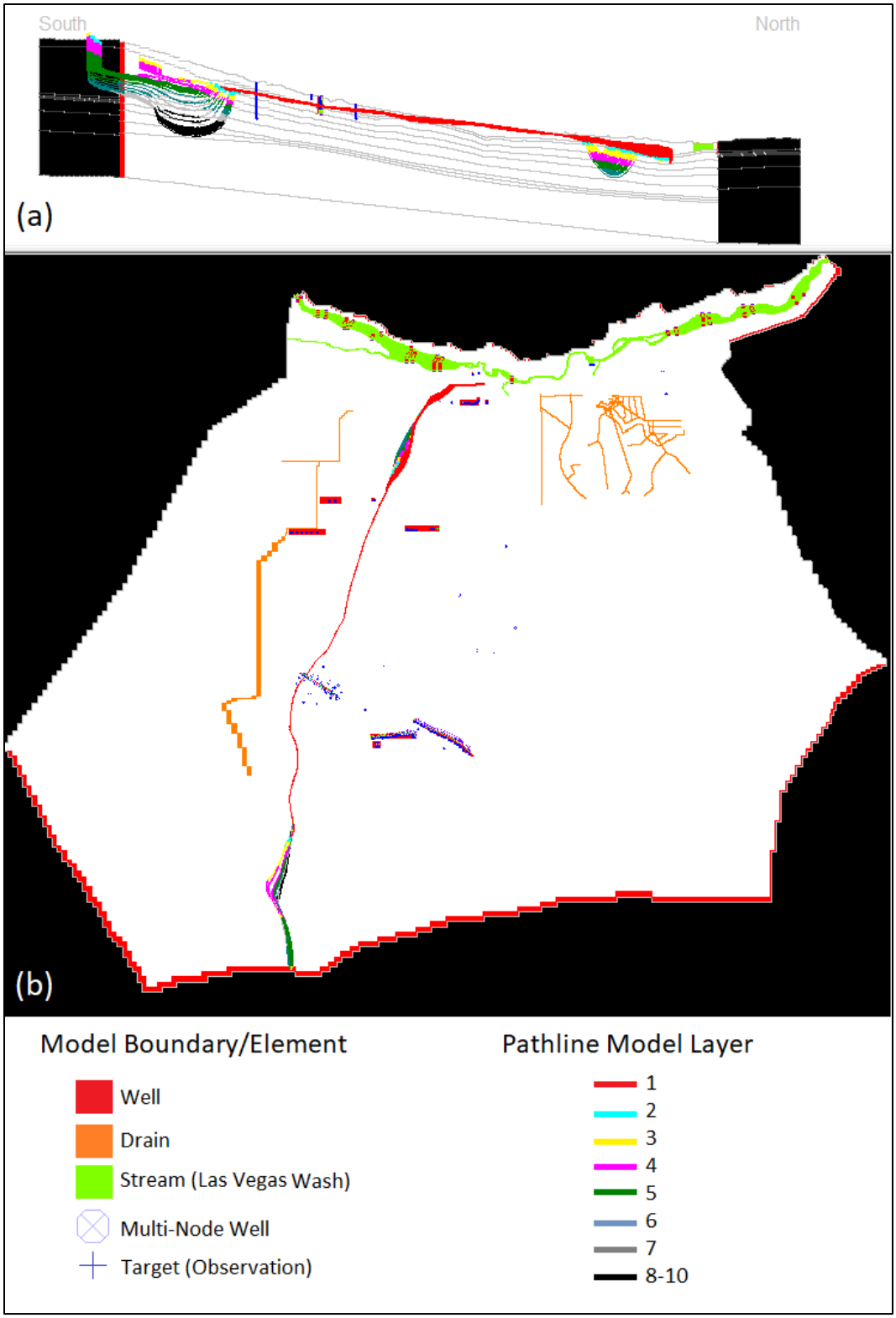

Figure 28. Backward tracking results for the baseline simulation well PC-157A/B. Pathlines are color coded by model layer in (a) a cross section along column 148 (north-south center of model) with layers delineated in light gray and (b) an aerial view.

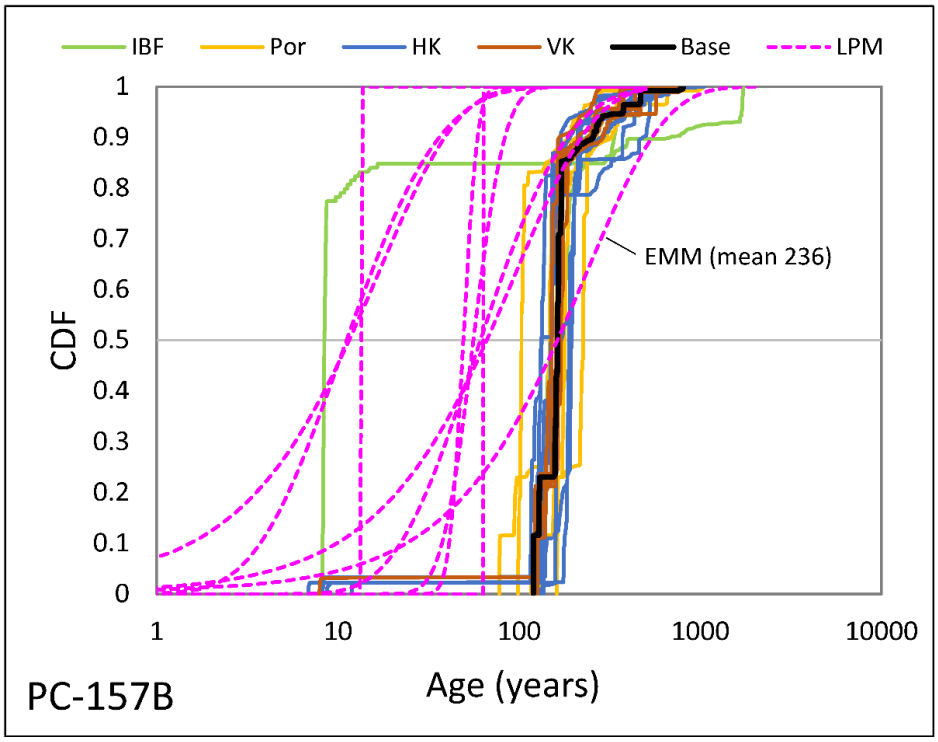

Figure 29. Age distributions calculated for the sensitivity analysis using the Phase 6 model and significant LPMs defined for PC-157B. Well PC-157A is nearly identical.

coarse-grained Upper Muddy Creek Formation and decreasing the vertical and horizontal hydraulic conductivity in the coarse-grained Muddy Creek. Tracer observations are slightly different in the two wells, but the LPM results are very similar, with water <70 years representing 16 to 100 percent of the well volume. Phase 6 model results are closest to the EMM, in which adjustments to the horizontal and vertical hydraulic conductivity and a reduction in porosity can aid in matching younger water ages.

MW-105: This well is located east of PC-56 in OU-1 and about 2 miles downgradient from ES-28 (which is located in the fine-grained unit of the Muddy Creek Formation and discussed in Section 4.3.3). Most water is derived from the southern boundary at depth, although a portion of water sourced to this well comes from shallower boundary fluxes (layer 2) and a small component comes from surface recharge (Figure 30). Deep flows move upward through the coarse-grained and fine-grained Muddy Creek Formation to emerge into the more conductive alluvium in layer 1. A component of flow from the surface in OU-3 does travel downward into layer 5 before moving upward into the well. Phase 6 modeled age distributions (Figure 31) indicate a mean age of 208 years (sensitivity range from 146 to 271 years) and a median of 130 years (sensitivity range from 89 to 167 years). Modern water accounts for 5 percent of well volume (range from 0 to 39 percent). Binary mixing models (Table 14) suggested 15 to 68 percent of modern water, with the lower young water fraction calibrated using ^{3}H and most similar to the Phase 6 output. Although the baseline Phase 6 model does not emulate the LPM, increasing flow across the southern boundary or decreasing porosity in one of the Muddy Creek units (fine- or coarse-grained) can individually mimic the LPM ages.

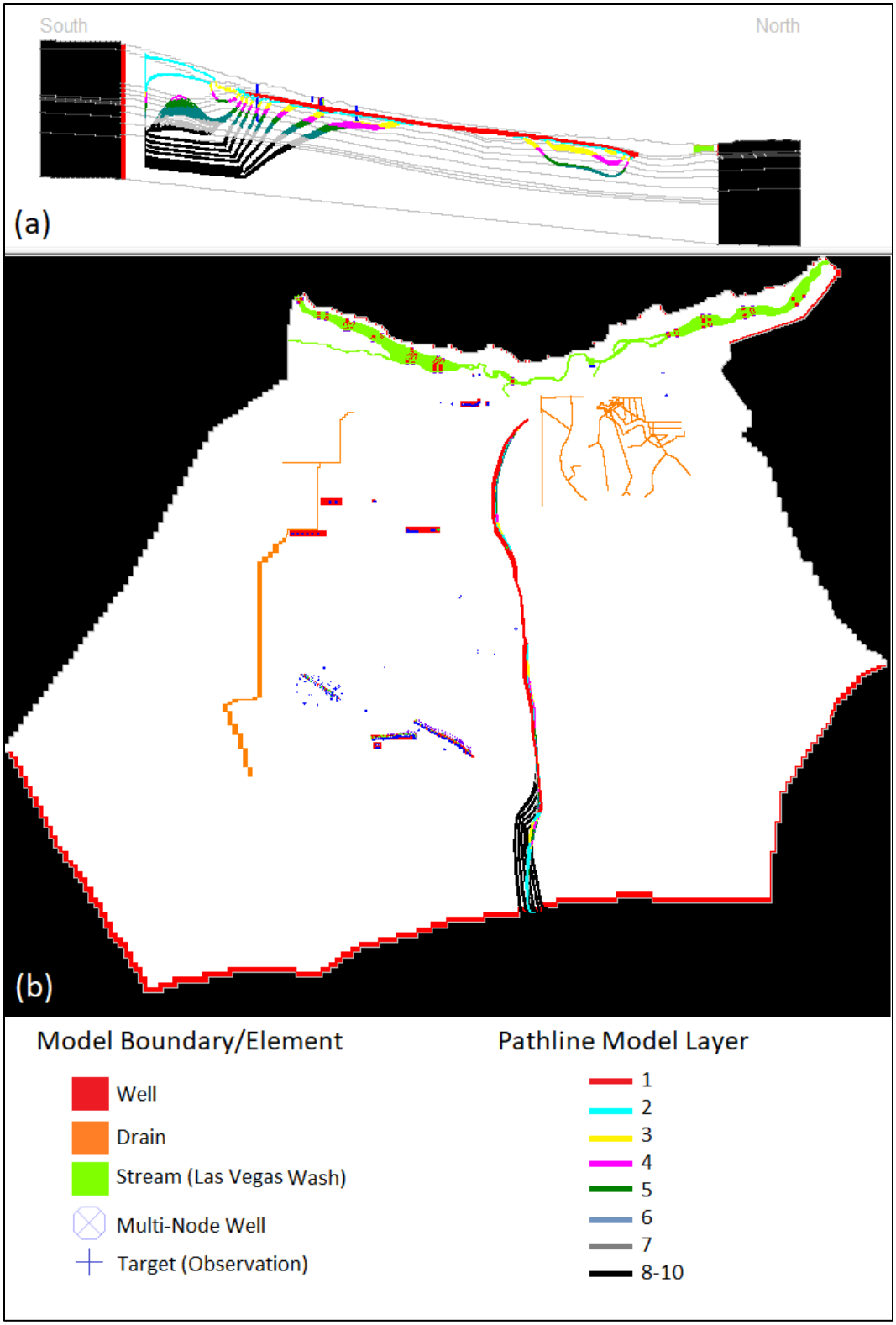

Figure 30. Backward tracking results for the baseline simulation well MW-105. Pathlines are color coded by model layer in (a) a cross section along column 148 (north-south center of model) with layers delineated in light gray and (b) an aerial view.

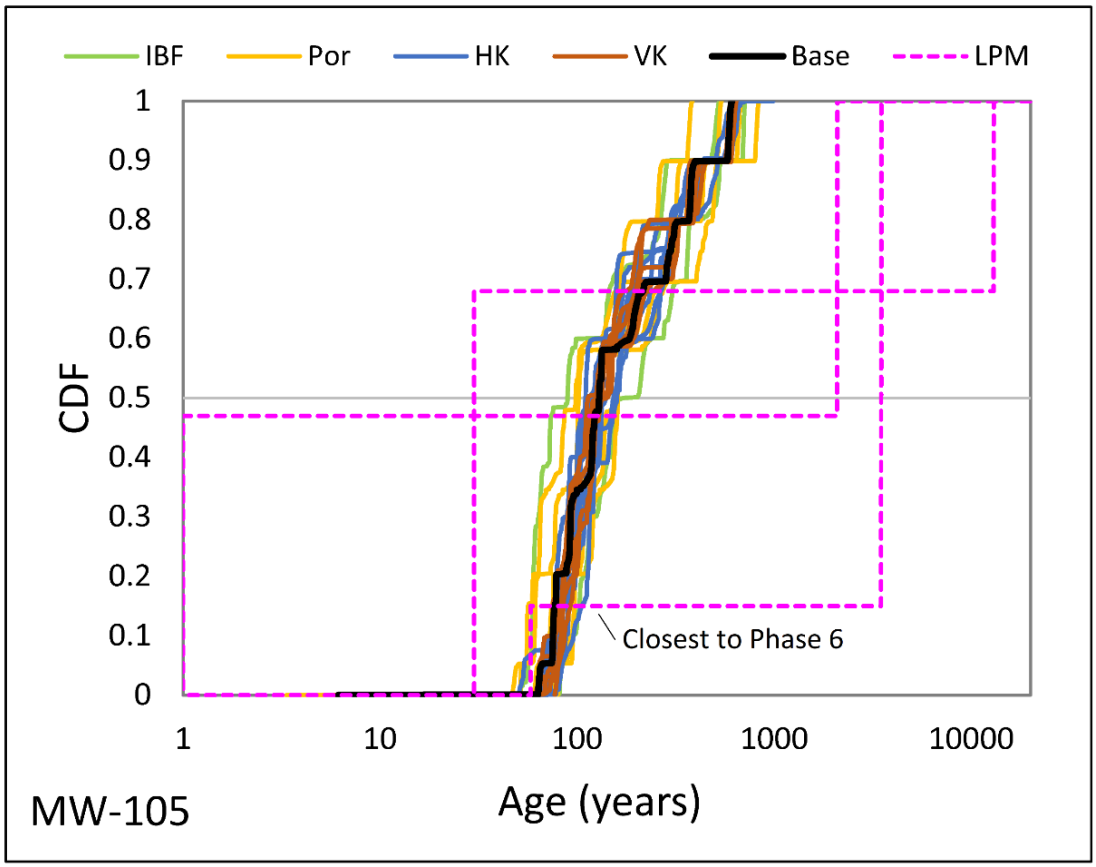

Figure 31. Age distributions for well MW-105 calculated for the sensitivity analysis using the Phase 6 model and multiple binary mixing model LPMs. Phase 6 model results most closely resemble the model with the young water calibrated using ^{3}H.

NERT5.49S1: This well is located in the Las Vegas Wash gravels downgradient from PC-157A/B. Phase 6 model results indicated all the water sourced in this well is derived from the Las Vegas Wash (Figure 32). Flow paths are very fast with a mean of 36 days (sensitivity range from 18 days to 408 years). The older water is obtained in the sensitivity analysis by reducing the horizontal hydraulic conductivity in the paleochannels and wash gravels or increasing the flow across the southern GBF (Figure 33). Both of these changes allow a component of water in the well to be sourced from the southern boundary to produce a "heavy tail" in the age distribution that is not simulated with the baseline Phase 6 model. The median age for this well is 29 days (sensitivity range from 15 to 44 days) and the fraction of water <70 years with the sensitivity analysis ranging from 82 to 100 percent. Observed tracers suggest ages are primarily modern although EMMs and DMs based on the CFCs suggest the possibility of median ages on the order of several hundred years. As a result, the fraction of water <70 years for LPMs ranges from 11 to 100 percent. Given large uncertainty in the LPMs and the position of the well in the Wash gravels, it is likely the well water is all modern and the Phase 6 model is reasonable.

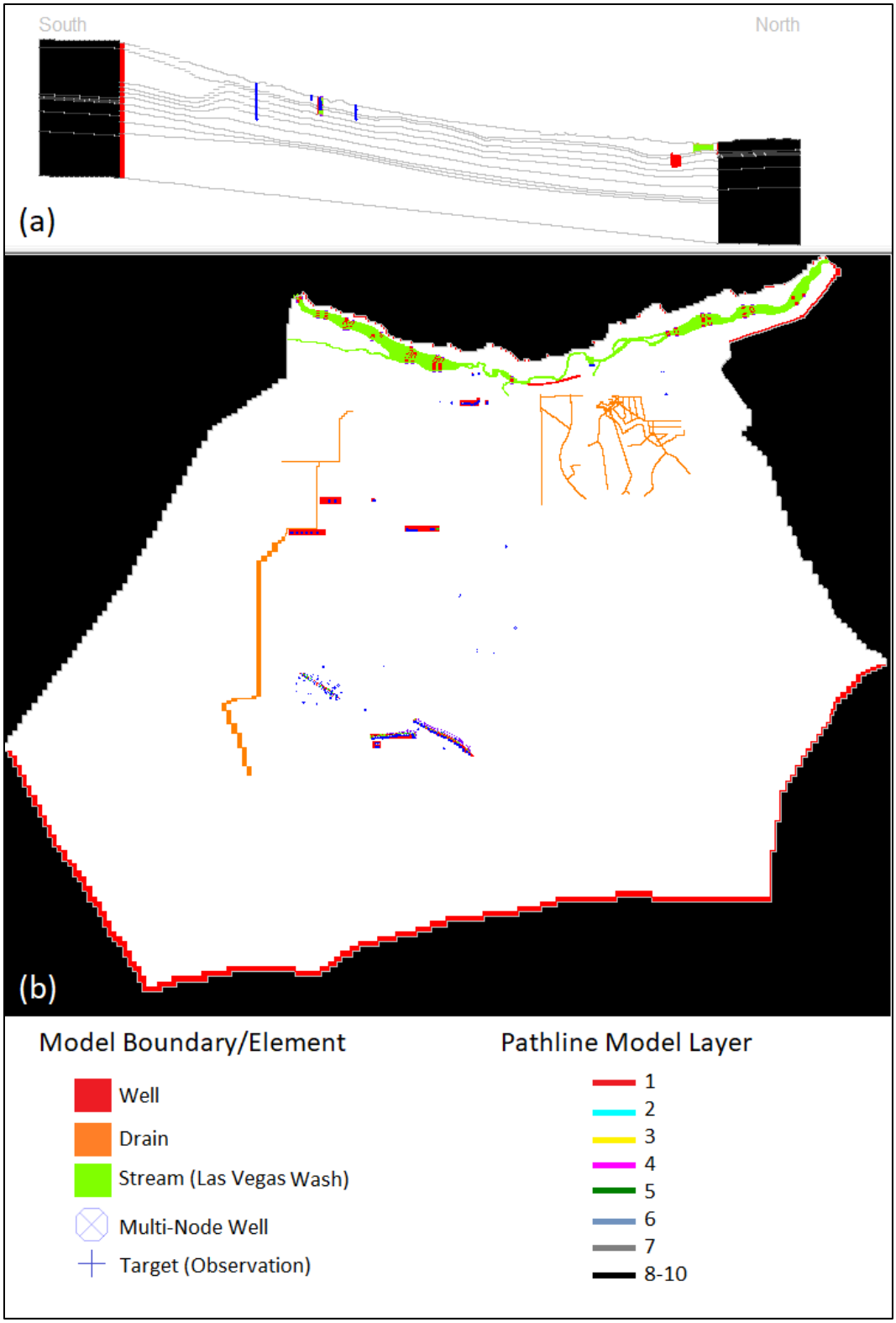

Figure 32. Backward tracking results for the baseline simulation well NERT5.49S1. Pathlines are color coded by model layer in (a) a cross section along column 148 (north-south center of model) with layers delineated in light gray and (b) an aerial view.

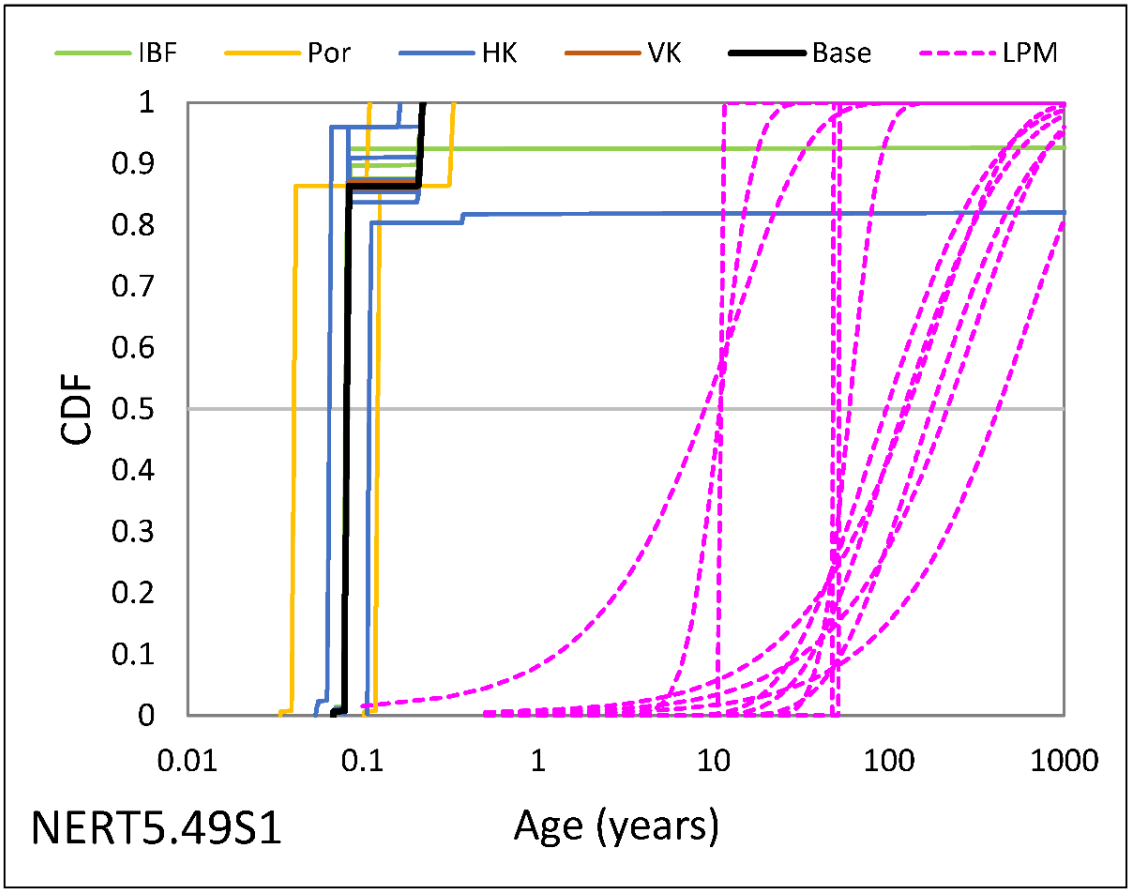

Figure 33. Age distributions for well NERT5.49S1 calculated for the sensitivity analysis using the Phase 6 model and all significant LPM (see Table 9).

MW-201A: This well is located downgradient from well NERT5.49S1 and is situated in the Las Vegas Wash gravels. Similar to NET5.49S1, this well also receives all its water from surface water loss from the Las Vegas Wash (Figure 34) but the range in its estimates from the sensitivity analysis do not shift a portion of flow paths from the southern boundary and remain much younger (Figure 35). Specifically, the mean age and the median age are the same, with baseline equal to 42 days (sensitivity range from 21 to 63 days). Mean and median age ranges for LPMs are much larger (range 19 to 84 years) with the fraction of water <70 years ranging from 62 to 100 percent. Similar to well NERT5.49S1, the large uncertainty in the LPMs and the position of the well in the Wash gravels, it is likely the well water is all modern and the Phase 6 model is reasonable.

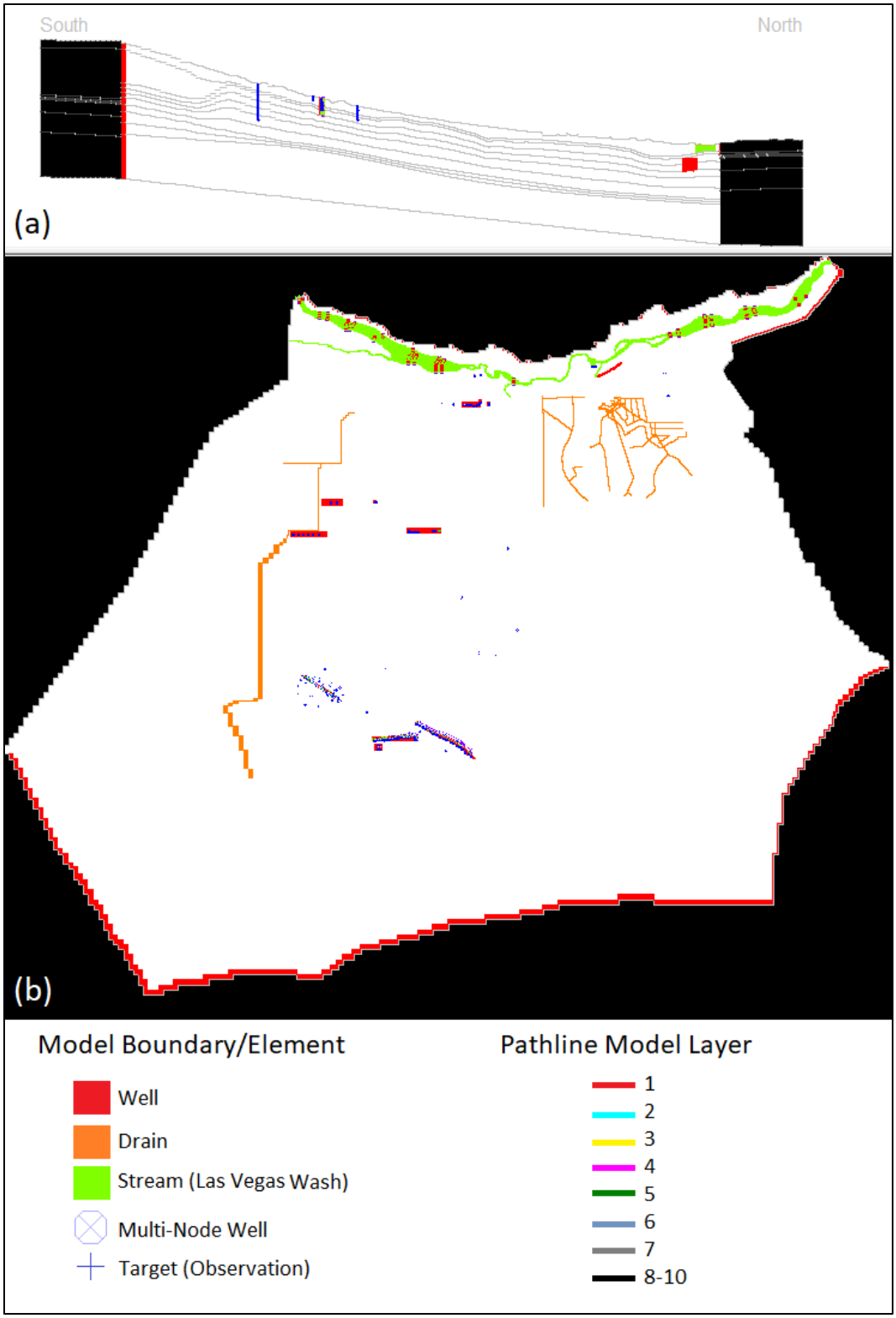

Figure 34. Backward tracking results for the baseline simulation well MW-201A. Pathlines are color coded by model layer in (a) a cross section along column 148 (north-south center of model) with layers delineated in light gray and (b) an aerial view.

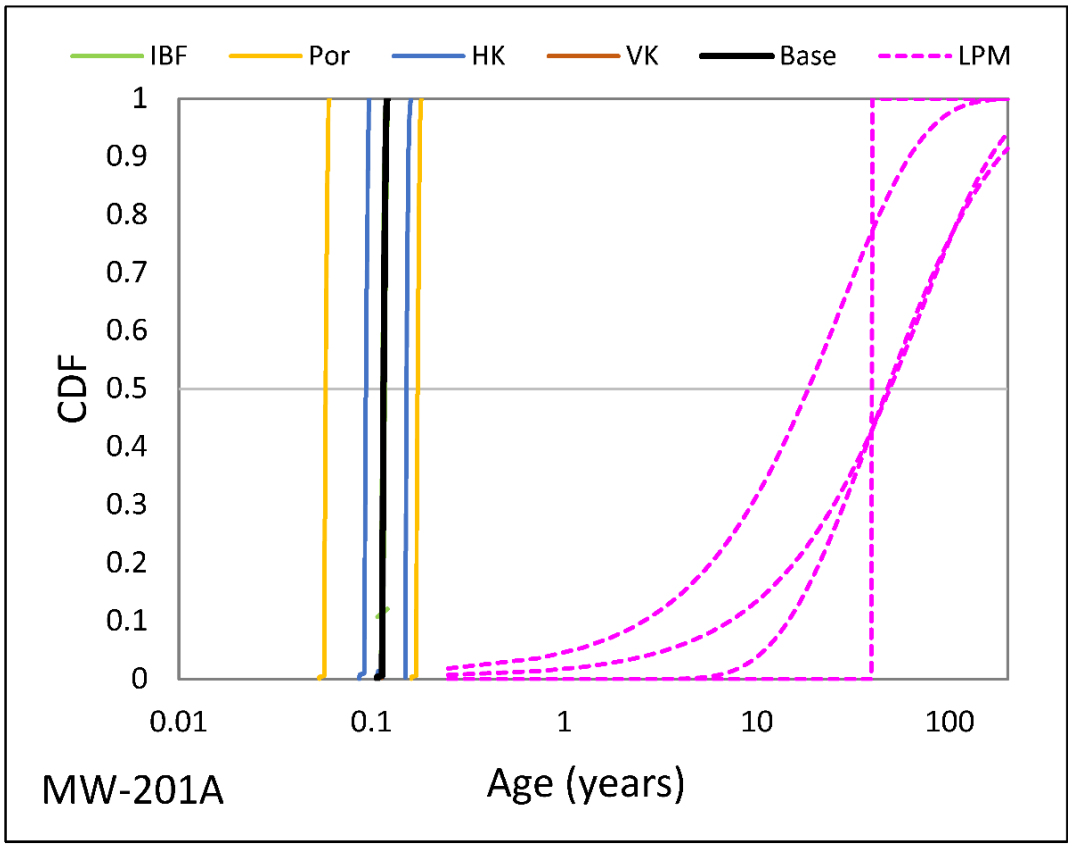

Figure 35. Age distributions for well MW-201A calculated for the sensitivity analysis using the Phase 6 model and significant LPMs (see Table 12).

NERT4.93S1: This well is located in the Las Vegas Wash gravels downgradient from MW-201A. The Phase 6 model estimates water in this well is solely sourced from the southern boundary with particles originating across depth (Figure 36). Flow at depth moves upward at the northern terminus of its flow path prior to entering the well located in the alluvium. Subsequently, the age distribution contains older water with a mean age of 837 years (sensitivity range from 529 to 1,145 years) and a median of 857 years (sensitivity range from 551 to 1,174 years) (Figure 37). Very little modern water was simulated in this well at 0.4 percent (sensitivity range is 0 to 1 percent). In contrast, the single significant PFM suggests that the mean (and median) age is 24 years. No version of the Phase 6 model can replicate the observed tracer information because of an over reliance on simulated deep flow paths originating along the southern GBF that are not supported because of the lack of old water in the well (^{14}C >80 pmC).

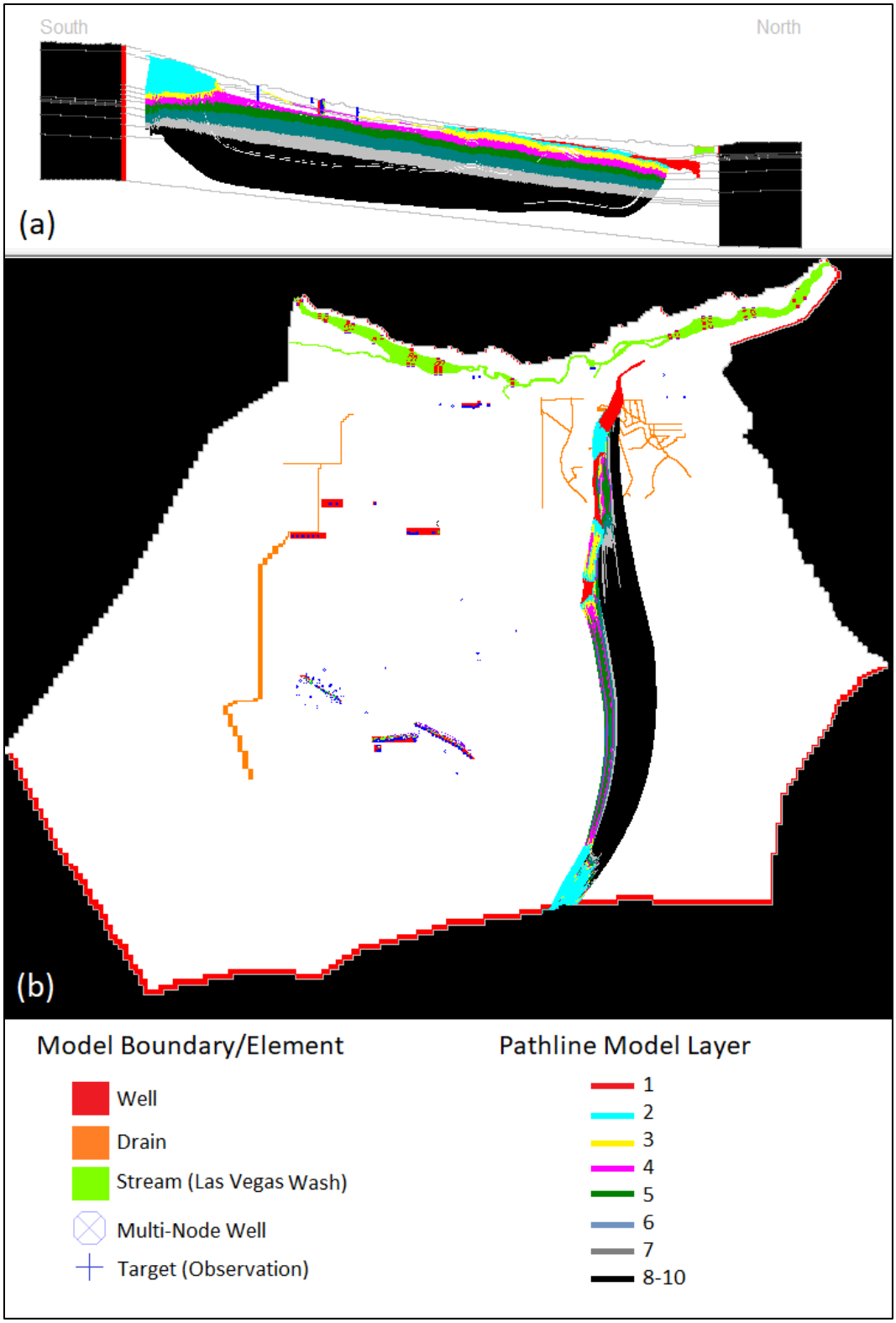

Figure 36. Backward tracking results for the baseline simulation well NERT4.93S1. Pathlines are color coded by model layer in (a) a cross section along column 148 (north-south center of model) with layers delineated in light gray and (b) an aerial view.

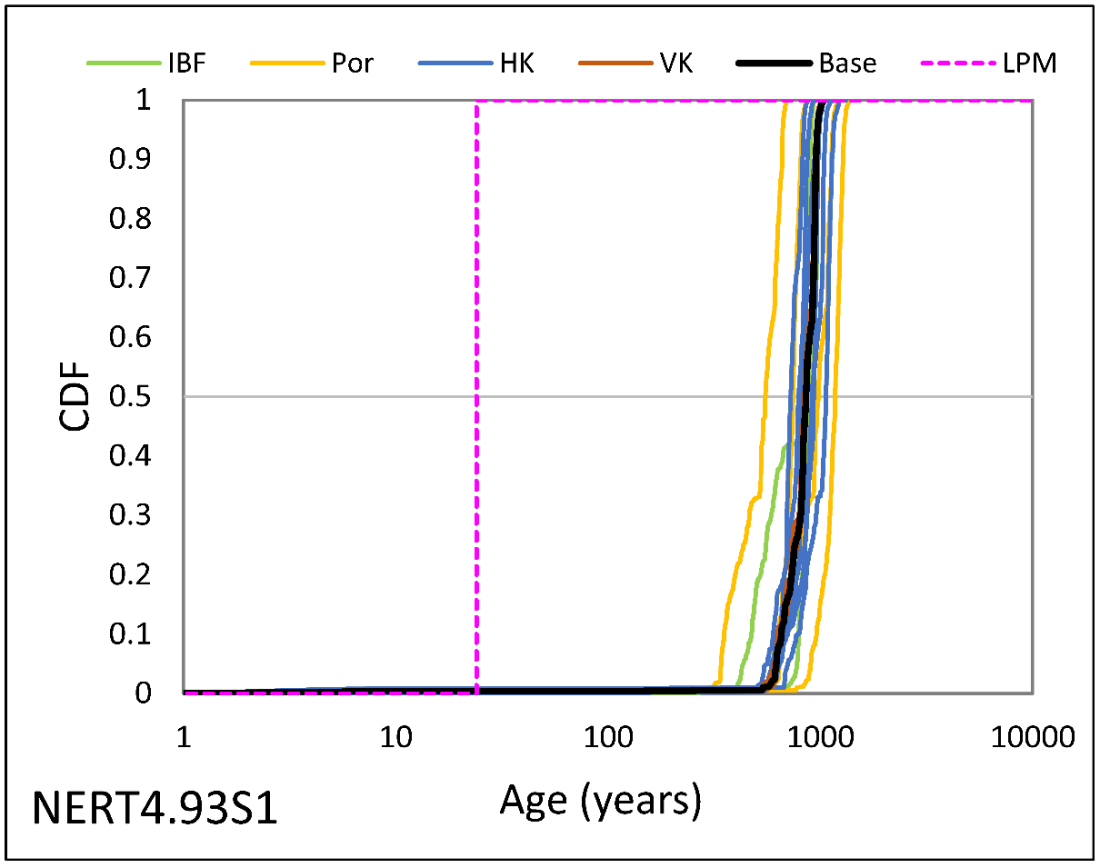

Figure 37. Age distributions for well NERT4.93S1 calculated for the sensitivity analysis using the Phase 6 model and a single significant LPM defined as a PFM calibrated using SF_6 with a mean age of 24 years.

MW-224A: This well is located a small distance from the Las Vegas Wash and does not reside in the gravels but in the alluvium proper. Similar to NERT4.93S1, it is simulated with the Phase 6 model to receive all its water from the southern boundary (Figure 38). Flow paths originate in the shallower layer 2 and subsequently dive into layer 10, the bottom-most layer. At the northern edge of its flow path, all flow moves toward the surface and into the well. Flow paths are homogenous to produce relative uniformity in age distributions (Figure 39). Mean and median ages are nearly equivalent at 1,019 years (sensitivity range from 759 to 1,280 years) and no modern water is simulated in this well. Two BMMs are found significant, but the model with the mean young age calibrated to ^{3}H is assumed most representative at 58 years and 15 percent modern water. The Phase 6 model cannot replicate this young water because it does not simulate any surface recharge entering the well.

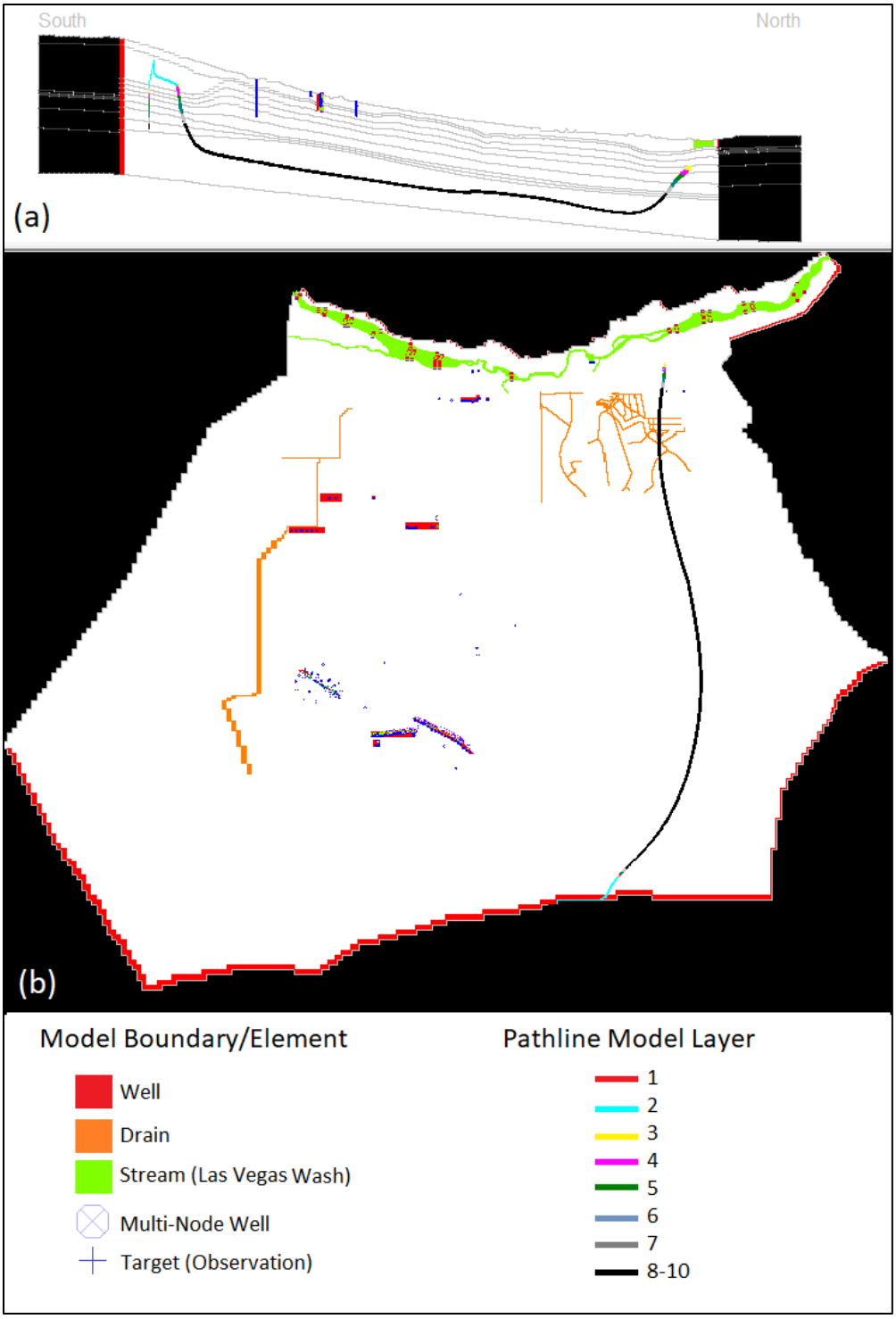

Figure 38. Backward tracking results for the baseline simulation well MW-224A. Pathlines are color coded by model layer in (a) a cross section along column 148 (north-south center of model) with layers delineated in light gray, and (b) an aerial view.

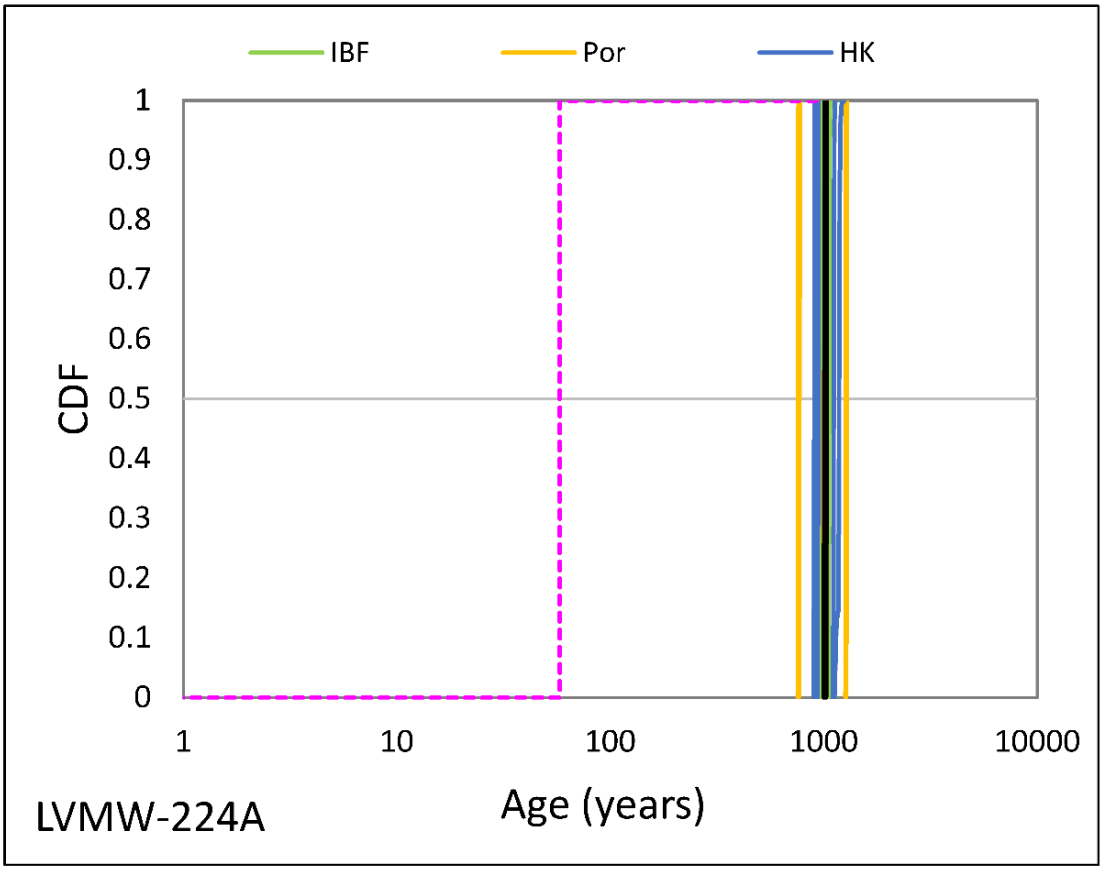

Figure 39. Age distributions for well MW-224A calculated for the sensitivity analysis using the Phase 6 model and a single significant LPM defined as a PFM calibrated using ^{3}H with a mean age of 58 years.

NERT4.71S1: This well is in the Wash gravels downgradient of NERT4.93S1 and MW-224A. Similar to both these wells, NERT4.71S is simulated by the Phase 6 model to receive all its water from the southern boundary flux (Figure 40). The age distribution contains a mean of 933 years (sensitivity range from 635 to 1,230 years) and a median of 989 years (sensitivity range from 623 to 1,289 years) (Figure 41). No modern water is simulated. In contrast, observed tracer data indicate no water >1,000 years flows to the well because ^{14}C is >80 pmC. Only a PFM using ^{3}H can produce a significant LPM with a mean of 63 years. No model variation tested can replicate the observed modern water and lack of older water.

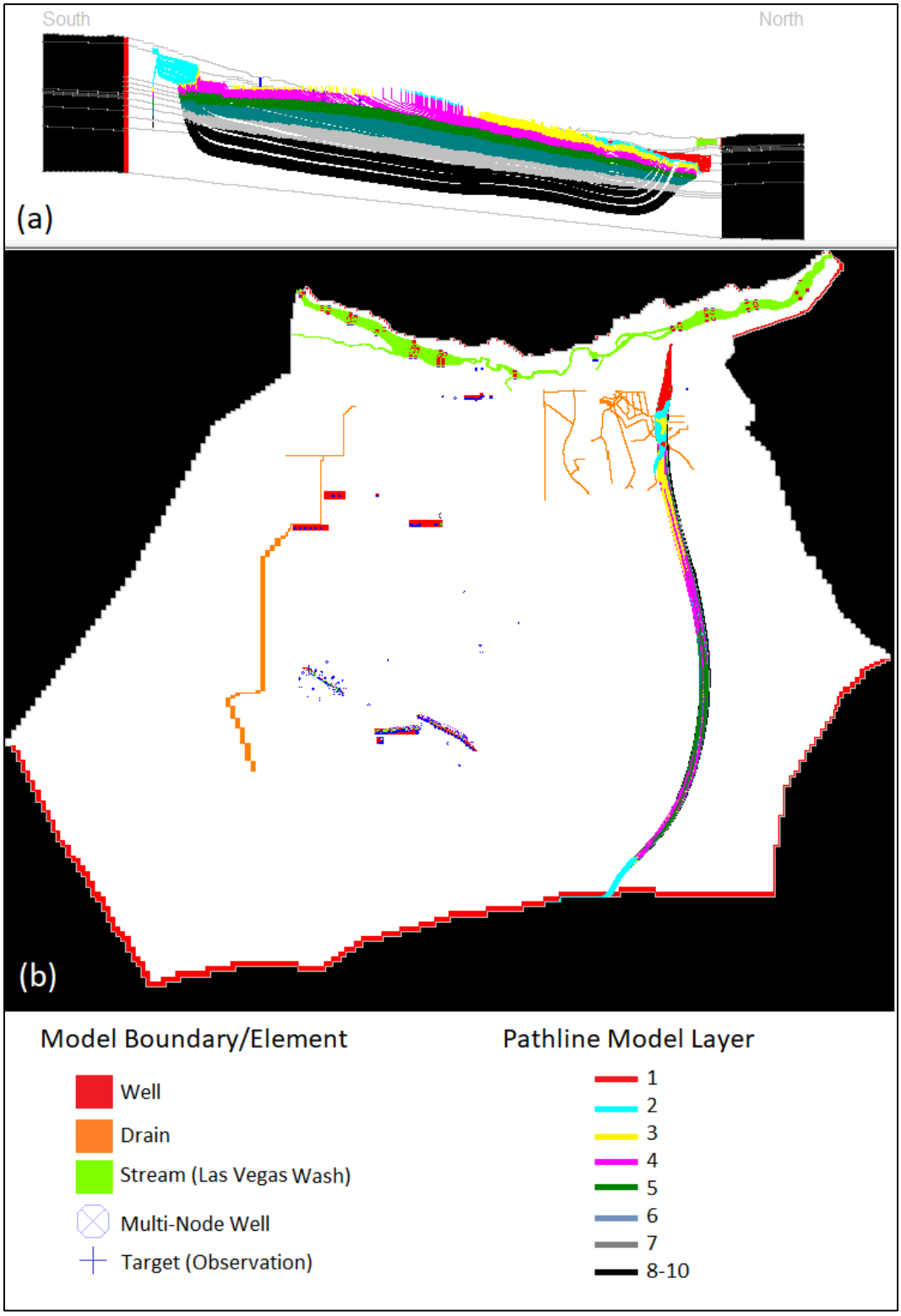

Figure 40. Backward tracking results for the baseline simulation well NERT4.71S1. Pathlines are color coded by model layer in (a) a cross section along column 148 (north-south center of model) with layers delineated in light gray and (b) an aerial view.

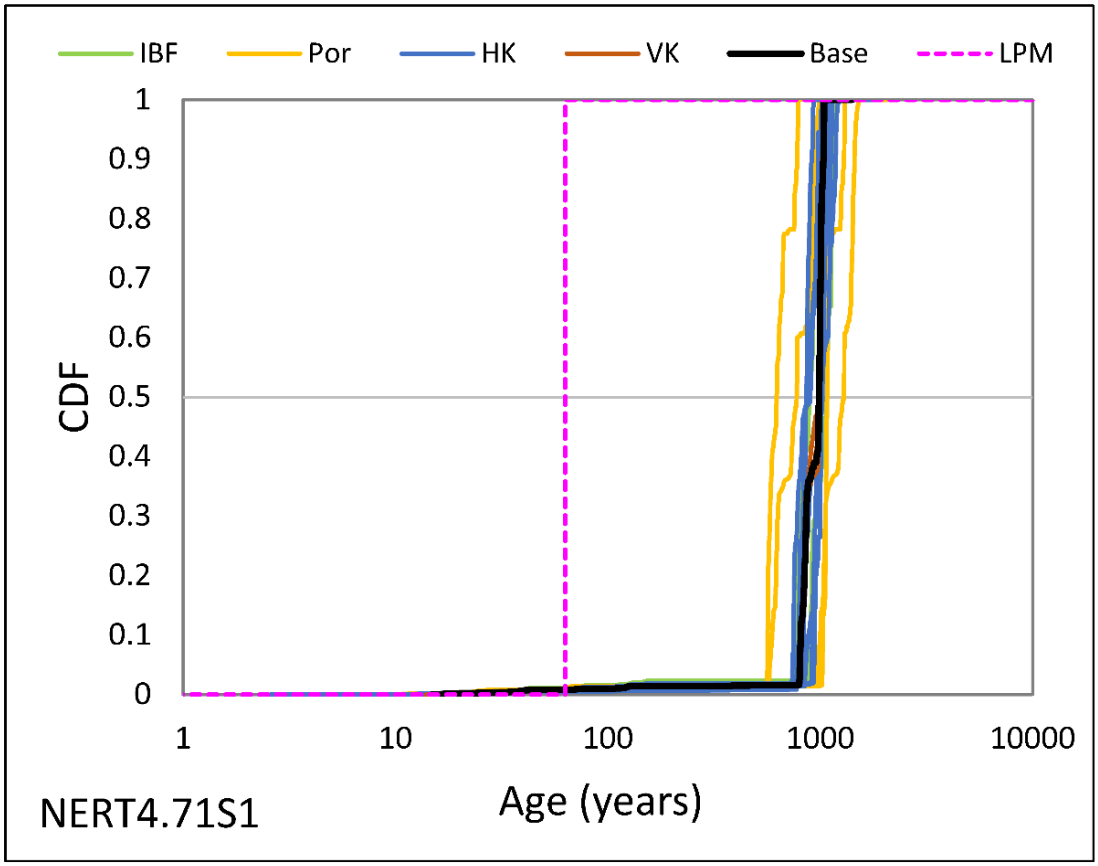

Figure 41. Age distributions for well NERT4.71S1 calculated for the sensitivity analysis using the Phase 6 model and a single significant LPM defined as a PFM calibrated using ^{3}H with a mean age of 63 years.

MW-25: This well represents the furthest eastern flow paths in the model. It is not in the Wash gravels but in the alluvium butted up against the lower permeable Horse Springs unit. All simulated groundwater flow to this well originates from the southern boundary flux (Figure 42). The water moves vertically into layers 5 to 8 and then as groundwater travels further north it moves upward into layer 1 prior to discharging into the well. The age distribution simulated for this well produces a mean age of 1,262 years (sensitivity range from 846 to 3,970 years) and a median age of 1,248 years (sensitivity range from 799 to 1,697 years) (Figure 43). No modern water is simulated, and no parameter adjustments can produce water in the well <70 years. Tritium exists in this well and is used to calibrate the mean age of the young fraction in the LPM. The amount of young water in the well is estimated at only one percent. The LPM produces an error of 6.4 percent for ^{3}H, which does not meet the significance level of <5 percent (see Table 16). Therefore, we consider this well uncertain with respect to the existence of modern water and we are unable to determine the accuracy of the Phase 6 model with respect to MW-25.

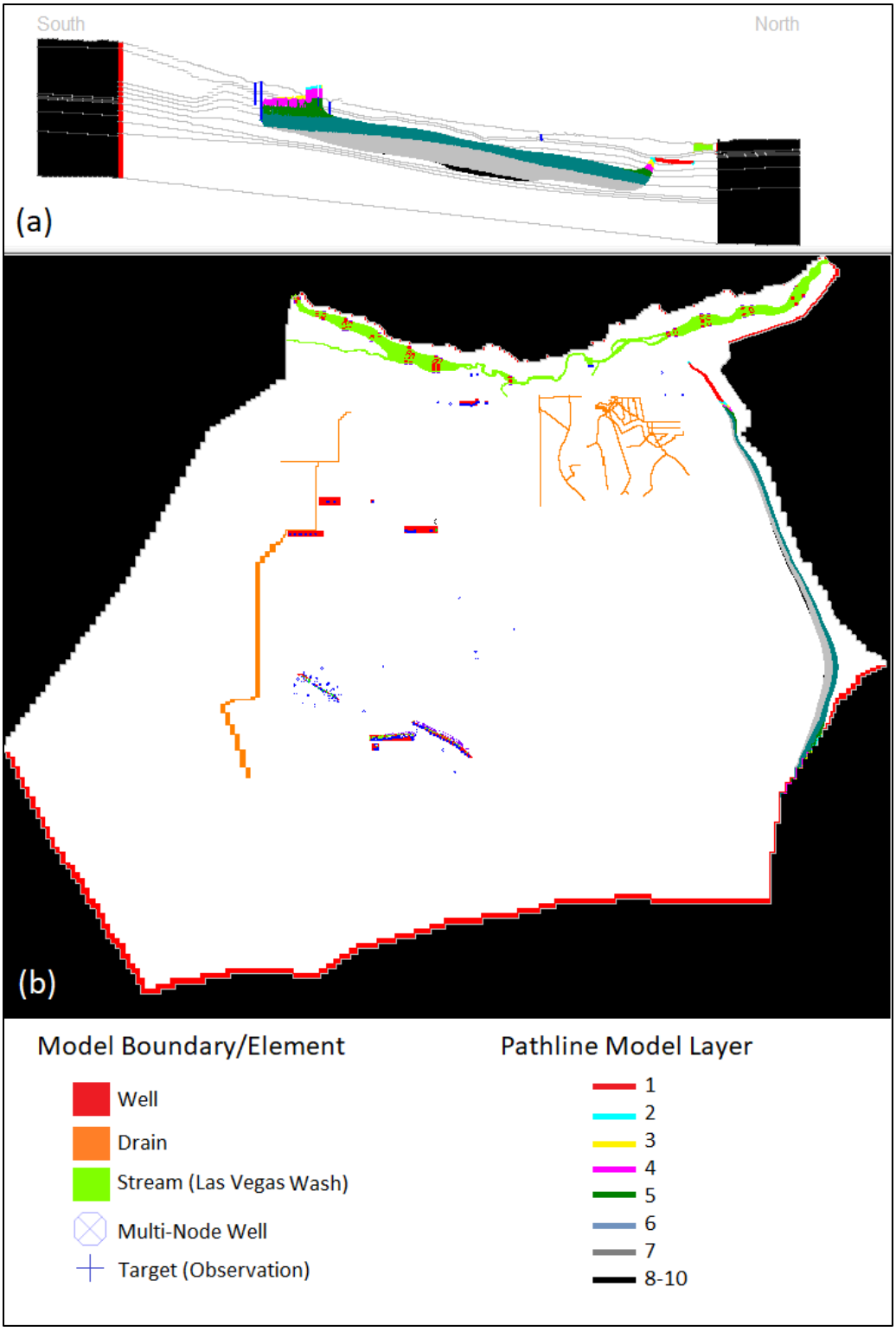

Figure 42. Backward tracking results for the baseline simulation well MW-25. Pathlines are color coded by model layer in (a) a cross section along column 148 (north-south center of model) with layers delineated in light gray and (b) an aerial view. Note that the IBF inputs for this well are further north and appear to be in the center of the model domain based on the location of the cross section.

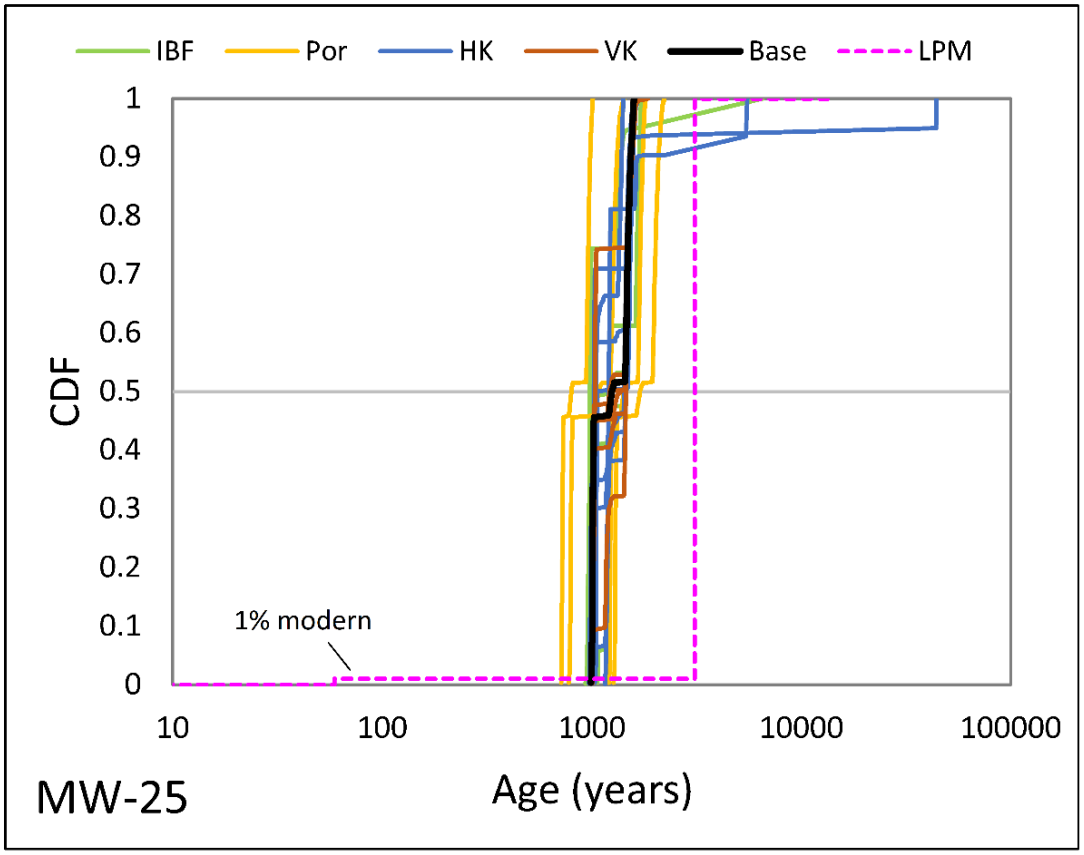

Figure 43. Age distributions for well MW-25 calculated for the sensitivity analysis using the Phase 6 model and a single LPM with the young water mean and fraction of young water calibrated to ^{3}H.

3.4.2 Age Distributions for Wells in the UMCf-cg1,2

Two sampled wells are screened in coarse-grained units of the Upper Muddy Creek. The shallower well (TR-8) pulls from the first unit (cg1) while the deeper well (TR-7) pulls from the second unit (cg2). These wells represent the most proximal wells to the southern boundary flux with an attempt to capture groundwater mixing behavior close to the upgradient boundary flux and to assess the difference in this behavior as a function of a vertical gradient.

TR-8: This relatively shallow well is screened in layer 2 with the screened interval 63 to 93 feet below land surface. Water is simulated by the Phase 6 model to originate from the southern boundary flux as a mix of shallower water (layer 2) and deeper water (layer 9) (Figure 44). The mean age in the well is simulated as 271 years (sensitivity range from 152 to 373 years) and the median age is 86 years (sensitivity range from 43 to 216 years) (Figure 45). The fraction of water <70 years is 39 percent (sensitivity range from 17 to 50 percent). Three significant LPMs indicate young fractions of 4, 15, and 35 percent, with the Phase 6 baseline model replicating two of the results (4 and 35 percent). The LPM ages that are greater than the Phase 6 model are appropriate for flow originating at boundary faces to allow for age accrual prior to entering the model domain.

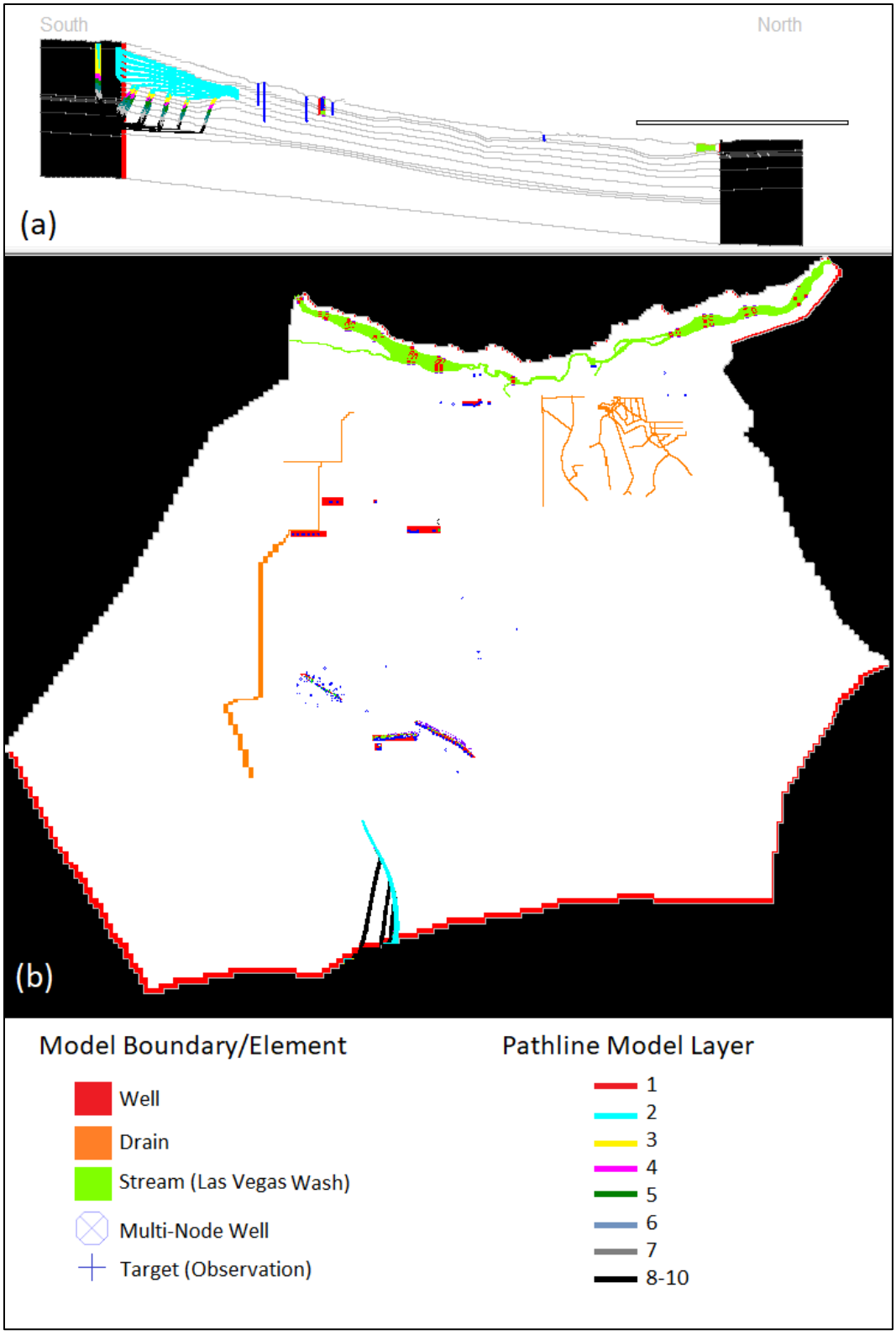

Figure 44. Backward tracking results for the baseline simulation well TR-8. Pathlines are color coded by model layer in (a) a cross section along column 148 (north-south center of model) with layers delineated in light gray and (b) an aerial view.

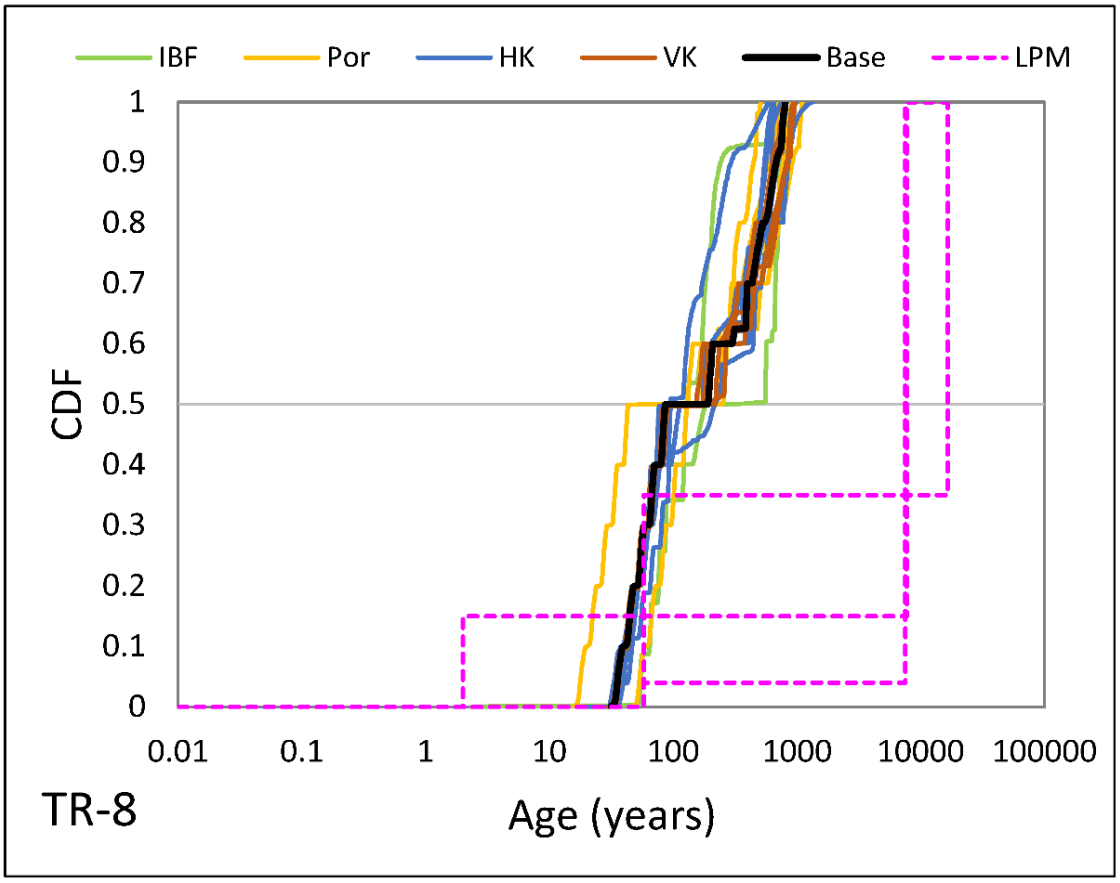

Figure 45. Age distributions for well TR-8 calculated for the sensitivity analysis using the Phase 6 model and significant LPMs (see Table 18).

TR-7: This well is screened 260 to 290 feet below the ground surface. It is modeled in layer 10 and represents the deepest well sampled for age tracers. The Phase 6 model estimates all water in this well is sourced from layer 10 along the southern boundary flux (Figure 46). Mean age is estimated at 383 years (sensitivity range from 206 to 561 years) and a median equal to 283 years (sensitivity range from 156 to 412 years) (Figure 47). No young water is simulated in this well. No tritium was observed, but an LPM calibrated to CFC-12 suggests the possibility of 12 percent modern water with a mean age of 16 years. CFCs are detectable at lower concentrations than ^{3}H and can be considered a more sensitive indicator of modern water. However, contamination of groundwater samples can potentially limit CFC dating. For example, organic contaminants may contain small amounts of CFCs that effect samples on the order of parts per trillion. These impacts can be significant for industrial areas (Solomon et al. 1998; Hinkle and Snyder 1997; https://wwwrcamnl.wr.usgs.gov/isoig/period/cfc_iig.html). Since contamination is anthropogenic, one might consider it still modern. A possible exception might be if hydrocarbons were introduced during the drilling process. It is also possible contamination occurred during sampling through the tubing or inadequately flushed sample bottles. Therefore, we are uncertain about the existence of young water in TR-7, especially given that

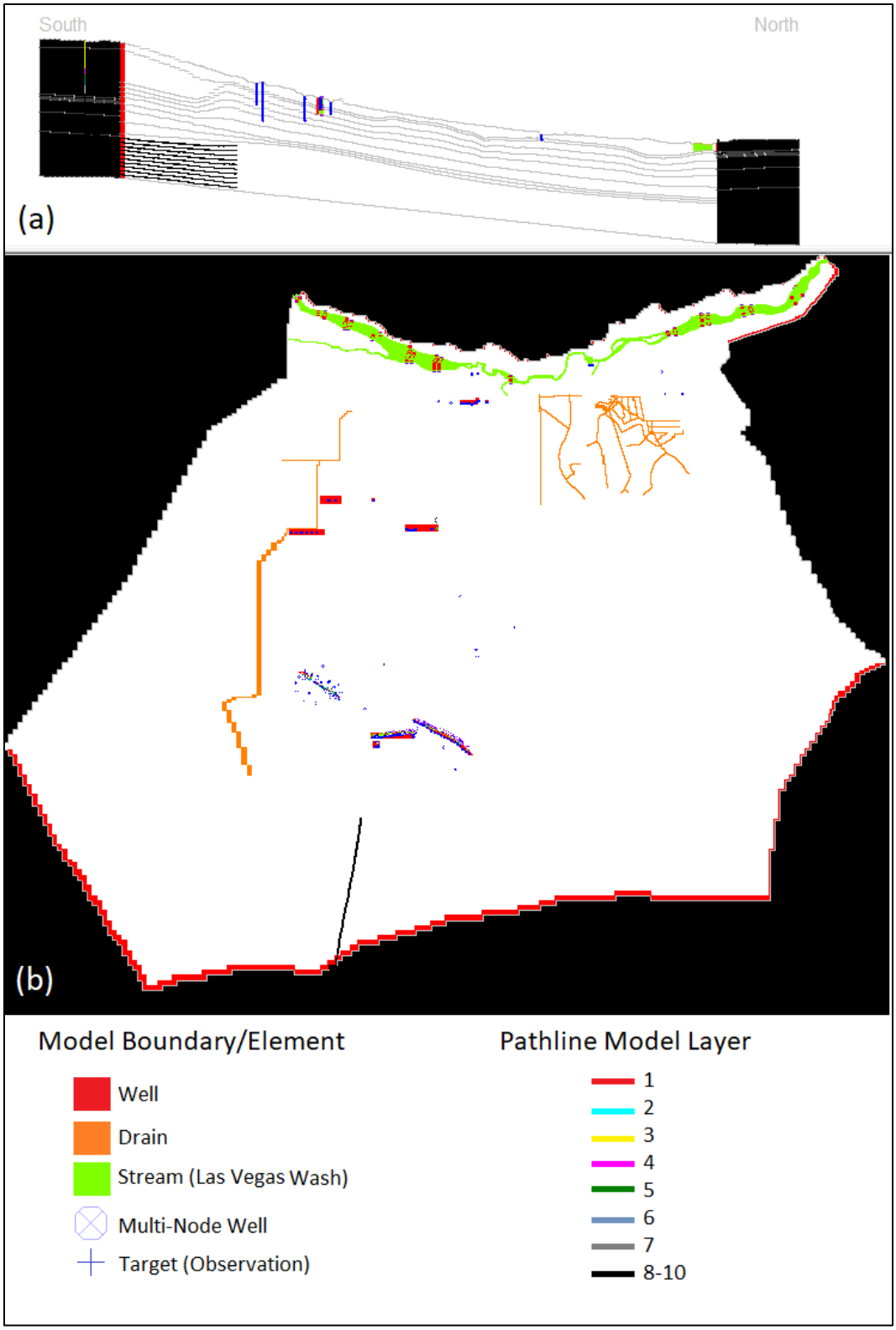

Figure 46. Backward tracking results for the baseline simulation well TR-7. Pathlines are color coded by model layer in (a) a cross section along column 148 (north-south center of model) with layers delineated in light gray and (b) an aerial view.

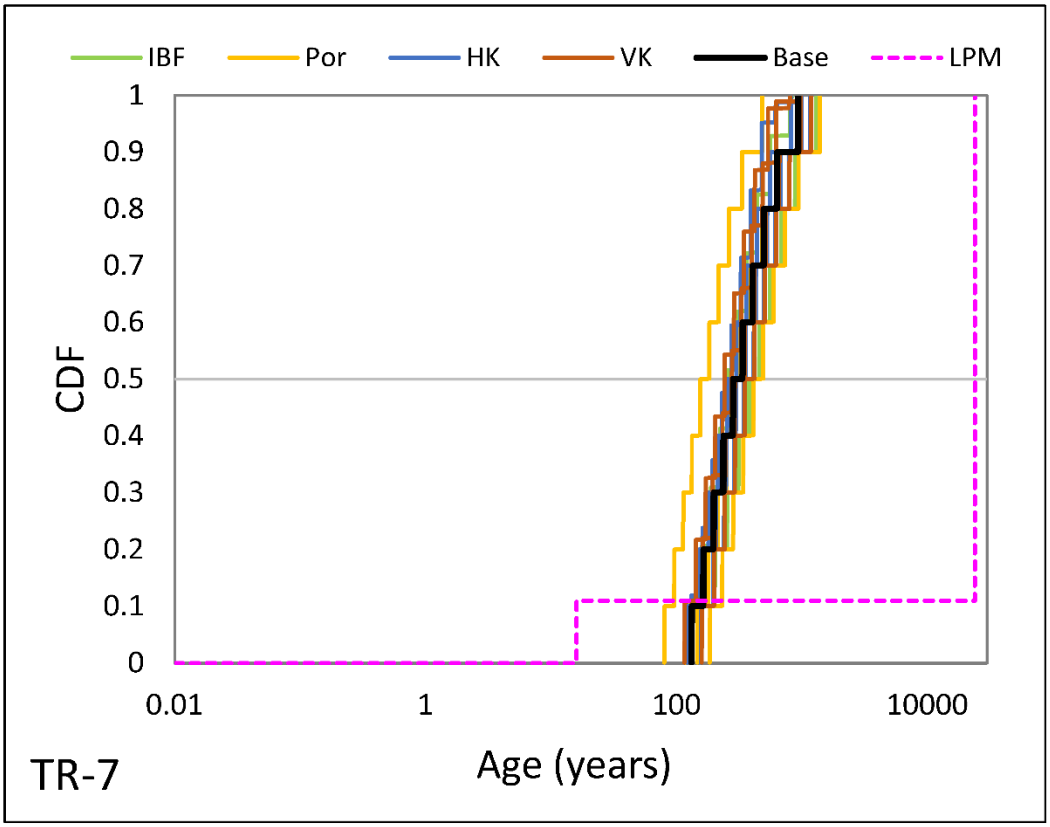

Figure 47. Age distributions for well TR-7 calculated for the sensitivity analysis using the Phase 6 model and a single significant LPM calibrated using CFC-12 with an 11 percent young fraction. No ^{3}H was observed in this well nor any perchlorate to suggest no modern water despite observations of SF_6 and CFCs.

this well, this is screened at considerable depth and there is no observed perchlorate contamination (an additional indicator there is a lack of modern water). If no modern water exists in the well, then Phase 6 conceptual model for groundwater mixing in TR-7 is appropriate.

3.4.3 Age Distributions for Wells in the UMCf-fg

Five sampled wells are screened in the fine-grained units of the Upper Muddy Creek and are described in detail below.

M-31A: This well is located in OU-1 just to the northeast of TR-7 and TR-8. It is screened between 35 and 55 feet below ground level and situated in layer 2 in the fine-grained unit of the Upper Muddy Creek Formation. The Phase 6 model estimates well water is sourced from the southern GBF, with shallower inputs (layer 2) responsible for younger ages and deeper flow rising vertically into layer 2 prior to entering the well (Figure 48). The simulated mean age is 340 years (sensitivity range from 234 to 1,493 years) and the median age is 176 years (sensitivity range from 113 to 678 years) (Figure 49). The fraction of water <70 years is low at 3.2 percent (sensitivity range from 0 to 9 percent). The LPM using a

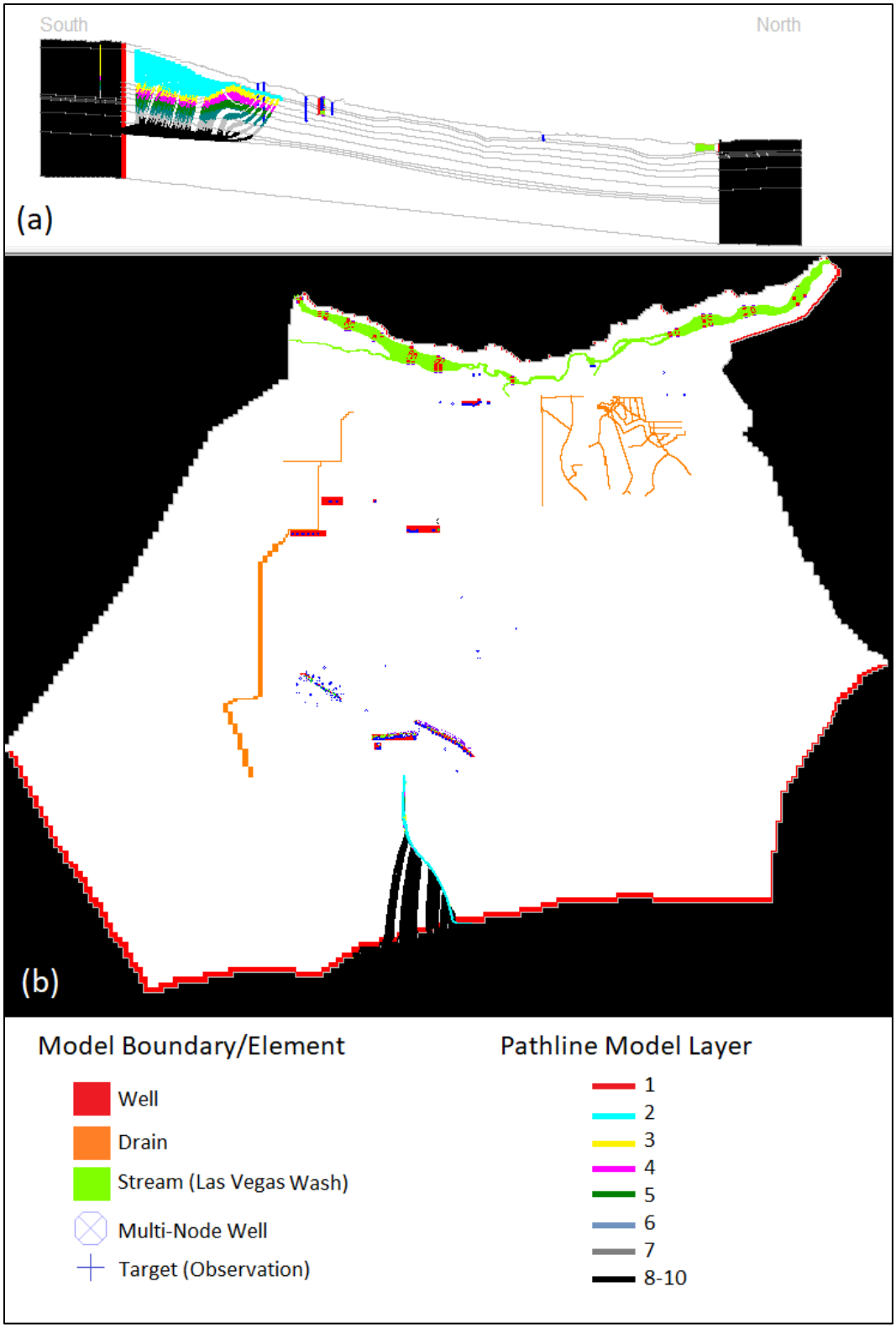

Figure 48. Backward tracking results for the baseline simulation well M-31A. Pathlines are color coded by model layer in (a) a cross section along column 148 (north-south center of model) with layers delineated in light gray and (b) an aerial view.

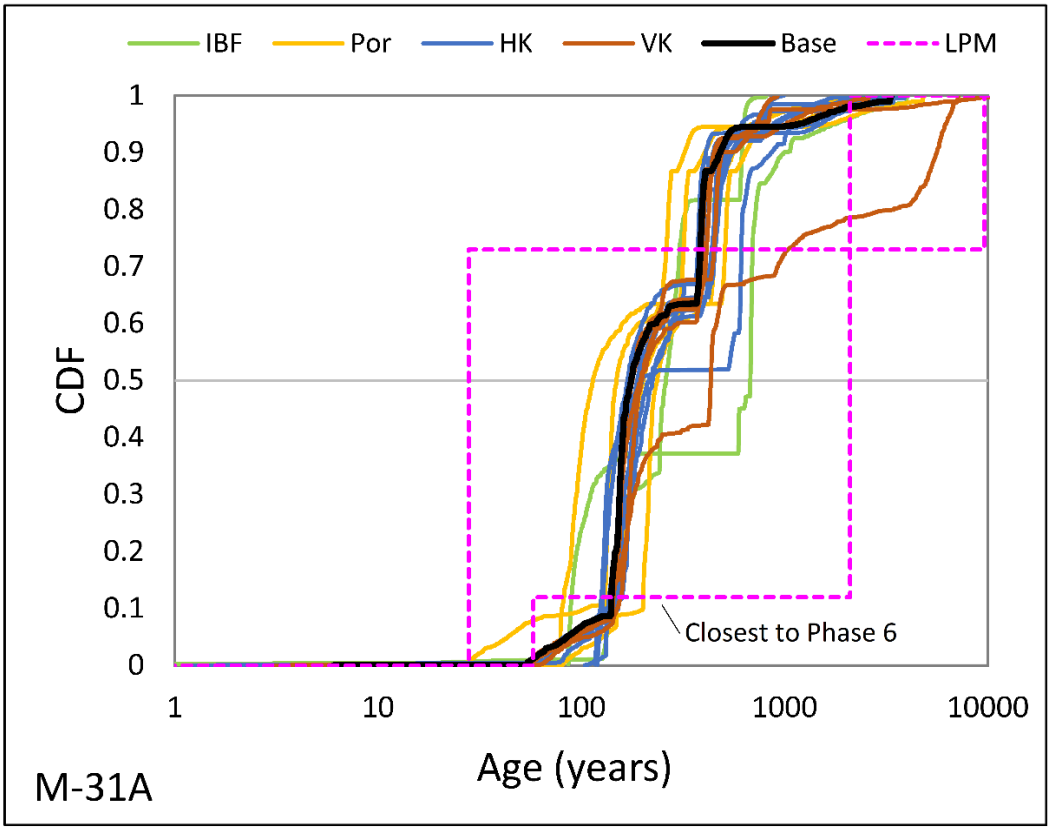

Figure 49. Age distributions for well M-31A calculated for the sensitivity analysis using the Phase 6 model. The LPM most closely representing the Phase 6 model was calibrated using ^{3}H.

binary distribution indicates modern water is between 12 to 73 percent. To increase the young water fraction in order to replicate the LPM young fraction of 12 percent requires increasing the southern boundary flux and/or decreasing the porosity in both the fine-grained and coarse-grained UMCf, with sensitivity greatest in the coarse-grained UMCf unit. Lumped parameter model ages older than the Phase 6 estimates for water sourced from an GBF account for age of groundwater gained prior to entering the model domain.

ES-28: This well is located to the east of M-31A in OU-2 (to the north of State Route 582). It is screened 65 to 85 feet below ground level and situated in model layer 3. Simulated flow paths suggest all flow is sourced from depth along the southern GBF (Figure 50). Homogenous flow paths result in similar mean and median ages of 249 years (sensitivity range from 182 to 317 years) (Figure 51). No modern water is estimated to enter the well. Tracer observations suggest the well contains predominantly younger water with the young fraction equal to 85 to 100 percent of the well volume and this is supported by uncorrected ^{14}C of > 80 pmC. Tracer observations suggest surface recharge is an important source to this well but is not simulated by the Phase 6 model. The ponds in eastern OU-2 held effluent water from the manufacturers located in OU-1 and contributed significant recharge to the shallow aquifers but the Phase 6 model doesn't include it because the ponds existed before the simulated period of Phase 6 model. It is suggested modern recharge needs to be considered in eastern OU-2 locations for future modeling efforts of the NERT site.

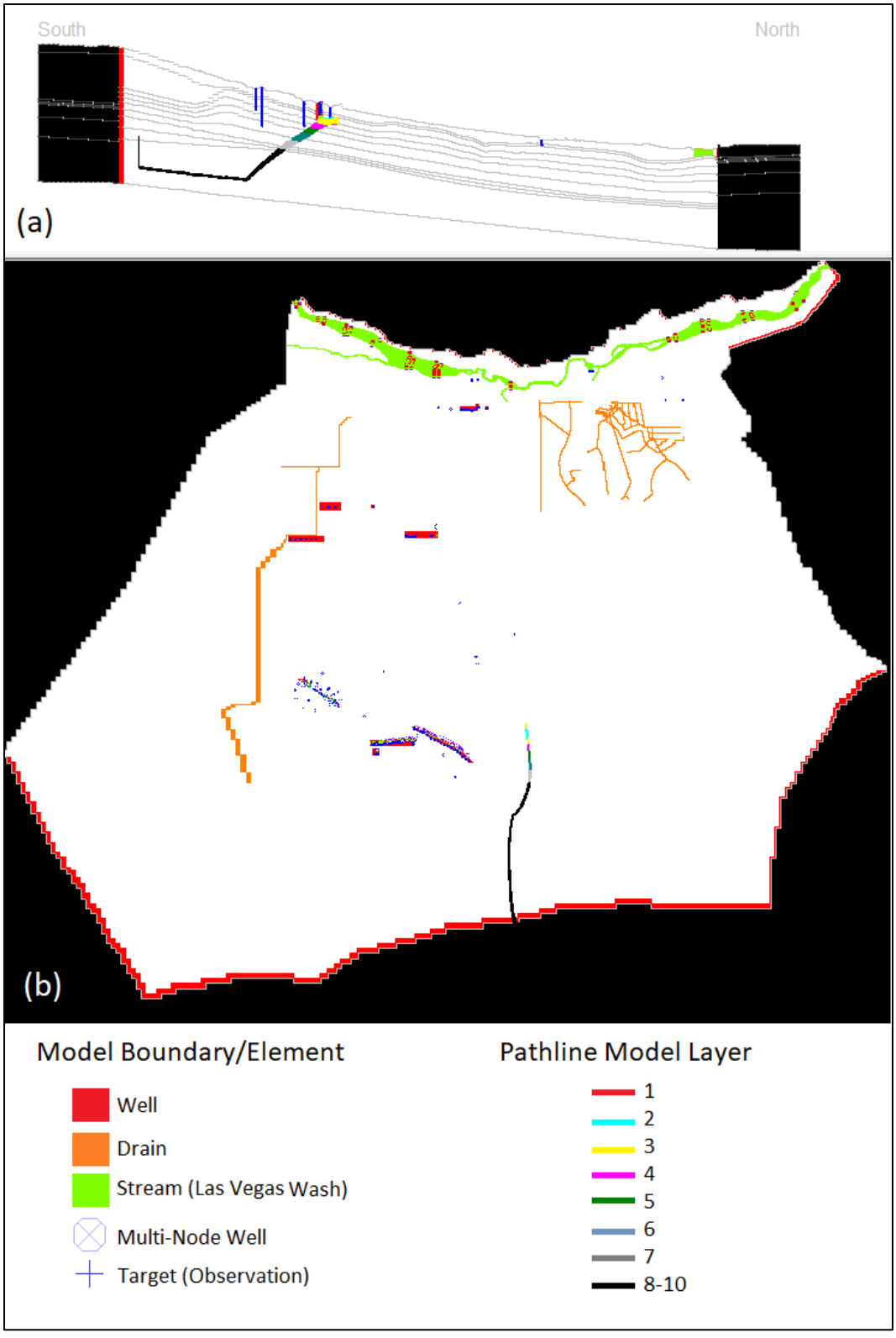

Figure 50. Backward tracking results for the baseline simulation well ES-28. Pathlines are color coded by model layer in (a) a cross section along column 148 (north-south center of model) with layers delineated in light gray and (b) an aerial view.

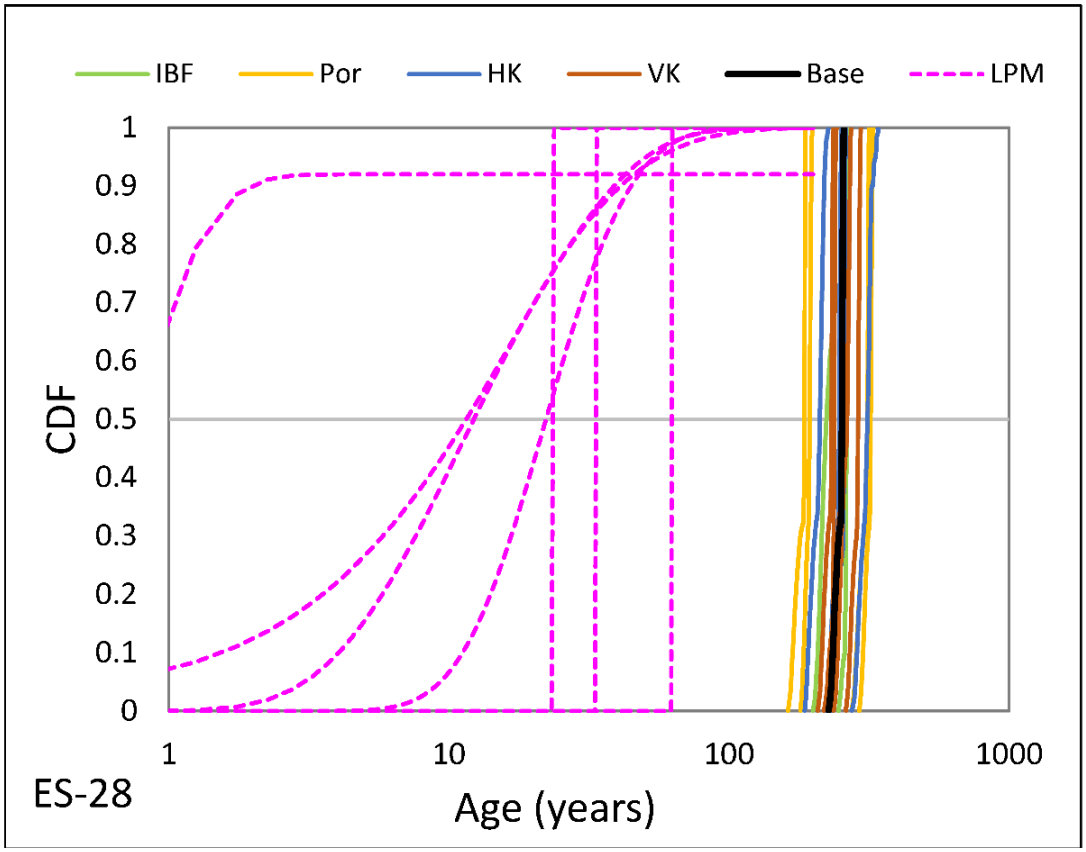

Figure 51. Age distributions for well ES-28 calculated for the sensitivity analysis using the Phase 6 model and significant LPMs calibrated to ^{3}H, SF_6, and CFC-113 (see Table 17).

M-155: This well is located downgradient from M-31A in the northern portion of OU-1. It is situated in model layer 10 with a screened interval between 200 and 220 feet below ground level. Phase 6 simulations indicate all water is sourced from depth along the southern boundary flux (Figure 52). Mean age is 650 years (sensitivity range from 370 to 962 years) and a median of 548 years (sensitivity range from 285 to 810 years) (Figure 53). No modern water is estimated by the Phase 6 model to occur in this deep well. The absence of ^{3}H suggests the Phase 6 model mixing representation is correct. In contrast, very small concentrations of SF_6 and CFCs were observed and hint at a small portion of modern water (LPM estimates are one to two percent) but none of the LPMs could significantly match these tracer observations in combination with the corrected ^{14}C. Given the uncertainty in the existence of modern water because of a lack of ^{3}H and lack of LPM significance, and the depth of this well, it is assumed, similar to TR-7, that no surface recharge has infiltrated into this well. Therefore, the current Phase 6 conceptualization of groundwater sourcing in this well is assumed correct.

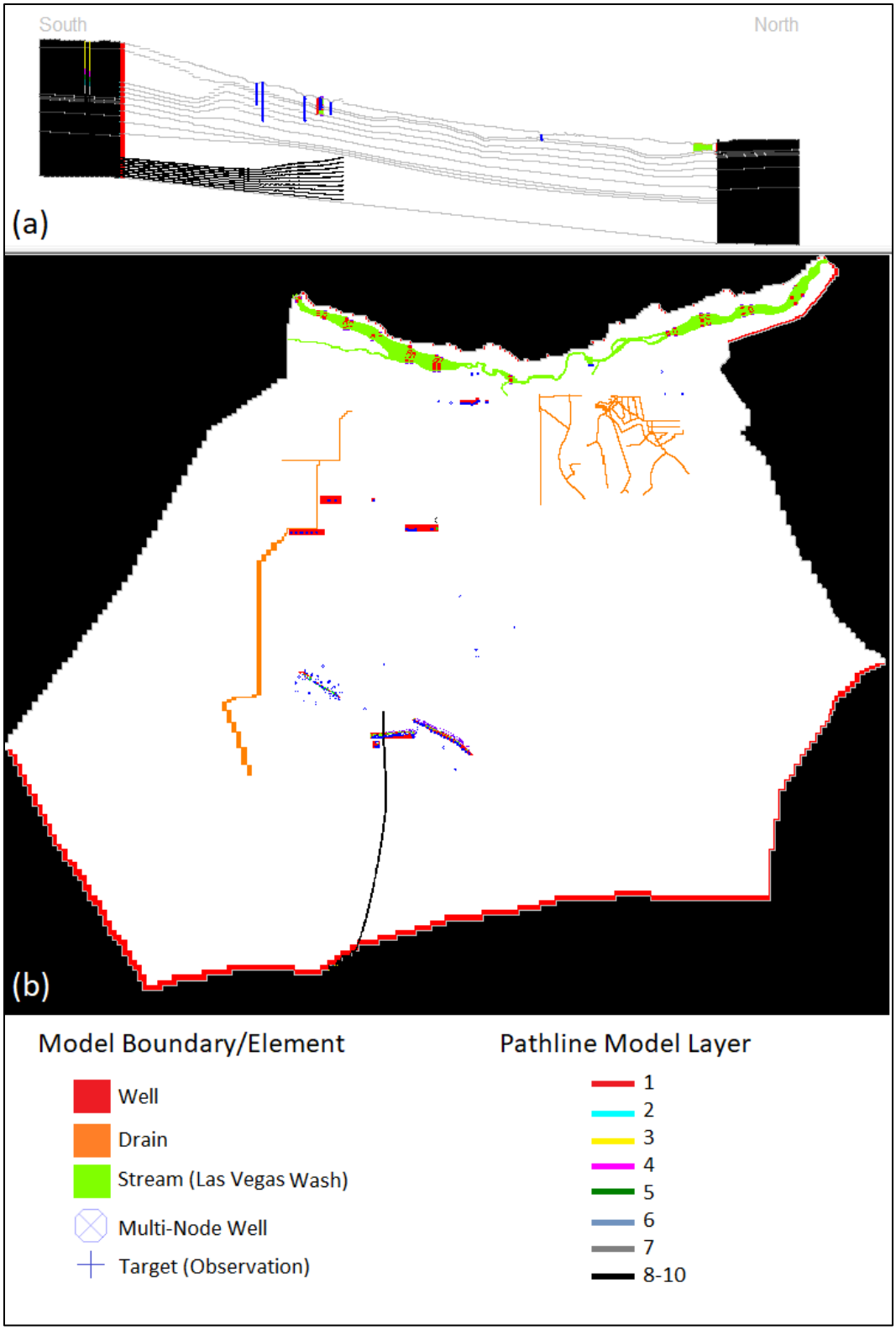

Figure 52. Backward tracking results for the baseline simulation well M-155. Pathlines are color coded by model layer in (a) a cross section along column 148 (north-south center of model) with layers delineated in light gray and (b) an aerial view.

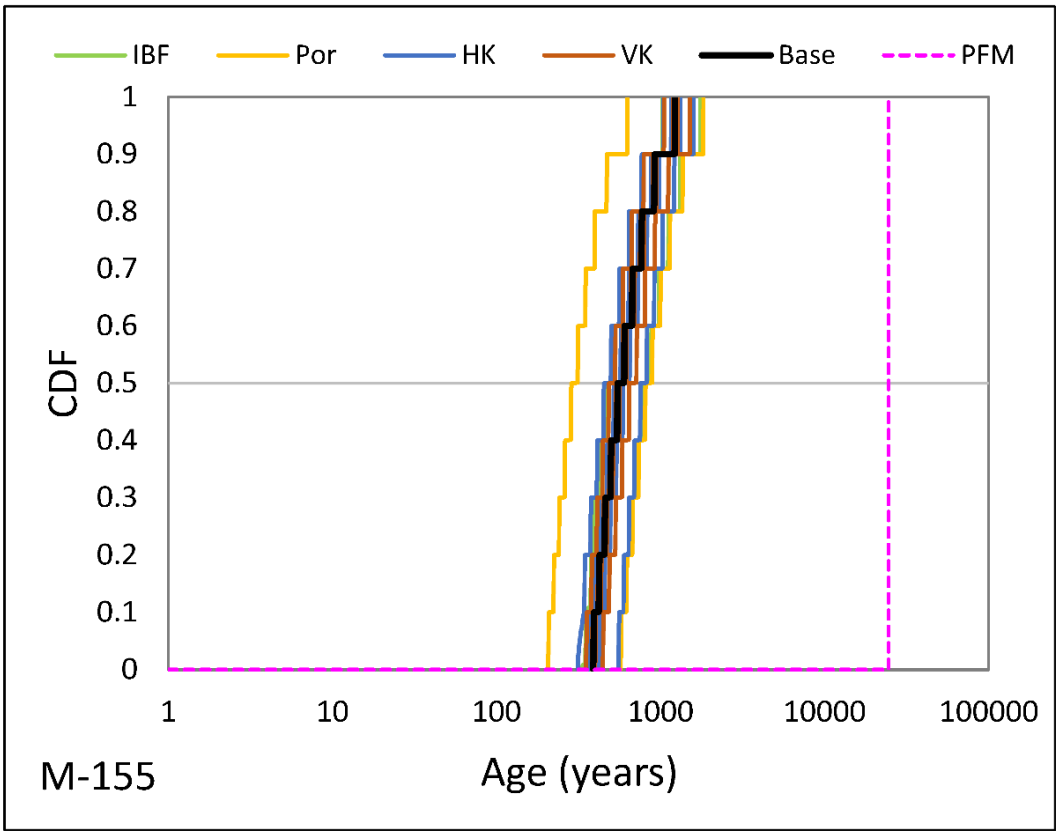

Figure 53. Age distributions for well M-155 calculated for the sensitivity analysis using the Phase 6 model. No binary mixing model could replicate the young water defined using SF6 or CFCs. Plotted is a single significant LPM defined using a PFM calibrated to ^{14}C.

M-207: This well is located adjacent to M-155 but screened much shallower (25 to 45 feet below ground level) and is situated in model layer 2. All sourced water is simulated by the Phase 6 model to originate at depth from the southern boundary with younger flows <150 years rising more quickly into shallower layers before moving horizontally toward the well (Figure 54). The numerical model estimates a mean age of 350 years (sensitivity range from 180 to 469 years) and a median age of 206 years (sensitivity range from 149 to 274 years) (Figure 55). The fraction of water <70 years is 0 percent (sensitivity range from 0 to 5 percent) with younger water generated by moving more water quickly from the southern GBF to the well. Specifically, water is moved more quickly by decreasing porosity in both the fine-grained and coarse-grained UMCf units and lowering horizontal hydraulic conductivity in the alluvium. No single Phase 6 model parameter adjustment can replicate the larger estimate of the young age fraction of 14 percent based on LPM calibration to observed ^{3}H, but multiple parameter adjustments may improve the Phase 6 estimate of young water to more than 5 percent. In addition to moving GBF water more quickly, the modeled young water fraction would benefit from surface recharge entering the well that is currently not simulated by the Phase 6 model to better replicate the observed ^{3}H in the well.

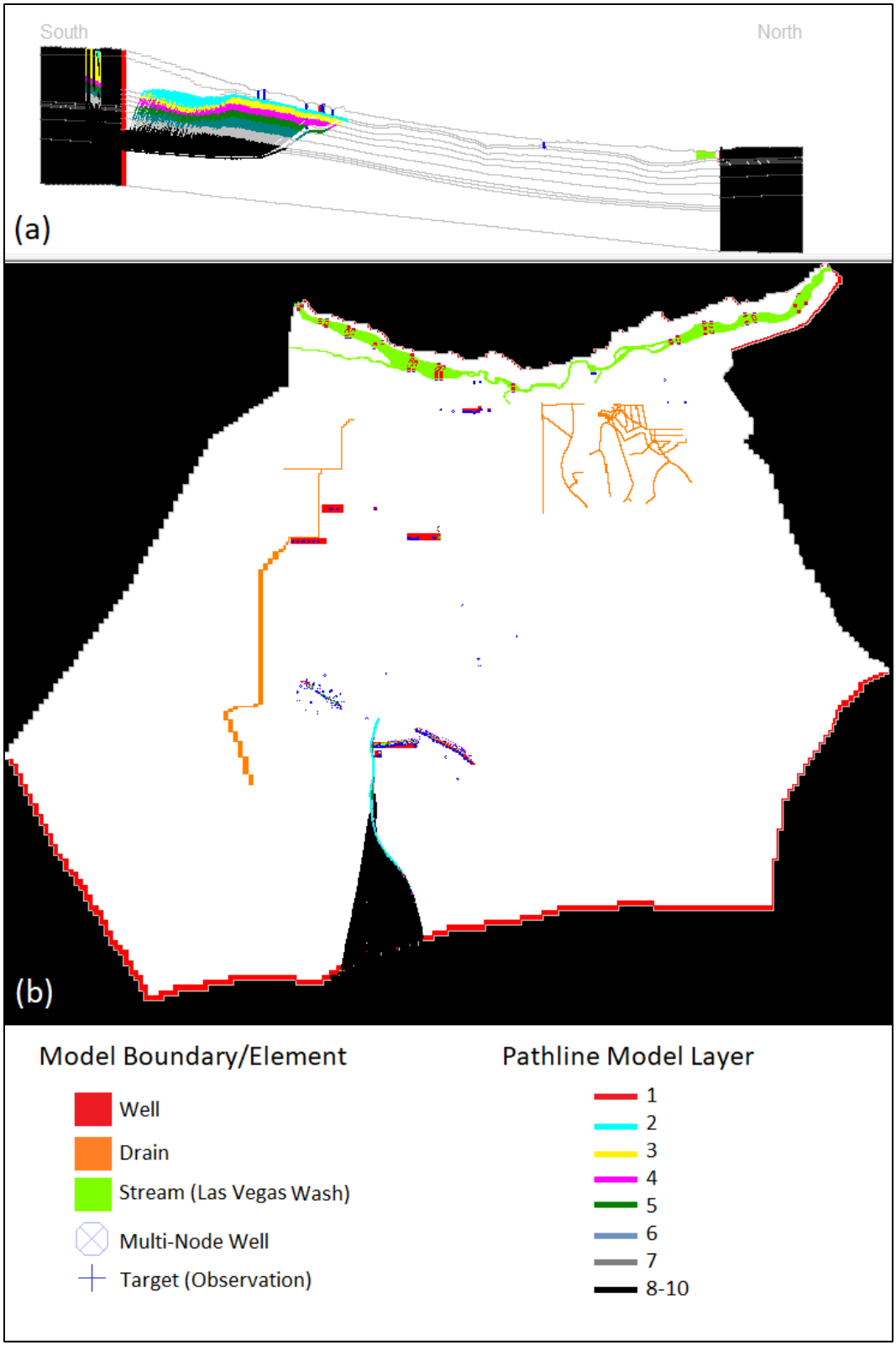

Figure 54. Backward tracking results for the baseline simulation well M-207. Pathlines are color coded by model layer in (a) a cross section along column 148 (north-south center of model) with layers delineated in light gray and (b) an aerial view.

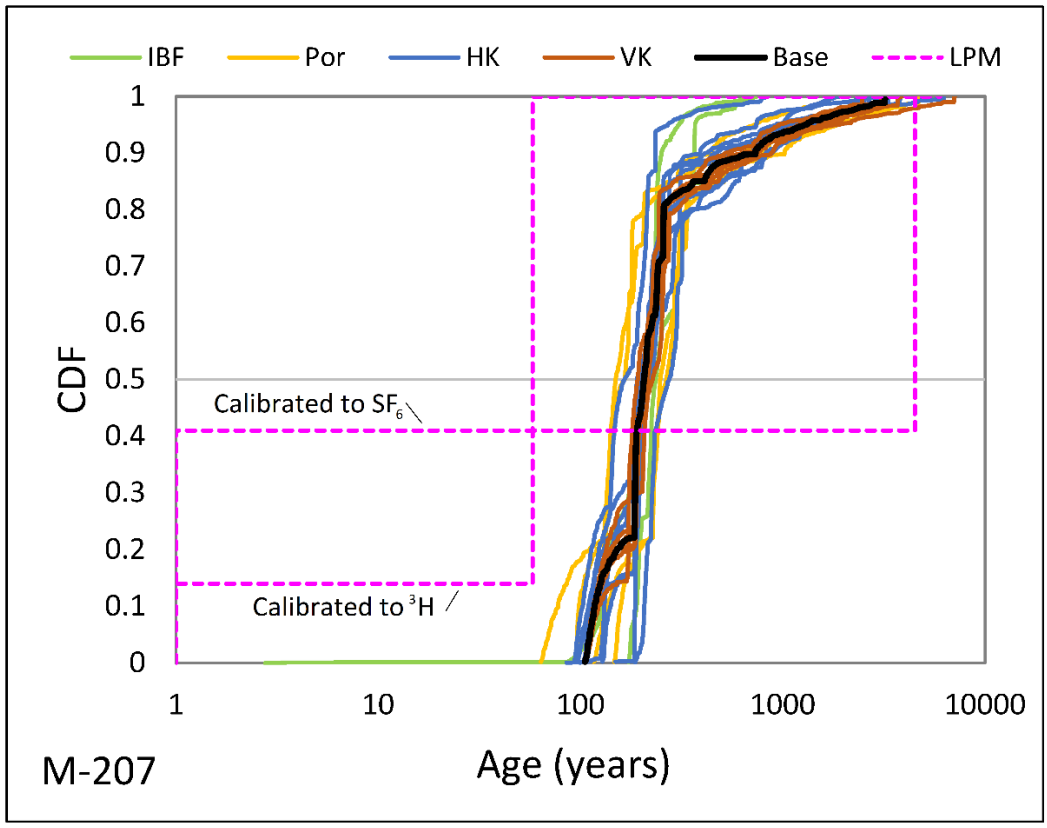

Figure 55. Age distributions for well M-207 calculated for the sensitivity analysis using the Phase 6 model and a single significant LPM defined as a PFM calibrated using ^{3}H with a mean age of 64 years.

PC-195: This well is in OU-3 near the interface of OU-2. It is screened between 60 and 70 feet below ground level and situated in model layer 3. Similar to upgradient well M-155, Phase 6 simulations indicate all water to M-207 is sourced from depth along the southern boundary flux (Figure 56). Mean age is 857 years (sensitivity range from 491 to 1,224 years) and median age is 855 years (sensitivity range from 489 to 1,221 years) (Figure 57). No modern water is estimated to enter PC-195. In contrast to Phase 6 model results, SF_6 and CFCs were present during our survey indicating the presence of modern water in the well. These contradictory observations add uncertainty to the presence or absence of modern water. Unlike M-155, LPMs for PC-195 can match observed SF_6, as well as CFC-12 and CFC-113 in combination with ^{14}C with low error (young water fraction = 5 to 70 percent). Consequently, we consider the presence of modern water in PC-195 uncertain and the ability to assess the Phase 6 model with respect to groundwater mixing also uncertain.

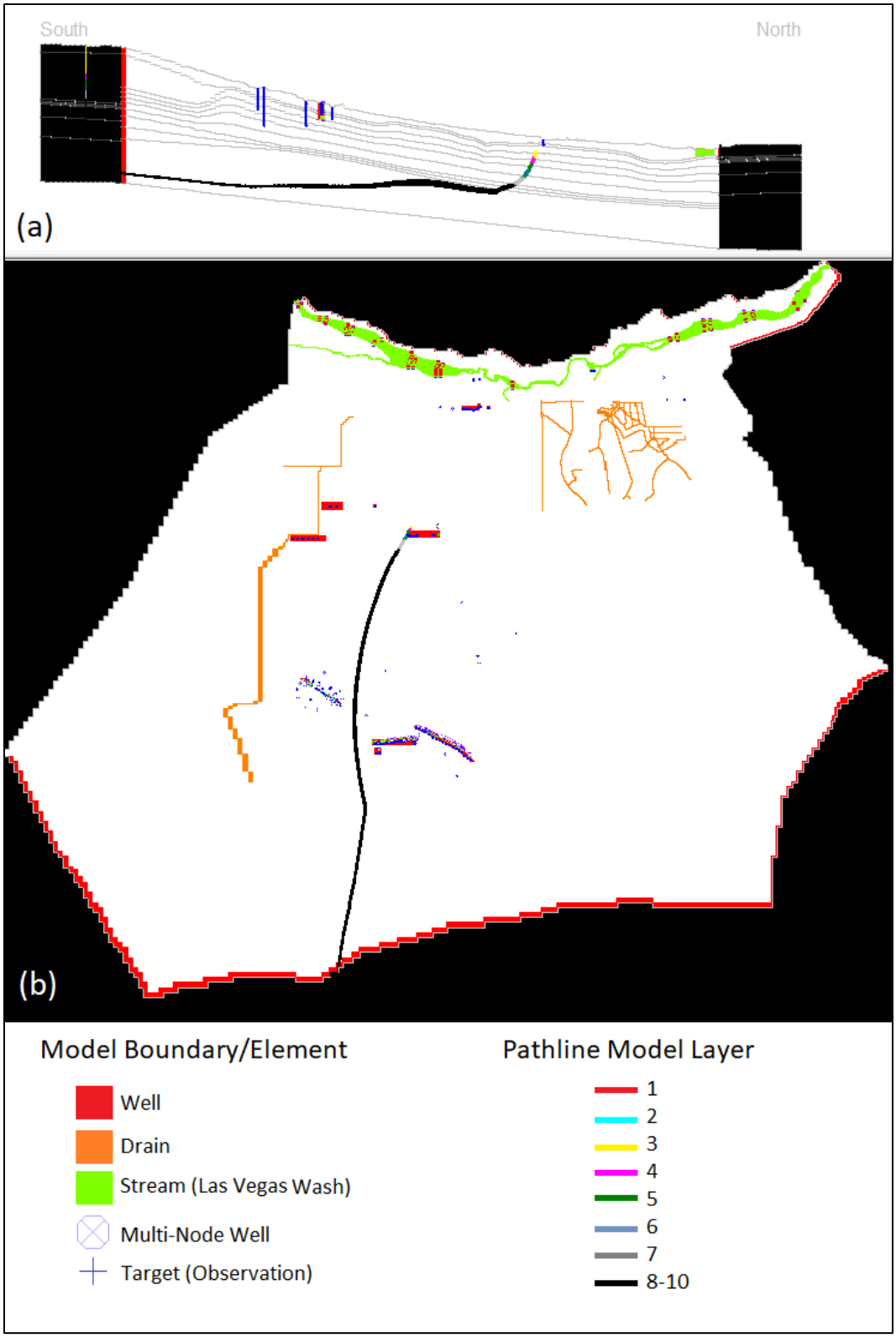

Figure 56. Backward tracking results for the baseline simulation well PC-195. Pathlines are color coded by model layer in (a) a cross section along column 148 (north-south center of model) with layers delineated in light gray and (b) an aerial view.

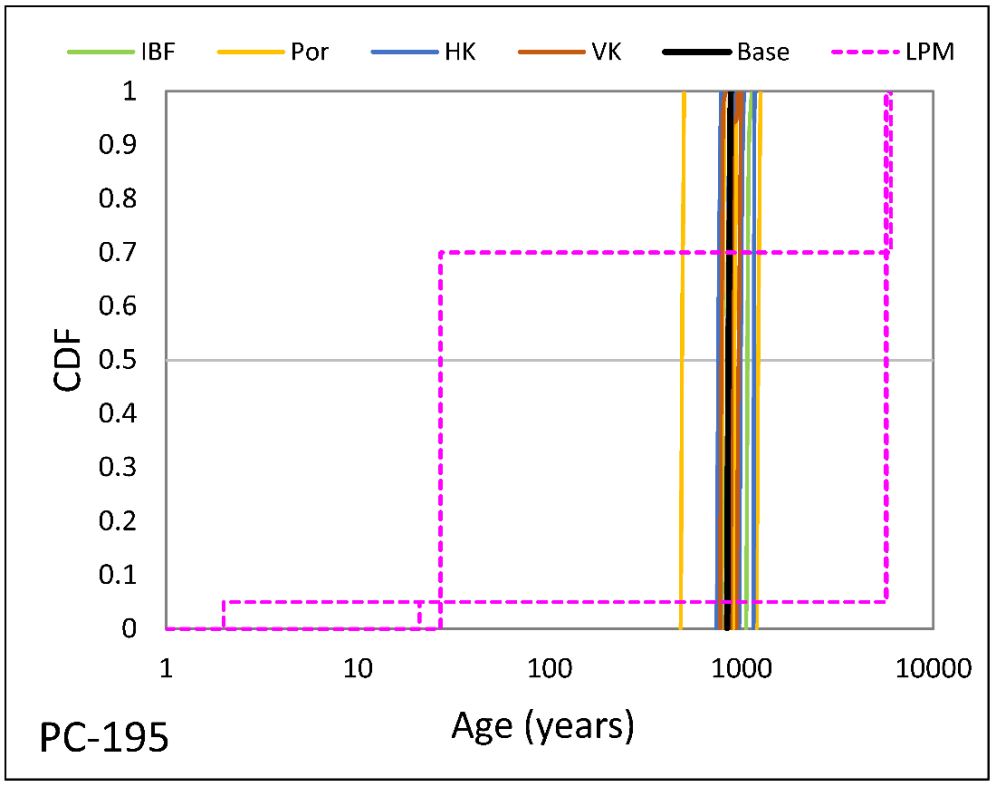

Figure 57. Age distributions for well PC-195 calculated for the sensitivity analysis using the Phase 6 model and significant LPMs. Young ages are calibrated to SF^6 and CFCs. No ^3H is found in this well making the young water ages from the LPM uncertain.

3.4.4 Overview of Sensitivity Analysis

Table 24 consolidates sensitivity results for each of the 19 sampled wells. It also includes the lithologic unit in which the well is completed, the model layer, and the fractions of young water (age <70 years) based on *NETPATH*-only estimates, as well as the LPM and the Phase 6 sensitivity run that most closely replicate one another. The results for each sensitivity scenario are provided by weight. A weight equal to 1 indicates the adjusted parameter moved the Phase 6 simulated age distribution closer toward the young water fraction as calculated by an LPM, but the single parameter adjusted in the sensitivity analysis could not fully replicate the LPM. A weight of 2 was given if a single parameter adjustment could reproduce the LPM young water fraction. No weight was given if the baseline already matched the LPM or the Phase 6 model could not match the LPM based on any of the parameters adjusted. The sum of weights was then tabulated to highlight those parameters most important to improving the simulated age distributions in the Phase 6 model domain. Where contradictory results occurred (e.g., increasing and decreasing southern GBF inflows improves the young water age fraction at different wells), then the best scenario was chosen based on the largest weight. We acknowledge global change in parameters such as the southern GBF is not a realistic calibration. Actual calibration to observed age targets will require breaking apart parameter groups as they are defined. Parameter adjustments that improve age distribution estimates in the Phase 6 model are listed below from highest weight to lowest weight:

Table 24. Calculated weights of sensitivity analysis with a comparison to the fraction of young water (fY), or water <70 years old calculated from the Phase 6 model, LPM, and *NETPATH*-only. Criteria for Phase 6 model able to mimic correct mixing of young and old water: (Y) the baseline or a single parameter is adjusted; (M) multiple parameters need to be adjusted but not tested; (U) fY is uncertain; (N) unable to match fY. Lithology: Qal = alluvium, G = Wash gravels, P = paleochannel, cg1=Upper Muddy Creek Formation-coarse grained unit 1, cg2 = Upper Muddy Creek Formation-coarse grained unit 2. Fg = Upper Muddy Creek Formation-fine grained unit. Only sensitive parameters included. Model parameters that did not affect or improve simulated results with respect to LPMs are not listed.

			Sampled Well																		
Param.	**Zone**	**Mult^.**	**ARP-7**	**ES-28**	**MW-105**	**MW-201A**	**MW-224A**	**M-31A**	**M-155**	**M-207**	**NERT4.71S1**	**NERT4.93S1**	**NERT5.49S1**	**PC-56**	**PC-64**	**PC-157A**	**PC-157B**	**PC-195**	**TR-7**	**TR-8**	**MW-25**	**Weight**
GBF	South	1.25			1			1														2
		0.8														2	2					4
Por	UMCf-fg	0.5			2			1		1						1	1					6
	UMCf-cg	0.5			2			2		1						1	1					7
HK	Qal	0.75													1							1
	UMCf-fg	1.25													1							1
	UMCf-cg	1.25								1												1
		0.75													1	1	1					3
VK	UMCf-cg	0.75													1	1	1					3
Correct Mixing Possible			N	N	Y	Y	N	Y	U	M	N	N	Y	N	M	M	M	U	U	Y	U	
Screened Unit			P	fg	Qal	G	LVW	fg	fg	fg	G	G	G	P	Qal	G	G	fg	cg2	cg1	Qal	
Model Layer			1	3	1	1	1	2	10	2	1	1	1	1	1	1	1	3	10	2	1	
Modeled fY*			0.09	0.00	0.15	1.00	0.00	0.09	0.00	0.05	0.00	0.01	1.00	0.22	0.02	0.03	0.03	0.00	0.00	0.39	0.00	
LPM fY*			1.00	0.98	0.15	1.00	0.85	0.12	0.00	0.14	1.00	1.00	1.00	1.00	0.17	0.16	0.16	0.05	0.11	0.35	0.01	
NETPATH-only fY			1.00	1.00	0.85	1.00	0.83	0.44	0.00	0.09	1.00	1.00	1.00	1.00	0.44	1.00	1.00	0.03	0.02	0.35	0.02	

^Mult = multiplier applied to baseline Phase 6 model parameter. *Closest fit between significant LPM and Phase 6 model across sensitivity scenarios (max. 1 parameter adj.).

- Decrease porosity in the UMCf-cg units.
- Decrease porosity in the UMCf-fg unit.
- Decrease flow across the southern GBF.
- Decrease horizontal hydraulic conductivity in the UMCf-cg units.
- Decrease vertical hydraulic conductivity in the UMCf-cg units.
- Increase horizontal hydraulic conductivity in the Qal.
- Increase horizontal hydraulic conductivity in the UMCf-fg unit.

Individual wells are then classified as:

- (Y) Phase 6 modeled age distribution can replicate a LPM based on observed tracers either with the original baseline model or adjustment of a single parameter.
- (M) Phase 6 modeled age distribution can possibly replicate a LPM based on multiple parameter adjustments, but this was not tested.
- (U) Phase 6 modeled age distribution is correct if the tracer-derived young water fraction is ignored. Uncertainty in age tracer observations is due to a lack of ^{3}H and/or LPMs for age tracers are insignificant.
- (N) Phase 6 modeled age distributions are unable to replicate the observed young water fraction. Inability is due to lack of modern water accounted for by the Phase 6 simulation and no parameter tested in the sensitivity analysis can improve the model outcome.

The spatial distribution of these results is provided in Figure 58. Overall, the Phase 6 model can replicate the young fraction delineated with age tracers in 26 percent of the wells with either the baseline model or the adjustment of a single parameter. Another 21 percent of the age-distributions in sampled wells could potentially be represented by the Phase 6 model if multiple parameters are adjusted simultaneously. There is some evidence of young water in MW-25, PC-195, M-155, and TR-7, but we consider the existence of young water uncertain given the lack of ^{3}H, perchlorate, and/or inability of LPMs to match observed tracer data. If we assume no modern water exists in these four wells, then the Phase 6 model can replicate the age-distributions calculated using observed tracers in 68 percent of the wells sampled. The young fraction in the remaining 32 percent of the wells cannot be captured by the current model structure. These wells are observed to contain a majority of modern water, but the Phase 6 model currently estimates limited or no modern water in these wells.

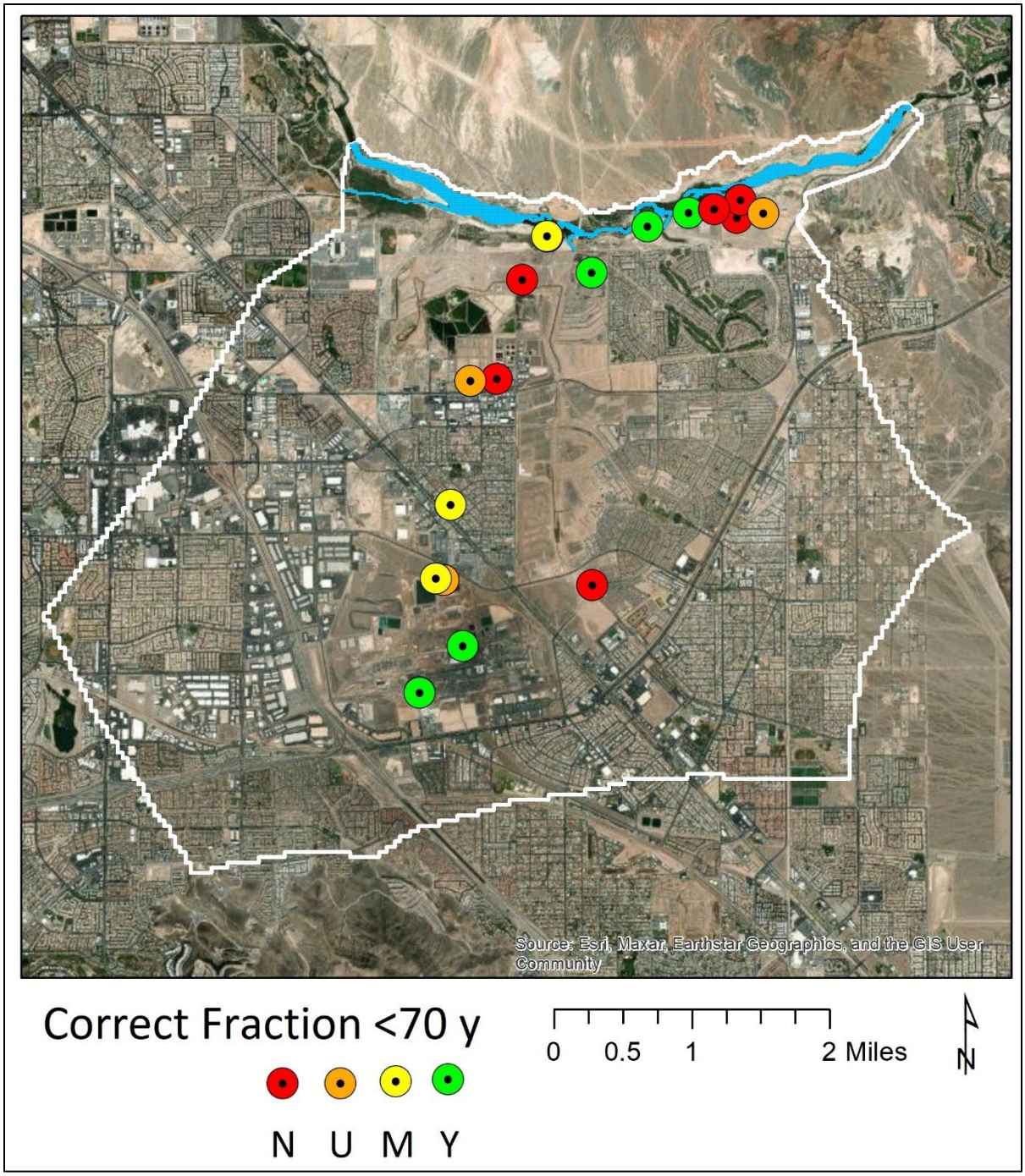

Figure 58. Spatial distribution of the Phase 6 model ability to replicate the young fraction in sampled wells with the baseline or a single parameter adjustment (Y), multiple parameter adjustments (M), excluding any modern water (U), and unable to match (N) indicated. Note that symbols for TR-7 (U) and PC-157B (Y) are hidden by symbols for shallower wells (TR-8 and PC-157A, respectively).

3.5 Las Vegas Wash Analysis

Figure 59 shows the spatial distribution of simulated particle pathlines contributing to each of the six reaches in the Las Vegas Wash for the baseline scenario. Particles entering reaches 1A and 1B generally enter the model domain from the western boundary and have relatively short flow paths compared with the other reaches. Pathlines entering reach 2 extend to the southern model boundary but are clustered along the western side of the model domain. The spatial distribution of particle path lines associated with reach 3 is quite narrow, which is not surprising given the comparatively small number of gaining SFR cells in that reach. Pathlines entering reaches 4 and 5 are well distributed and cover much of the model domain.

Summary statistics for simulated ages in each reach of the Las Vegas Wash are presented in Table 25 for the baseline model and in Table 26 for the sensitivity model that combines all parameter adjustments found to improve estimated age distributions by the Phase 6 model. A comparison of age distributions for each reach is provided in Figure 60. In both models, anomalous results were removed before tabulating the summary statistics. For example, particles exceeding one billion years in age were removed (three particles from

Table 25. Summary age statistics by reach for the baseline scenario. Values presented are recharge weighted.

Reach	Volume	Mean Age (Years)	Median Age (Years)	Max. Age (Years)	<10 Years	>100 Years
1a	25.8%	0.9	0.4	427	99.6%	0.1%
1b	3.1%	0.5	0.4	2	100%	0%
2	47.6%	10.5	0.5	3,357	98.3%	1.1%
3	0.01%	122.5	120.8	175	0%	100%
4	1.3%	759.9	816.5	6,098	2.5%	97.4%
5	22.3%	52.4	1.7	13,844	95%	3.8%
All	100%	26.6	0.5	13,844	96.7%	2.7%

Table 26. Summary age statistics by reach for the sensitivity scenario using optimized parameters. Values presented are recharge weighted.

Reach	Volume	Mean Age (Years)	Median Age (Years)	Max. Age (Years)	<10 Years	>100 Years
1a	22.0%	0.8	0.4	160	99.5%	0%
1b	2.2%	0.5	0.4	2	100%	0%
2	51.1%	2.1	0.5	2,084	99.5%	0.4%
3	0.01%	13.6	6.7	125	69%	1%
4	7.3%	171.9	1.5	2,898	70%	28.8%
5	17.3%	40.0	1.7	9,066	92.3%	6.3%
All	100%	17.3	0.5	9,066	96.7%	2.8%

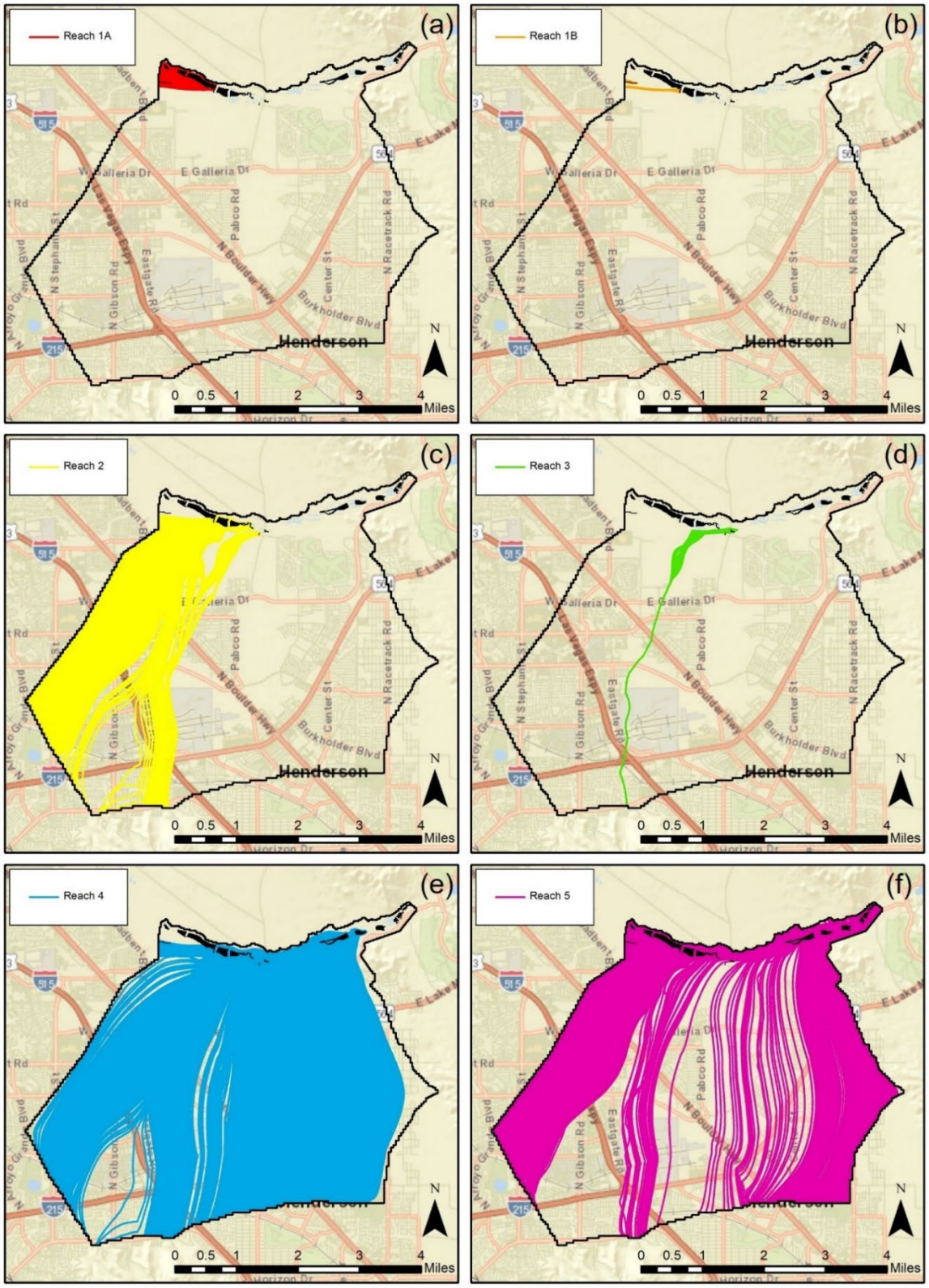

Figure 59. Particle pathline distribution contributing to each of the six identified reaches in the Las Vegas Wash.

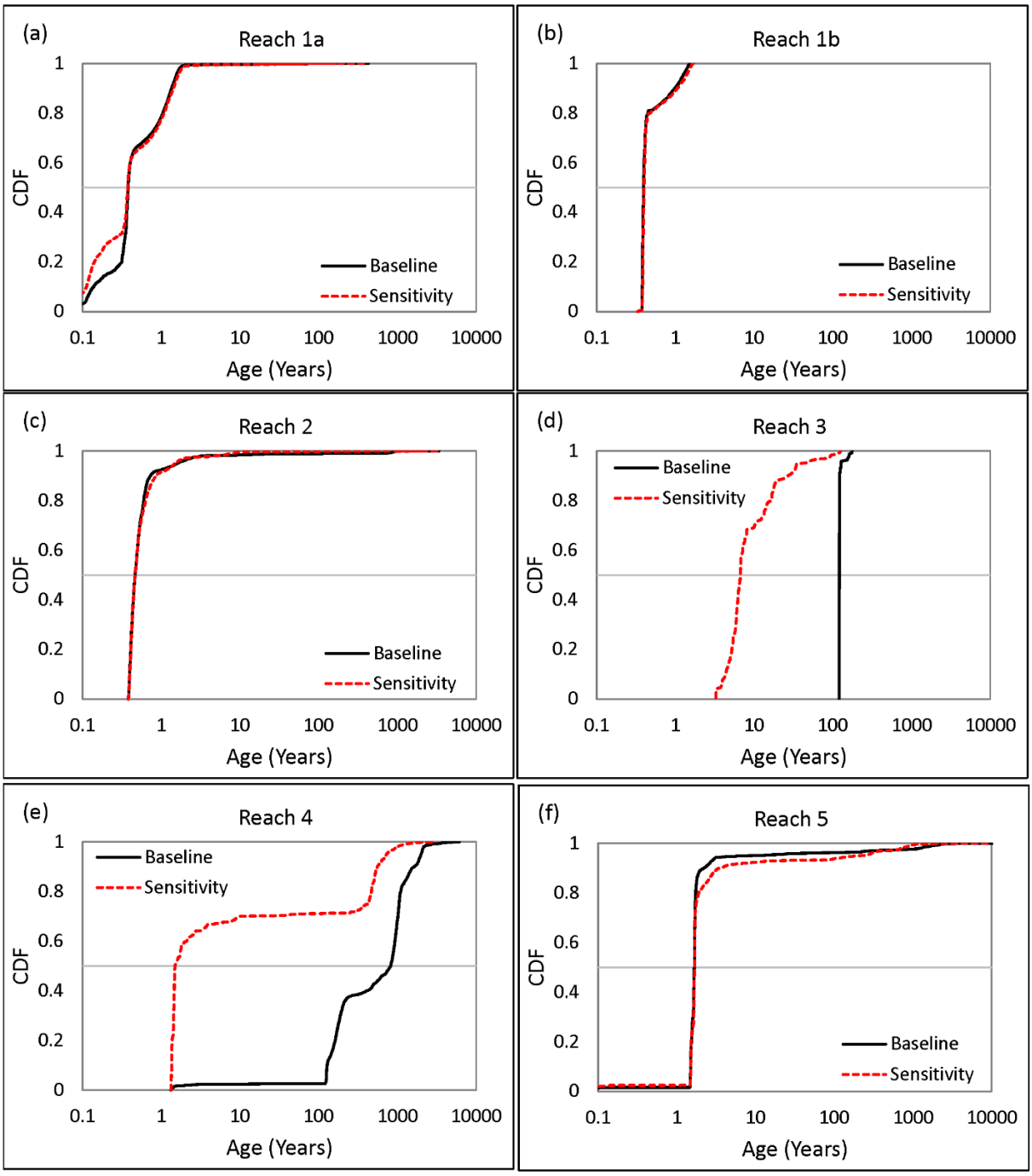

Figure 60. Recharge weighted CDF plots comparing the age distribution in the baseline and sensitivity model runs by reach.

reach 5 in the baseline model and one particle from reach 5 in the sensitivity model). Particles originating from cells with no source of recharge were also eliminated, as by definition they cannot contribute to a volume weighted CDF (62 particles removed from reach 5 in the baseline model and 59 particles removed from reach 5 in the sensitivity

model). With the exception of the maximum age, all statistics presented in Tables 25 and 26 are weighted by the recharge at each particle's endpoint, meaning that they are representative of the simulated volume of water entering the Las Vegas Wash in each reach.

A spatial comparison of pathline ages in the baseline and sensitivity runs are presented in Figure 61. Pathlines are displayed with the youngest ages on top for visibility. The oldest water flowing into the Las Vegas Wash in the baseline scenario is derived from the southern boundary flux with emphasis on older ages generally occurring along the eastern half of the modeled domain. Younger ages are generated along the western edge of the domain and from surface recharge, with the fastest flow paths through shallow paleochannels. This is particularly evident in recharged water from the Henderson Bird Viewing Preserve (refer to Figure 1) moving quickly through highly permeable paleochannels. Overall, the youngest groundwater contributions to the Las Vegas Wash travel through the proximal Wash gravels, which indicates surface and groundwater circulation between the different stream reaches is important in the current Phase 6 model. The spatial distribution of the pathlines is very similar but not identical between the baseline and sensitivity scenarios. A reduction in pathline age between the two scenarios is shown to take place over most of the model domain, with notable exceptions along the western model boundary where path line ages in the sensitivity run are greater than in the baseline run, and in the area north of the Wash where path line ages remain approximately the same.,. These flow paths are dependent on the northern GBF that was not impactful on observed tracers in wells to the south of the Las Vegas Wash.

The baseline model estimates the majority of water entering the Las Vegas Wash is occurring in reaches 1a, 2, and 5. Age distributions in these reaches (Figure 60) are dominated by young water and this biases ages across the entire Las Vegas Wash to receiving 96.7 percent of its water <10 years in age. Heavy tails in the age distributions for reaches 2 and 5 suggest water in excess of 100 years is likely accounting for one to four percent of their respective volumes, although the potential of very old water is also possible (>1,000 years). With Phase 6 parameter adjustments to better match observed tracer concentrations in sampled wells, the high-volume reaches (reaches 1a, 2, and 5) experience only small changes in their age distributions, with changes largely related to reductions in water >100 years. The exception is in reach 5 which experiences an increase in water ages >100 years despite the removal of the oldest ages from the distribution. Under baseline conditions, reaches 3 and 4 are sourced with nearly all water >100 years. These two reaches experience the largest changes in their age distributions as a result of modifying the Phase 6 parameters from the sensitivity analysis. For reach 3, mean and median ages decrease by 88.9 and 94.5 percent, respectively, and the fraction of water entering this reach <10 years old increases from 0 to 69 percent. For reach 4, the mean and median ages decrease by 77.4 and 99.8 percent, respectively, and the fraction of water <10 years increases from 2.5 percent to more than 70 percent. The contributing volume to both of these reaches is relatively low. This is especially true for reach 3, which is simulated as primarily losing water back into the Wash gravels and only contributing 0.01 percent to the total Las Vegas Wash volume. Reach 4 contributes 1.3 percent of the baseline volume and this increases with the sensitivity parameter suite to 7.3 percent of the total Wash volume.

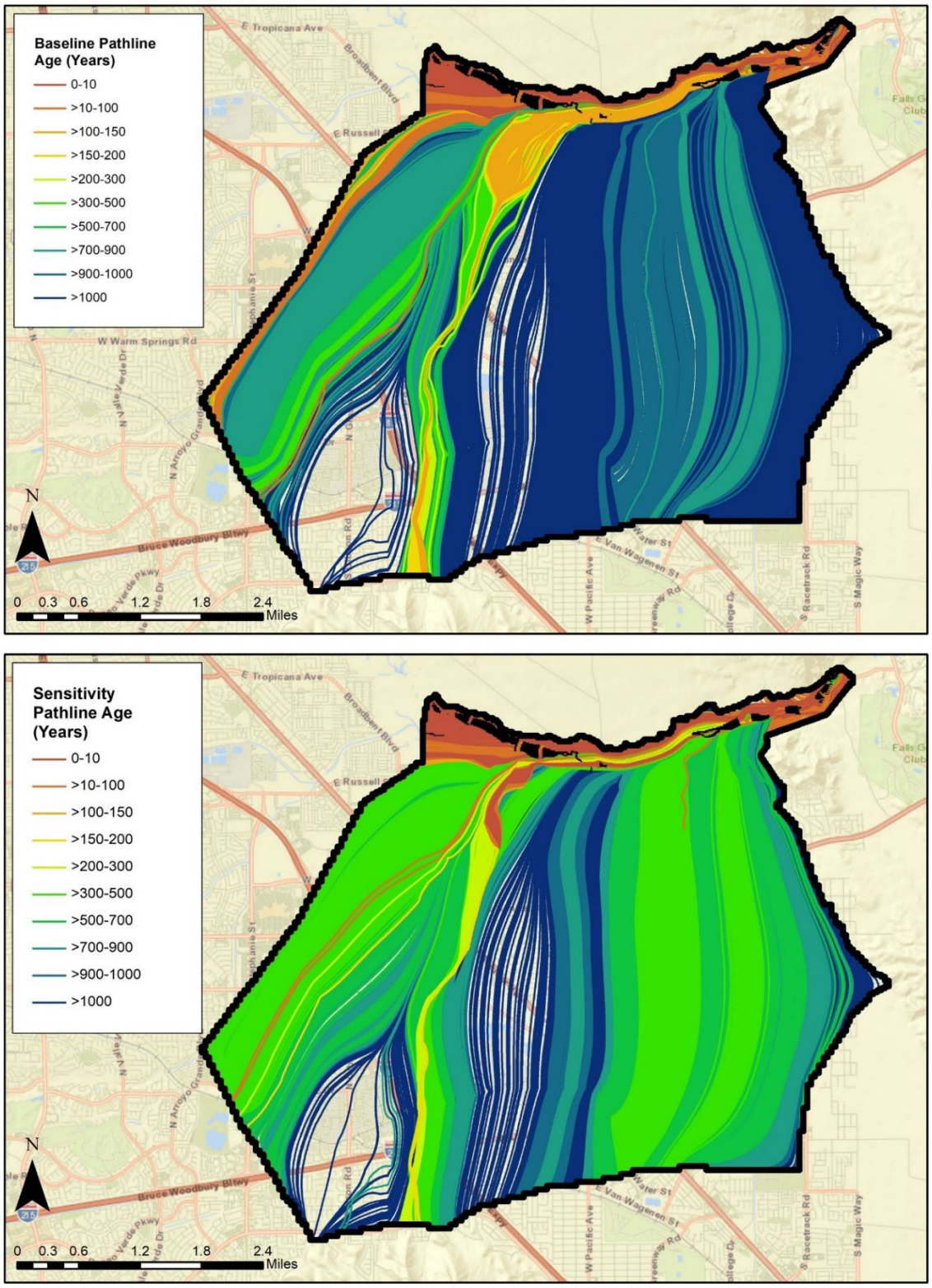

Figure 61. Pathline ages for the baseline (top) and sensitivity (bottom) scenarios.

4.0 DISCUSSION: SUMMARY, INSIGHTS, AND LIMITATIONS

An investigation was conducted to evaluate the NERT Phase 6 groundwater model using observed age tracers within monitoring wells across the NERT site. The goal of the work was to improve the conceptual understanding of groundwater flow paths and mixing behavior in the model domain, provide insight on age distributions into the Las Vegas Wash, and qualify possible impacts on remediation. The water balance from the Phase 6 model indicates 83 percent of the inflow is derived from interbasin groundwater flow, 12 percent is from areal recharge (summer sprinkler application), and 5 percent is from focused recharge (golf course irrigation, retention ponds, and miscellaneous injection) (Ramboll 2019). Therefore, the tracers selected for the project reflect the anticipated bimodal ages with modern water (<70 years) identified using tracers of ^{3}H, SF_6, and CFCs and older water (>1,000 years) based on ^{14}C. The use of ^{39}Ar could be useful in future studies and provide greater constraint on simulated flow paths in the midrange (70 to 1,000 years) though it is acknowledged this tracer is difficult to sample and costly to analyze.

Tracer sampling locations were selected through an iterative approach of backward particle tracking from monitoring wells located in the Phase 6 model domain and discussions with NDEP. Priority was given to wells following principal groundwater flow paths while also spanning different depths and lithologic units. Well selection also targeted several wells east of the NERT site, as well as a sequence of wells in the alluvium running parallel to the Las Vegas Wash. Wells near the Las Vegas Wash were selected to understand the relative importance of upwelling deep, old groundwater into the Las Vegas Wash versus more contemporary shallow flow through the alluvium. Wells were selected to minimize logistical issues related to restricted access and were limited to wells already targeted for sampling in the May 2022 sampling event conducted by Tetra Tech. Lastly, well selection was refined to wells with a minimum pumping rate (>100 mL/min) observed in previous NERT sampling campaigns to expediate sample collection for age tracers. In several cases, alternative wells had to be selected during the May 2022 sampling campaign because pumping rates in originally selected wells were much lower than anticipated, with corresponding large drops in water levels during pumping, than previously observed. Although the cause of decreased pumping rates and large water-level drops during the May 2022 sampling campaign is unknown, it may be related to the ongoing drought in the western United States. Wells to the east of the NERT site are relatively scarce and several identified for sampling were found with too low a pumping rate for sampling gas tracers. In the end, 19 wells were sampled out of the 25 initially proposed. Of the 19 wells, 12 wells were sampled for age tracers in the alluvial units (3 in the Quaternary alluvium, 2 in paleochannel deposits, and 7 in the Wash gravels), 5 wells were sampled in the fine-grained Upper Muddy Creek Formation, and 2 were sampled in the coarse-grained Upper Muddy Creek Formation.

Lumped parameter models for individual wells were calibrated to different tracer observations based on a variety of travel time distributions (piston flow, exponential and dispersion) to provide a range of reasonable estimates of the young water fraction (<70 years). While LPMs provide specific age statistics we rely on broad definitions of young water in acknowledgement of uncertainty in tracer-based approaches and to allow a direct comparison to the Phase 6 age estimates based on backward particle tracking. All sampled wells contained observable SF_6 and/or CFCs that is potentially indicative of some modern water. Additionally, all wells contained observable ^{3}H (also indicative of modern

water) except for three wells (M-155, PC-195, and TR-7). These three wells also contained no perchlorate and both M-155 and TR-7 are screened very deep in the subsurface (>200 feet). These conditions do not preclude the presence of modern water, per se, but add additional ambiguity to the young water fraction defined only with SF_6 and/or CFCs. Phase 6 modeling results suggest these three wells contain only deep, old groundwater obtained from the southern boundary flux and have no surface recharge contributions. With respect to M-155, LPMs could not adequately simulate the observed concentrations of SF_6 and CFCs, adding additional uncertainty to the analytical results. Therefore, we conclude that the Phase 6 model results are likely correct and M-155 lacks modern water. TR-7 is also a very deep well, but water-rock reaction modeling and observed groundwater stable isotopic signatures indicate that young water fractions occur on the order of 2 percent. The LPMs corroborate this result with 11 percent young water obtained using CFC-12 in the LPM calibration. Similarly, LPMs can match observed SF_6, as well as CFC-12 and CFC-113 in PC-195 with low error indicating this well may contain 5 percent modern water. However, the lack of ^3H in both TR-7 and PC-195 still make young water estimates suspect and thus the presence of modern water in both these wells remains uncertain. Consequently, the ability the Phase 6 model to replicate groundwater mixing in these wells cannot be assessed based on observed age tracers collected as part of this study.

Of the 19 wells sampled, 7 wells were observed to contain a mixture of young and old water. Two of these wells (MW-224A and MW-25) are screened in the shallow alluvium in the northeastern portion of the model domain. Age tracers indicate M-224A contains 15 percent young water, whereas MW-25 contains only 1 percent to 2 percent young water. The LPM results for MW-25 match observed ^3H with a 6.4 percent error. This is above the maximum error defining a significant result (5 percent) and we consequently consider the young water fraction in this well uncertain. However, both MW-224A and MW-25 contain measurable perchlorate concentrations providing additional evidence of modern water in these wells. In both cases, the Phase 6 model estimates all water in the vicinity of these wells is sourced from deep flow paths with no surface recharge contributions. Future modeling of the NERT model domain should consider this inconsistency in the conceptual model and if impacts on remediation efforts are significant. In contrast, the other five wells observed with a mixture of young and old groundwater can be accurately simulated by the Phase 6 model. Two of these wells are located in the Quaternary alluvium (M-105, PC-64), two are located in the Upper Muddy Creek Formation fine-grained unit (M-31A, M-207) and one is located in the Upper Muddy Creek formation coarse-grained unit (TR-8). In general, the Phase 6 model is consistent with the observed age tracers in replicating groundwater mixing relationships along the principal flow path from OU-1 to OU-3.

Nine wells contain ^3H, CFCs, and SF_6, which indicates the presence of young water and high ^{14}C content indicating minimal old water (>1,000 years). These wells are assumed to contain all modern groundwater (<70 years) with some variation in age distribution statistics calculated with LPMs as a function of the assumed groundwater flow process (e.g., piston flow, exponential, or dispersion) and the age tracers used in their calibration. Of the nine wells observed to contain only modern water, only one is completed in the fine-grained Upper Muddy Creek (ES-28). This well is located east of the NERT site and far upgradient from the Las Vegas Wash. The Phase 6 model estimates all water in this well is old and sourced from the southern boundary. The simulated reliance on old water contradicts the tracer observations. The remaining eight wells dominated by modern water are in the

alluvium. ARP-7 (layer 1) is a shallow well located close to the slightly deeper well PC-195 (layer 3). Both ARP-7 and PC-195 are simulated by the Phase 6 model to contain only old water derived from the southern boundary flux. As discussed above, there is uncertainty in PC-195 age tracer observations, but it likely contains mostly old water and, if so, it is properly simulated by the Phase 6 model. In contrast, tracers in the proximal well ARP-7 indicate only young water, which is not consistent with the Phase 6 model estimates. Importantly, age tracers suggest the old water in PC-195 and young water in ARP-7 do not mix and future work should consider resampling these wells to reduce uncertainty in age tracer concentrations and explore the significance of a possible flow divide between these wells to perchlorate transport and associated remediation efforts.

The remaining six wells observed with only modern water are situated in the Wash gravels. Two of these wells (MW-201A, NERT5.49S1) are simulated by the Phase 6 model to receive all their water from the Las Vegas Wash. The resulting young water agrees with the age tracer results. Wells PC-157A and PC-157B are nested approximately 20 feet apart. Calibrated LPMs provide a range in young water fractions (<70 years) from 16 percent to 100 percent. The Phase 6 model sensitivity analysis indicates the numerical model can potentially mimic the lower range in the young water fraction estimated by LPMs by reducing the southern boundary flux and forcing groundwater to move quickly through the shallow alluvial units. The last two wells running parallel to the Las Vegas Wash (NERT4.71S1, NERT4.93S1) are simulated by the Phase 6 model to contain little to no modern water (0 percent to 1 percent) and cannot replicate the observed age tracers, which indicates the majority of water in these wells is young water. The reliance on old water from the southern boundary flux in the Phase 6 model appears inaccurate. It is more likely that these wells are dependent on surface recharge or have access to reach 3 surface water that flows out of the Las Vegas Wash and into the adjacent gravels.

Overall, if we assume no modern water exists in MW-25, M-155, PC-195, and TR-7 given the uncertainty in their age tracer observations, then the Phase 6 model replicates the groundwater age distributions in approximately two-thirds of the sampled wells. This is done either with the baseline Phase 6 model or with adjustments to various parameters. Parameter adjustments include increasing the speed of water travel by reducing porosity in the coarse- and fine-grained units of the UMCf. Decreasing porosity, however, increases error in perchlorate estimates at well locations and the Las Vegas Wash (Ramboll 2019). Improved estimates in simulated age distributions occurred with adjustments to hydraulic conductivity. Specifically, increasing horizontal hydraulic conductivity in the alluvium outside paleochannels and in the UMCf-fg unit and decreasing horizontal and vertical hydraulic conductivity in the UMCf-cg units. These parameter adjustments generally improve estimates of groundwater levels but do not improve estimated Las Vegas Wash discharge (Ramboll 2019). The age distribution in one-third of the wells sampled cannot be adequately simulated with the Phase 6 model without decreasing the influence of the southern boundary flux and potentially increasing surface recharge. However, these parameter adjustments, if done across the entire NERT site, decrease the ability of the Phase 6 model to replicate observed groundwater levels and Las Vegas Wash discharge (Ramboll 2019). To improve the match between observed age tracers and the Phase 6 model while still meeting hydrologic metrics of groundwater and Wash discharge will require localized adjustments to model parameters as opposed to global shifts, as tested in this study.

Phase 6 baseline results indicate the majority of water entering the Las Vegas Wash is derived along reaches 1a, 2, and 5 in which the majority of water is <10 years old. Although most of the reaches contribute some fraction of older water, only reaches 3 and 4 contain a predominance of water >100. With the combined adjustment of parameters to improve age distribution estimates at the 19 sampled well locations, reaches 3 and 4 experience large shifts in their age distributions toward significantly more young water. Despite this shift toward younger ages, old water contributions (or heavy tails) from reaches 3 and 4 remain on the order of 1 percent (reach 3) and 29 percent (reach 4). The Phase 6 model estimates reach 3 contributes very little volume to the Las Vegas Wash. It is simulated as mostly losing water back into the Wash gravels and is simulated to support water for wells MW-201A and NERT5.49S1. This may be contradictory to mass balance estimates of perchlorate that suggest reach 3 is gaining groundwater. In contrast to reach 3, reach 4 volumetric contributions to the Las Vegas Wash appear more substantial and the effect of 29 percent old water (>100 years) discharged into reach 4 implies that remediation efforts may be required over a significant time period.

We acknowledge several major limitations to quantifying the Las Vegas Wash age distributions that require further study. First, the steady-state solution based on contemporary conditions (2014-2018) does not account for the widespread surface disposal of wastewater from the 1940s to the 1970s throughout much of the study site. However, most sampled wells in this study contain low to no contamination and are likely not sourcing younger water (i.e., <70 years) from these mid-twentieth-century wastewater ponds. Instead, stable isotopic data indicate local recharge is a combination of evaporated Lake Mead water and isotopically heavy and evaporated precipitation. This areal recharge may be underrepresented by the Phase 6 model. Nonetheless, the steady-state solution does limit younger water representation in the Phase 6 model by not replicating seasonal dynamics between surface and groundwater in the Las Vegas Wash, as well as ignoring episodic flood events and the diurnal variations in wastewater effluent. Despite these limitations, several wells in the Phase 6 model are simulated as majority (or exclusively) old water. The complete lack of simulated young water, even in the steady-state model, suggests a possible underrepresentation of local recharge in the model. The mixing behavior at these locations deserves further study to ensure the Phase 6 conceptual model is adequate for the purposes of remediation. The second major limitation is that no wells were sampled near reaches 1, 2, and 5 so we could not confidently evaluate the sourcing of young water to these portions of the Wash. Additional uncertainty in estimated age distributions in the Las Vegas Wash occurs in reach 4 because no model scenario tested could replicate the young water fraction observed in the wells adjacent to this reach. Instead, modeled ages in these wells appear to be overly reliant on old water sourced from the southern boundary. To improve model estimates of ages in these wells, future work can revisit localized influences of decreasing flow across the southern boundary and increasing surface recharge.

5.0 REFERENCES

Aggarwal, P.K., T. Matsumoto, N.C. Sturchio, H.K. Chang, D. Gastmans, and L.J. Araguas-Araguas, 2015. Continental Degassing of 4He by Surficial Discharge of Deep Groundwater. *Nature Geoscience* 8 (1): 35–39. https://doi.org/https://doi.org/10.1038/ngeo2302.

Ameli, A.A., N. Amvrosiadi, T. Grabs, H. Laudon, I.F. Creed, J J. McDonnell, and K. Bishop, 2016. Hillslope Permeability Architecture Controls on Subsurface Transit Time Distribution and Flow Paths. *Journal of Hydrology* 543: 17–30. https://doi.org/10.1016/j.jhydrol.2016.04.071.

Carroll, R.W.H., A.H. Manning, R. Niswonger, D. Marchetti, and K.H. Williams, 2020. Controls on Baseflow Age Distributions in a Snow-Dominated Mountain Headwater Stream. *Water Resources Research* 56, https://doi.org/10.1029/2020WR028161 .

Clark, I., 2015. *Groundwater Geochemistry and Isotopes*. CRC Press, Boca Raton, FL.

Clark, I., and P. Fritz, 1997. *Environmental Isotopes in Hydrology*. Lewis Publishers, Boca, Raton, FL.

Condon, L.E., K.H. Markovich, C.A. Kelleher, J.J. McDonnell, G. Ferguson, and J.C. McIntosh, 2020. Where Is the Bottom of a Watershed? *Water Resources Research* 56 (3): 0–3. https://doi.org/10.1029/2019WR026010.

Craig, H., 1961. Isotopic Variations in Meteoric Waters. *Science* 133:1702-1703.

Danesh-Yazdi, M., J. Klause, L.E. Condon, and R.M. Maxwell, 2018. Bridging the Gap Betwen Numerical Solutions of Travel Time Distributions and Analytical Storage Selection Functions. *Hydrological Processes* 32 (8): 1063–76. https://doi.org/doi:org/10.1002/hyp.11481.

Engdahl, N.B., J.L. McCallum, and A. Massoudieh, 2016. "Transient Age Distributions in Subsurface Hydrologic Systems." *Journal of Hydrology* 543: 88–100. https://doi.org/10.1016/j.jhydrol.2016.04.066.

Epstein, B., G.M. Pohll, J. Huntington, and R.W.H. Carroll, 2010. Development and Uncertainty Analysis of an Empirical Recharge Prediction Model for Nevada's Desert Basins. *Nevada Water Resources Association* 5 (1): 1–22.

Han, L-F., L.N. Plummer, and P. Aggarwal, 2014. The Curved ^{14}C vs. $\delta^{13}C$ Relationship in Dissolved Inorganic Carbon: A useful tool for groundwater age- and geochemical interpretations. *Chemical Geology* 387:111-125.

Hem, J.D., 1989. Study and Interpretation of the Chemical Characteristics of Natural Water. U.S. Geological Survey Water-Supply Paper 2254.

Hinkle, S.R., and D.T. Snyder, 1997. Comparison of Chlorofluorocarbon-Age Dating with Particle-Tracking Results of a Regional Ground-water Flow Model of the Portland Basin, Oregon and Washington. U.S. Geological Survey Water-Supply Paper 2483, 47 p.

Hounslow, A.W., 1995. *Water Quality Data, Analysis, and Interpretations*. Lewis Publishers, Boca Raton, FL.

Gleeson, T., A.H. Manning, A. Popp, M. Zane, and J.F. Clark., 2018. The Suitability of Using Dissolved Gases to Determine Groundwater Discharge to High Gradient Streams. *Journal of Hydrology* 557: 561–72. https://doi.org/10.1016/j.jhydrol.2017.12.022.

Jiang, W., K. Bailey, Z.-T. Lu, P. Mueller, T.P. O'Connor, C. Cheng, S.-M. Hu, R. Purtschert, N.C. Sturchio, Y.R. Sun, W.D. Williams, and G.-M. Yang, 2012. An Atom Counter for Measuring 81Kr and 85Kr in Environmental Samples. *Geochimica et Cosmochimica Acta* 91 (1–6). https://doi.org/doi:10.1016/j.gca.2012.05.019.

Jurgens, B.C., J.K. Böhlke, and S.M. Eberts, 2012. TracerLPM (Version 1): An Excel ® Workbook for Interpreting Groundwater Age Distributions from Environmental Tracer Data: U.S. Geological Survey Techniques and Methods Report 4-F3, 60 P., No. Version 1:60.

Kwicklis, E., I. Farnham, R.L. Hershey, A. Visser, and J. Hoaglund III, 2021. Understanding Long-term Groundwater Flow at Pahute Mesa and Vicinity, Nevada National Security Site, USA, from Naturally Occurring Geochemical and Isotopic Tracers. *Hydrogeology Journal* 29:2725–2749. https://doi.org/10.1007/s10040-021-02397-x.

Markovich, K.H., A.H. Manning, L.E. Condon, and C. Jennifer, 2019. Mountain-block Recharge: A Review of Current Understanding. https://doi.org/10.1029/2019WR025676.

Maxey, G.B., and T.E. Eakin. 1949. Ground Water in White River Valley, White Pine, Nye, and Lincoln Counties, Nevada. No. 8. Carson City, Nevada.

Maxwell, R.M., L.E. Condon, S.J. Kollet, K. Maher, R. Haggerty, and M. M. Forrester, 2016. The Imprint of Water and Geology on Residence Times in Groundwater. *Geophysical Research Letters* 43:701–8. https://doi.org/doi:10.1002/2015GL066916.

McGuire, K.J., J.J. McDonnell, M. Weiler, C. Kendall, B.L. McGlynn, J.M. Welker, and J. Seibert., 2005. The Role of Topography on Catchment-Scale Water Residence Time. *Water Resources Research* 41(5). https://doi.org/10.1029/2004WR003657.

McGuire, K.J., and J.J. McDonnell, 2006. A Review and Evaluation of Catchment Transit Time Modeling. *Journal of Hydrology* 330 (3–4):543–63. https://doi.org/10.1016/j.jhydrol.2006.04.020.

Niswonger, R.G., S. Panday, and M. Ibaraki, 2011. MODFLOW-NWT, A Newton Formulation for MODFLOW-2005. *U.S. Geological Survey Groundwater Resources Program, Techniques and Methods* 6-A37:44.

Niswonger, R.G., and D.E. Prudic, 2005. Documentation of the Streamflow-Routing (SFR2) Package to Include Unsaturated Flow beneath Streams - A Modification to SFR1. *U.S. Geological Survey Techniques and Methods* 6-A13:50.

Plummer, L.N., E.C. Prestemon, D.L., Parkhurst, 1994. An Interactive Code (NETPATH) for Modeling NET Geochemcial Reactions Along a Flow Path, Version 2.0. U.S. Geological Survey Water-Resources Investigations Report 94-4169.

Pohlmann, K., and K. Heintz, 2017. Investigation of the Sources of Selected Springs in the Lake Mead National Recreational Area using Stable Isotopes. Desert Research Institute Publication No. 41271, Las Vegas, Nevada.

Pollock, D.W., 2016. User Guide for MODPATH Version 7 -- A Particle-Tracking Model for MODFLOW. *U.S. Geological Survey Open-File Report* 2016–1086: 35 p. https://doi.org/10.3133/ofr20161086.

Quade, J., T.E. Cerling, and J.R. Bowman, 1989. Systematic variations in the carbon and oxygen isotopic composition of pedogenic carbonate along elevation transects in the southern Great Basin, United States. Geological Society of America Bulletin, 101:464-475.

Ramboll, 2019. Phase 6 Groundwater Flow and Transport Model, Nevada Environmental Response Trust Site, Henderson, Nevada. Prepared for the Nevada Environmental Trust. Project Number 1690011200-034. Ramboll, 2200 Powell St., Ste. 700, Emeryville, CA, November 27, 2019. https://nertjoomla3.azurewebsites.net/index.php/project-documents/access-project-documents/Reports/2019/2019-11-27 Phase 6 GW Flow and Transport Model.

Solomon, D.K., P.G., Cook, and W.E. Sanford, 1998. Dissolved Gases in Subsurface Hydrology. In: C. Kendall and J.J. McDonnell (Eds.), *Isotope Tracers in Catchment Hydrology*. Elsevier, pp. 291-318.

Solomon, D.K., and P.G. Cook, 2000. 3H and 3He. In *Environmental Tracers in Subsurface Hydrology*, edited by A.L. Cook, P.G., and Herczeg, 397–424. Boston, MA: Kluwer Academic Publishers.

Suckow, A., 2014. The Age of Groundwater - Definitions, Models and Why We Do Not Need This Term. *Applied Geochemistry* 50:222–30. https://doi.org/10.1016/j.apgeochem.2014.04.016.

Toth, J., 1963. A Theoretical Analysis of Groundwater Flow in Small Drainage Basins. *Journal of Geophysical Research* 68:4795–4812. https://doi.org/doi:10.1029/JZ068i008p02354.

Vogel, J.C., and D. Ehhalt, 1963. The Use of the Carbon Isotopes in Groundwater Studies. *In* Radioisotopes in Hydrology, Proceedings of a Symposium, Tokyo, 5-9 March, 1963. International Atomic Energy Agency, Vienna, 1963. P. 383-395.

Yokochi, R., 2016. Recent Developments on Field Gas Extraction and Sample Preparation Methods for Radiokrypton Dating of Groundwater. *Journal of Hydrology* 540. https://doi.org/10.1016/j.jhydrol.2016.06.020.

APPENDIX A. CHEMISTRY AND ISOTOPE LABORATORY RESULTS

Table A-1. Observed geochemical and isotopic data from sampled wells.

Sample Well	Date (m/d/y)	Time	Ca (mg/L)	Mg (mg/L)	Na (mg/L)	K (mg/L)	HCO_3 (mg/L $CaCO_3$)	Cl (mg/L)	SO_4 (mg/L)	NO_3 (mg/L as N)	SiO_2 (mg/L)	pH	EC (µS/cm)	$\delta^{18}O$ (‰)	$\delta^{2}H$ (‰)	$\delta^{13}C$ (‰)	^{14}C (pmC)	^{3}H (TU)	SF_6 Ave. Age (yrs)	CFC Ave. Age (yrs)
PC-157A	5/4/2022	13:59	200	72.9	443	23.2	302	528	839	0.665	73.2	7.69	3640	-9.4	-87	-16.0	92.79	5.91	18.3	47.1
PC-157B	5/5/2022	8:18	211	90.1	406	22.9	212	504	1010	1.84	73.5	7.67	3580	-9.6	-87	-14.0	81.17	4.82	14.6	47.4
LVWPS-MW224A	5/2/2022	9:50	531	154	358	123	80.0	494	2200	12.0	60.6	7.45	4950	-10.7	-90	-13.4	71.51	4.20	12.3	-
NERT4.71S1	5/3/2022	11:13	519	196	463	96.9	124	716	2200	23.5	54.8	7.44	5530	-10.7	-91	-15.3	81.77	5.39	0.8	26.6
LVWPS-MW105	5/5/2022	13:47	580	259	564	221	94.0	1220	2350	15.4	79.0	7.57	7130	-10.9	-92	-13.8	66.63	4.17	22.1	37.0
NERT5.49S1	5/4/2022	11:35	133	55.3	183	19.5	140	270	450	10.0	16.2	7.75	2050	-11.6	-95	-14.3	83.69	5.67	9.6	27.3
PC-56	5/6/2022	7:55	193	69.7	559	16.5	212	643	971	13.2	55.4	7.66	4200	-11.6	-96	-13.2	90.35	5.89	6.3	26.4
LVWPS-MW201A	5/3/2022	8:20	440	164	489	57.4	154	765	1780	14.8	47.8	7.37	5160	-11.7	-96	-14.1	82.88	5.41	C	32.3
NERT4.93S1	5/5/2022	11:30	438	165	465	67.7	154	754	1760	16.5	47.8	7.46	5120	-12.2	-99	-12.4	82.74	TBA	12.1	57.8
MW-25	5/2/2022	13:30	274	94.5	569	93.3	170	571	1780	1.97	68.5	7.40	4640	-12.3	-96	-13.3	64.99	0.09	9.8	76.5
ARP-7	5/9/2022	8:30	787	296	1110	27.1	114	2430	2340	28.1	87.3	7.44	10400	-11.8	-96	-14.6	81.61	5.02	C	-
PC-64	5/4/2022	8:55	579	154	911	10.7	210	750	2600	66.2	83.0	7.71	7100	-11.6	-95	-11.3	57.25	4.62	19.3	44.1
PC-195	5/10/2022	8:00	209	79.9	282	19.6	88.0	327	1200	<0.500	61.1	7.78	3120	-12.3	-95	-7.7	25.1	6.72	46.9	58.7
M-153	5/10/2022	9:00	*	*	*	*	*	*	*	*	*	*	*	-12.5	-95	*	*	*	*	*
M-212	5/10/2022	10:45	*	*	*	*	*	*	*	*	*	*	*	-12.2	-95	-7.7	29.3	*	*	*
M-207	5/9/2022	13:20	264	142	615	17.4	104	906	1160	19.4	70.1	7.79	5230	-11.6	-93	-7.0	44.2	3.79	24.6	17.4
M-155	5/10/2022	13:30	24.1	12.6	124	5.81	86.0	115	164	0.672	13.9	8.10	918	-12.6	-95	-10.4	4.42	BD	C	42.9
ES-28	5/9/2022	13:00	451	212	864	20.5	118	484	3430	12.0	81.6	7.75	6660	-11.0	-94	-9.5	87.29	5.92	23.9	33.6
M-31A	5/11/2022	8:00	280	112	628	13.3	144	382	1660	18.4	69.8	7.62	5420	-11.6	-95	-7.5	56.28	3.43	6.9	34.4
TR-8	5/10/2022	14:00	63.5	27.6	190	8.86	92.0	122	449	2.18	41.9	8.06	1540	-12.0	-93	-6.1	48.46	1.21	37.9	39.2
TR-7	5/10/2022	11:30	52.1	20.6	153	8.70	90.0	184	228	0.946	32.8	8.13	1280	-12.7	-95	-6.8	16.92	BD	24.4	41.8

*Not collected; "-" = no result; C = concentration elevated above datable range; BD = below detection; TBA = to be analyzed.

Table A-2. The CFC results for sampled wells. Data provided by the U.S. Geological Survey.

Sample Name	Sampling Date (m/d/y)	Excess Air (cc/kg)	Recharge Temp (°C)	Recharge Elevation (feet)	CFC-11 (pptv)	CFC-12 (pptv)	CFC-113 (pptv)	Piston Flow Ages (years)*					
								CFC-11 1	CFC-11 2	CFC-12 1	CFC-12 2	CFC-113 1	CFC-113 2
MW224A	5/2/2022	0.9	22.8	1527	1439.56	29159.79	101.29	C	C	C	C	C	C
MW224A	5/2/2022	0.9	22.8	1527	780.70	30016.18	102.35	C	C	C	C	C	C
MW-25	5/2/2022	0.9	23.2	1530	1142.12	817323.62	132.30	C	C	C	C	C	C
MW-25	5/2/2022	0.9	23.2	1530	0.00	0.00	0.00	77.84	NP	82.34	NP	69.34	NP
MW-201A	5/3/2022	2.4	24.8	1523	194.79	530.19	32.91	39.34	NP	27.34	11.34	39.34	NP
MW-201A	5/3/2022	2.4	24.8	1523	196.96	496.58	32.55	38.84	NP	31.84	2.34	39.84	NP
NERT4.71S1	5/3/2022	1.2	22.6	1520	558.42	628.18	85.51	C	C	C	C	26.34	26.84
NERT4.71S1	5/3/2022	1.2	22.6	1520	564.75	605.70	91.05	C	C	C	C	C	C
PC-64	5/4/2022	3.8	26.8	1573	104.84	906.17	325.12	48.34	NP	C	C	C	C
PC-64	5/4/2022	3.8	26.8	1573	190.39	903.37	369.76	39.84	NP	C	C	C	C
PC-64	5/4/2022	3.8	26.8	1573	993.50	904.64	366.51	C	C	C	C	C	C
NERT5.49S1	5/4/2022	2.7	29.1	1544	14.92	230.45	10.21	60.34	NP	47.34	NP	48.34	NP
NERT5.49S1	5/4/2022	2.7	29.1	1544	21.79	0.00	8.52	58.34	NP	82.34	NP	49.84	NP
PC-157A	5/4/2022	5.7	25.5	1545	29.70	291.82	36.71	56.84	NP	42.84	NP	38.84	NP
PC-157A	5/4/2022	5.7	25.5	1545	26.04	288.66	21.39	57.84	NP	43.34	NP	42.84	NP
PC-157B	5/5/2022	3.8	22	1545	39.57	264.61	12.34	54.84	NP	45.34	NP	46.84	NP
PC-157B	5/5/2022	3.8	22	1545	147.81	263.76	11.80	44.84	NP	45.34	NP	47.34	NP
NERT4.93S1	5/5/2022	1.8	24.5	1524	205.98	507.11	45.10	37.84	NP	30.84	3.84	36.84	NP
NERT4.93S1	5/5/2022	1.8	24.5	1524	208.34	503.05	46.95	37.84	NP	31.34	3.34	36.84	NP
MW-105	5/5/2022	4.9	24	1532	171.94	621.49	74.64	41.84	NP	C	C	32.34	8.84
MW-105	5/5/2022	4.9	24	1532	197.03	622.86	59.24	38.84	NP	C	C	34.84	NP
PC-56	5/6/2022	3.8	15.6	1573	253.04	518.52	59.53	33.85	17.85	29.35	7.35	34.85	NP
PC-56	5/6/2022	3.8	15.6	1573	256.35	514.08	59.76	33.35	19.35	30.35	6.35	34.85	NP

*NP = not possible, C= contaminated.

Table A-2. The CFC results for sampled wells. Data provided by the U.S. Geological Survey (continued).

Sample Name	Sampling Date (m/d/y)	Excess Air (cc/kg)	Recharge Temp (°C)	Recharge Elevation (feet)	CFC-11 (pptv)	CFC-12 (pptv)	CFC-113 (pptv)	Piston Flow Ages (years)*					
								CFC-11 1	CFC-11 2	CFC-12 1	CFC-12 2	CFC-113 1	CFC-113 2
ARP-7	5/9/2022	0.9	24.9	1600	3131.16	3035.87	101.73	C	C	C	C	C	C
ARP-7	5/9/2022	0.9	24.9	1600	3387.91	3058.49	100.08	C	C	C	C	C	C
ES-28	5/9/2022	1.9	26.2	1750	1099.48	11785.54	66.77	C	C	C	C	33.85	NP
ES-28	5/9/2022	1.9	26.2	1750	1120.35	11341.16	67.54	C	C	C	C	33.35	NP
M-207	5/9/2022	3	21.6	1729	666.40	496.03	98.73	C	C	31.85	2.35	C	C
M-207	5/9/2022	3	21.6	1729	621.21	477.06	93.75	C	C	32.85	NP	C	C
PC-195	5/10/2022	1.5	24.1	1613	312.02	30.82	6.89	C	C	63.36	NP	51.36	NP
PC-195	5/10/2022	1.5	24.1	1613	405.94	19.84	5.17	C	C	66.86	NP	53.36	NP
TR-7	5/10/2022	0.6	25.4	1814	258.18	59.40	28.48	33.36	19.86	58.36	NP	40.86	NP
TR-7	5/10/2022	0.6	25.4	1814	621.26	65.26	31.35	C	C	57.86	NP	39.86	NP
TR-7	5/10/2022	0.6	25.4	1814	579.79	61.94	28.80	C	C	58.36	NP	40.86	NP
M-155	5/10/2022	1.6	26.8	1728	252.12	50.51	15.61	34.36	17.36	59.86	NP	45.36	NP
M-155	5/10/2022	1.6	26.8	1728	596.50	52.86	28.11	C	C	59.36	NP	40.86	NP
TR-8	5/10/2022	4	15.9	1600	400.19	197.12	30.28	C	C	48.86	NP	40.36	NP
TR-8	5/10/2022	4	15.9	1600	278.14	192.62	29.29	28.36	28.36	48.86	NP	40.36	NP
TR-8	5/10/2022	4	15.9	1600	625.13	182.47	29.29	C	C	49.36	NP	40.36	NP
M-31A	5/11/2022	1.6	21.9	1797	448.07	592.78	64.28	C	C	C	C	34.36	NP
M-31A	5/11/2022	1.6	21.9	1797	424.93	618.18	60.78	C	C	C	C	34.36	NP

*NP = not possible, C= contaminated.

Table A-3. The SF_6 results for sampled wells. Data provided by the U.S. Geological Survey.

Sample Name	Sampling Date (m/d/y)	Excess Air (mL)	Recharge Temp (°C)	Elevation (feet)	SF_6 Pressure (pptv)*	Piston Flow Ages (years)*
MW224A	5/2/2022	0.9	22.8	1527	7.84	9.84
MW224A	5/2/2022	0.9	22.8	1527	6.36	14.84
MW-25	5/2/2022	0.9	23.2	1530	7.96	9.84
MW-25	5/2/2022	0.9	23.2	1530	7.80	9.84
MW201A	5/3/2022	2.4	24.8	1523	12.06	C
MW201A	5/3/2022	2.4	24.8	1523	NS	NS
NERT4.71S1	5/3/2022	1.2	22.6	1520	11.79	-0.16
NERT4.71S1	5/3/2022	1.2	22.6	1520	10.60	1.84
PC-64	5/4/2022	3.8	26.8	1573	5.28	19.34
PC-64	5/4/2022	3.8	26.8	1573	5.33	19.34
NERT5.49S1	5/4/2022	2.7	29.1	1545	7.26	11.84
NERT5.49S1	5/4/2022	2.7	29.1	1545	7.10	12.34
PC-157A	5/4/2022	5.7	25.5	1544	5.31	19.34
PC-157A	5/4/2022	5.7	25.5	1544	5.77	17.34
PC-157B	5/5/2022	3.8	22	1545	6.87	13.34
PC-157B	5/5/2022	3.8	22	1545	6.16	15.84
NERT4.93S1	5/5/2022	1.8	24.5	1524	7.54	10.84
NERT4.93S1	5/5/2022	1.8	24.5	1524	8.44	8.34
MW-105	5/5/2022	4.9	24	1532	4.06	24.84
MW-105	5/5/2022	4.9	24	1532	5.34	19.34
PC-56	5/6/2022	3.8	15.6	1573	9.25	5.85
PC-56	5/6/2022	3.8	15.6	1573	8.98	6.85
ARP-7	5/9/2022	0.9	24.9	1750	21.43	C
ARP-7	5/9/2022	0.9	24.9	1750	21.38	C
ES-28	5/9/2022	1.9	26.2	1729	4.31	23.85
ES-28	5/9/2022	1.9	26.2	1729	4.27	23.85
M-207	5/9/2022	3	21.6	1600	3.65	26.85
M-207	5/9/2022	3	21.6	1600	4.65	22.35
PC-195	5/10/2022	1.5	24.1	1613	0.31	49.86
PC-195	5/10/2022	1.5	24.1	1613	0.72	43.86
TR-7	5/10/2022	0.6	25.4	1814	4.10	24.86
TR-7	5/10/2022	0.6	25.4	1814	4.32	23.86
M-155	5/10/2022	1.6	26.8	1728	23.31	C
M-155	5/10/2022	1.6	26.8	1728	23.83	C
TR-8	5/10/2022	4	15.9	1600	1.44	37.86
TR-8	5/10/2022	4	15.9	1600	1.46	37.86
M-31A	5/11/2022	1.6	21.9	1797	8.91	6.86
M-31A	5/11/2022	1.6	21.9	1797	8.88	6.86

*NS = no sample received, C = contaminated.

Table A-4. Dissolved gas results from sampled wells. Data provided by the U.S. Geological Survey.

Sample	Date	Field Temp (°C)	Recharge Elevation (feet)	Concentration in mg/L		
				CH_4	CO_2	N_2
MW 224A	5/2/2022	23.57	1527	0.00	4.16	14.31
MW 224A	5/2/2022	23.57	1527	0.00	4.36	14.11
MW25	5/2/2022	26.5	1530	0.00	15.99	14.15
MW25	5/2/2022	26.5	1530	0.00	14.98	14.05
MW201A	5/3/2022	23.54	1523	0.00	11.73	15.36
MW201A	5/3/2022	23.54	1523	0.00	11.34	15.10
NERT4.71S1	5/3/2022	23.54	1520	0.00	7.89	14.61
NERT4.71S1	5/3/2022	23.54	1520	0.00	8.75	14.45
PC-64	5/4/2022	23.93	1573	0.00	2.18	16.14
PC-64	5/4/2022	23.93	1573	0.00	2.23	16.15
PC-157B	5/4/2022	22.36	1545	0.00	15.07	19.14
PC-157B	5/4/2022	22.36	1545	0.00	13.20	19.42
NERT5.49S1	5/4/2022	20.71	1544	0.00	4.02	15.15
NERT5.49S1	5/4/2022	20.71	1544	0.00	4.79	14.19
PC-157A	5/4/2022	22	1545	0.00	25.10	18.29
PC-157A	5/4/2022	22	1545	0.00	27.67	18.24
NERT4.93S1	5/5/2022	24.24	1524	0.00	12.53	14.82
NERT4.93S1	5/5/2022	24.24	1524	0.00	12.63	14.72
MW-105	5/5/2022	23.6	1532	0.00	4.61	17.85
MW-105	5/5/2022	23.6	1532	0.00	4.08	17.85
PC-56	5/6/2022	17.5	1573	0.00	13.99	20.99
PC-56	5/6/2022	17.5	1573	0.00	13.59	20.97
ES-28	5/9/2022	27.1	1750	0.00	3.29	14.32
ES-28	5/9/2022	27.1	1750	0.00	3.27	14.39
M-207	5/9/2022	26	1729	0.00	4.55	16.50
M-207	5/9/2022	26	1729	0.00	4.42	16.47
ARP-7	5/9/2022	25.2	1600	0.00	8.60	13.70
ARP-7	5/9/2022	25.2	1600	0.00	8.45	13.71
PC-195	5/10/2022	23	1613	0.00	2.57	14.52
PC-195	5/10/2022	23	1613	0.00	3.09	14.51
TR-7	5/10/2022	25.2	1814	0.00	1.41	13.20
TR-7	5/10/2022	25.2	1814	0.00	1.50	13.18
M-155	5/10/2022	24.1	1728	0.00	1.18	13.87
M-155	5/10/2022	24.1	1728	0.00	1.23	14.15
TR-8	5/10/2022	25.1	1600	0.00	1.59	20.96
TR-8	5/10/2022	25.1	1600	0.00	1.50	21.10
M-31A	5/11/2022	24.4	1797	0.00	6.73	15.01
M-31A	5/11/2022	24.4	1797	0.00	7.09	14.96

APPENDIX B. *NETPATH* MODELING RESULTS

TR-8 + ES-28 = M-31A

```
           MODEL  31
 Init 1    + F        0.55556
 Init 2    + F        0.44444
 CO2 GAS              0.39374
 GYPSUM    +         -1.22129      (Constraint ignored)
 CALCITE              0.19650
 NaCl      +          2.79494
 PLAGAN45  +          5.85120
 DOLOMITE  +          0.15181
 Ca-MONT   -         -3.87311
 MONT-FEL  -         -0.14672
                Computed    Observed
Carbon-13       -7.0704     -7.4910
C-14 (% mod)    60.9572*    56.2800
Sulfur-34         Insufficient data
Strontium-87      Insufficient data
Nitrogen-15      0.0000   Undefined
-------------------------------------------------------------------
Adjusted C-14 age in years:    660.*     * = based on Original Data

           MODEL  32
 Init 1    + F        0.55556
 Init 2    + F        0.44444
 CO2 GAS              0.45239
 GYPSUM    +         -1.22129      (Constraint ignored)
 CALCITE              0.25523
 NaCl      +          2.79494
 PLAGAN45  +          5.85120
 DOLOMITE  +          0.09312
 Ca-MONT   -         -3.96123
 K-MONT    -         -0.05780
                Computed    Observed
Carbon-13       -7.3079     -7.4910
C-14 (% mod)    62.9360*    56.2800
Sulfur-34         Insufficient data
Strontium-87      Insufficient data
Nitrogen-15      0.0000   Undefined
-------------------------------------------------------------------
Adjusted C-14 age in years:    924.*     * = based on Original Data
```

TR-8 + ES-28 = M-31A

```
           MODEL  42
 Init 1    + F        0.55556
 Init 2    + F        0.44444
 CO2 GAS              0.56845
 GYPSUM    +         -1.22129      (Constraint ignored)
 CALCITE              0.32541
 NaCl      +          2.79494
 PLAGAN45  +          5.85120
 Ca-MONT   -         -3.82385
 K-MONT    -         -0.24592
 BIOTITE   +          0.06208
                Computed    Observed
Carbon-13       -7.7778     -7.4910
C-14 (% mod)    66.8523*    56.2800
Sulfur-34         Insufficient data
Strontium-87      Insufficient data
Nitrogen-15      0.0000   Undefined
-------------------------------------------------------------------------
Adjusted C-14 age in years:   1423.*     * = based on Original Data

           MODEL  62
 Init 1    + F        0.55556
 Init 2    + F        0.44444
 CO2 GAS              0.59025
 GYPSUM    +         -1.22129      (Constraint ignored)
 NaCl      +          2.79494
 ALBITE    +          2.18975
 PLAGAN45  +          4.85052
 DOLOMITE  +          0.15181
 MONT-FEL  -         -0.14672
 NA-MONT   -         -4.96780
                Computed    Observed
Carbon-13       -7.8661     -7.4910
C-14 (% mod)    67.5879*    56.2800
Sulfur-34         Insufficient data
Strontium-87      Insufficient data
Nitrogen-15      0.0000   Undefined
-------------------------------------------------------------------------
Adjusted C-14 age in years:   1514.*     * = based on Original Data
```

TR-8 + ES-28 = M-31A

```
           MODEL  64
 Init 1    + F        0.55556
 Init 2    + F        0.44444
 CO2 GAS              0.70762
 GYPSUM    +         -1.22129      (Constraint ignored)
 NaCl      +          2.79494
 ALBITE    +          0.49658
 PLAGAN45  +          4.94833
 DOLOMITE  +          0.09312
 K-SPAR    +          1.69003
 K-MONT    -         -5.17912
               Computed    Observed
Carbon-13       -8.3413     -7.4910
C-14 (% mod)    71.5484*    56.2800
Sulfur-34         Insufficient data
Strontium-87      Insufficient data
Nitrogen-15      0.0000   Undefined
-------------------------------------------------------------------------
Adjusted C-14 age in years:   1984.*     * = based on Original Data

           MODEL 118
 Init 1    + F        0.55556
 Init 2    + F        0.44444
 CO2 GAS              0.70026
 GYPSUM    +         -1.22129      (Constraint ignored)
 NaCl      +          2.79494
 PLAGAN45  +          6.35453
 DOLOMITE  +          0.09680
 Ca-MONT   -         -4.22284
 MONT-FEL  -         -0.14672
 EXCHANGE            -0.13842
               Computed    Observed
Carbon-13       -8.3115     -7.4910
C-14 (% mod)    71.2999*    56.2800
Sulfur-34         Insufficient data
Strontium-87      Insufficient data
Nitrogen-15      0.0000   Undefined
-------------------------------------------------------------------------
Adjusted C-14 age in years:   1956.*     * = based on Original Data
```

TR-8 + ES-28 = M-31A

```
           MODEL 119
 Init 1    + F        0.55556
 Init 2    + F        0.44444
 CO2 GAS              0.27224
 GYPSUM    +         -1.22129      (Constraint ignored)
 NaCl      +          2.79494
 PLAGAN45  +          5.85120
 DOLOMITE  +          0.31081
 Ca-MONT   -         -3.18412
 MONT-FEL  -         -0.92236
 BIOTITE   +          0.10083
               Computed    Observed
Carbon-13       -6.5784     -7.4910
C-14 (% mod)    56.8571*    56.2800
Sulfur-34         Insufficient data
Strontium-87      Insufficient data
Nitrogen-15      0.0000   Undefined
-------------------------------------------------------------------------
Adjusted C-14 age in years:     84.*     * = based on Original Data

           MODEL 128
 Init 1    + F        0.55556
 Init 2    + F        0.44444
 CO2 GAS              0.53228
 GYPSUM    +         -1.22129      (Constraint ignored)
 NaCl      +          2.79494
 PLAGAN45  +          5.04895
 DOLOMITE  +          0.18079
 K-SPAR    +          1.53819
 K-MONT    -         -4.71898
 EXCHANGE             0.22062
              Computed    Observed
Carbon-13       -7.6314     -7.4910
C-14 (% mod)    65.6319*    56.2800
Sulfur-34         Insufficient data
Strontium-87      Insufficient data
Nitrogen-15      0.0000   Undefined
-------------------------------------------------------------------------
Adjusted C-14 age in years:   1271.*     * = based on Original Data
```

TR-7 + PC-157A = M-155

```
           MODEL   6
 Init 1    + F        0.96933
 Init 2    + F        0.03067
 CO2 GAS              0.53367
 GYPSUM    +         -0.86288      (Constraint ignored)
 CALCITE              -0.72932
 NaCl      +         -2.24719      (Constraint ignored)
 ALBITE    +          0.02145
 MONT-FEL  -         -0.65705
 ANORTH    +          0.99915
 EXCHANGE             0.28690
                Computed    Observed
Carbon-13       -9.1395    -10.4430
C-14 (% mod)    43.6742*     4.4200
Sulfur-34         Insufficient data
Strontium-87      Insufficient data
Nitrogen-15      0.0000   Undefined
-------------------------------------------------------------------
Adjusted C-14 age in years:  18936.*     * = based on Original Data

           MODEL   7
 Init 1    + F        0.96933
 Init 2    + F        0.03067
 CO2 GAS              0.81828
 GYPSUM    +         -0.86288      (Constraint ignored)
 CALCITE              -1.01393
 NaCl      +         -2.24719      (Constraint ignored)
 ALBITE    +          0.59526
 MONT-FEL  -         -1.30492
 ANORTH    +          1.19447
 BIOTITE   +          0.08422
                Computed    Observed
Carbon-13       -9.7068    -10.4430
C-14 (% mod)    51.8328*     4.4200
Sulfur-34         Insufficient data
Strontium-87      Insufficient data
Nitrogen-15      0.0000   Undefined
-------------------------------------------------------------------
Adjusted C-14 age in years:  20352.*     * = based on Original Data
```

TR-7 + PC-157A = M-155

```
           MODEL  15
 Init 1    + F        0.96933
 Init 2    + F        0.03067
 CO2 GAS              1.55268
 GYPSUM    +         -0.86288      (Constraint ignored)
 CALCITE             -1.74833
 NaCl      +         -2.24719      (Constraint ignored)
 PLAGAN45  +          3.77429
 MONT-FEL  -         -2.97661
 EXCHANGE            -0.74030
 BIOTITE   +          0.30154
               Computed    Observed
Carbon-13      -10.8170    -10.4430
C-14 (% mod)    67.8162*     4.4200
Sulfur-34         Insufficient data
Strontium-87      Insufficient data
Nitrogen-15      0.0000   Undefined
-------------------------------------------------------------------------
Adjusted C-14 age in years:  22573.*     * = based on Original Data
```

TR-8 + M-31A + PC-157A = M-207

```
           MODEL   2
 Init 1    + F        0.56465
 Init 2    + F        0.32340
 Init 3    + F        0.11195
 CO2 GAS              -0.59674
 GYPSUM    +          2.88635
 NaCl      +          5.46618
 ALBITE    +          5.67612
 SiO2                 0.00000
 K-MONT    -         -6.41416
 BIOTITE   +          2.25811
               Computed    Observed
Carbon-13       -7.2632     -6.9690
C-14 (% mod)    62.9587*    44.2000
Sulfur-34        5.2411   Undefined
Strontium-87      Insufficient data
Nitrogen-15      0.0000   Undefined
-------------------------------------------------------------------------
Adjusted C-14 age in years:   2924.*     * = based on Original Data

           MODEL  26
 Init 1    + F        0.36466
 Init 2    + F        0.56471
 Init 3    + F        0.07063
 CO2 GAS              -0.69055
 GYPSUM    +          0.00000
 ALBITE    +          3.92377
 ANORTH    +          2.52908
 K-MONT    -         -6.36007
 EXCHANGE             1.52876
 BIOTITE   +          2.22784
               Computed    Observed
Carbon-13       -6.3472     -6.9690
C-14 (% mod)    60.4237*    44.2000
Sulfur-34        0.0000   Undefined
Strontium-87      Insufficient data
Nitrogen-15      0.0000   Undefined
-------------------------------------------------------------------------
Adjusted C-14 age in years:   2585.*     * = based on Original Data
```

TR-8 + M-31A + PC-157A = M-207

```
           MODEL  59
 Init 1    + F        0.36466
 Init 2    + F        0.56471
 Init 3    + F        0.07063
 CO2 GAS              -0.25906
 CALCITE              -0.43149
 NaCl      +           0.00000
 PLAGAN45  +           6.71485
 K-MONT    -          -6.46954
 EXCHANGE              1.64407
 BIOTITE   +           2.26397
                Computed    Observed
Carbon-13        -7.9017     -6.9690
C-14 (% mod)    60.2347*    44.2000
Sulfur-34        0.0000   Undefined
Strontium-87      Insufficient data
Nitrogen-15      0.0000   Undefined
-------------------------------------------------------------------------
Adjusted C-14 age in years:   2559.*     * = based on Original Data
```

TR-7 + TR-8 + PC-157 A = PC-195

```
           MODEL   1
 Init 1    + F        0.44977
 Init 2    + F        0.52580
 Init 3    + F        0.02444
 CO2 GAS              3.23965
 GYPSUM    +          8.95330
 CALCITE             -7.08770
 NaCl      +          4.59943
 PLAGAN45  +          0.00000
 DOLOMITE  +          1.86037
 Ca-MONT   -         -0.11394
 BIOTITE   +          0.26877
                Computed    Observed
Carbon-13       -6.6947     -7.6590
C-14 (% mod)    46.2157*    25.1000
Sulfur-34       15.7319   Undefined
Strontium-87      Insufficient data
Nitrogen-15      0.0000   Undefined
-------------------------------------------------------------------------
Adjusted C-14 age in years:   5046.*     * = based on Original Data

           MODEL   3
 Init 1    + F        0.46358
 Init 2    + F        0.51491
 Init 3    + F        0.02151
 CO2 GAS              3.25014
 GYPSUM    +          8.94014
 CALCITE             -7.08747
 NaCl      +          4.65205
 PLAGAN45  +          0.00000
 DOLOMITE  +          1.86115
 NA-MONT   -         -0.11481
 BIOTITE   +          0.26980
                Computed    Observed
Carbon-13       -6.6986     -7.6590
C-14 (% mod)    46.2844*    25.1000
Sulfur-34       15.7088   Undefined
Strontium-87      Insufficient data
Nitrogen-15      0.0000   Undefined
-------------------------------------------------------------------------
Adjusted C-14 age in years:   5059.*     * = based on Original Data
```

TR-7 + TR-8 + PC-157 A = PC-195

```
           MODEL   7
 Init 1    + F        0.44977
 Init 2    + F        0.52580
 Init 3    + F        0.02444
 CO2 GAS              3.21956
 GYPSUM    +          8.95330
 CALCITE             -7.12020
 NaCl      +          4.59943
 SiO2                 0.00000
 DOLOMITE  +          1.88667
 MONT-FEL  -         -0.12827
 BIOTITE   +          0.28544
               Computed    Observed
Carbon-13       -6.6353     -7.6590
C-14 (% mod)    45.7284*    25.1000
Sulfur-34       15.7319   Undefined
Strontium-87      Insufficient data
Nitrogen-15      0.0000   Undefined
-------------------------------------------------------------------
Adjusted C-14 age in years:   4959.*     * = based on Original Data

           MODEL  10
 Init 1    + F        0.44977
 Init 2    + F        0.52580
 Init 3    + F        0.02444
 CO2 GAS              3.33591
 GYPSUM    +          8.95330
 CALCITE             -7.02950
 NaCl      +          4.59943
 SiO2                 0.00000
 DOLOMITE  +          1.78314
 K-MONT    -         -0.15602
 BIOTITE   +          0.32026
               Computed    Observed
Carbon-13       -6.9044     -7.6590
C-14 (% mod)    47.9498*    25.1000
Sulfur-34       15.7319   Undefined
Strontium-87      Insufficient data
Nitrogen-15      0.0000   Undefined
-------------------------------------------------------------------
Adjusted C-14 age in years:   5351.*     * = based on Original Data
```

M-31A = PC-64

```
          MODEL   5
 CO2 GAS              3.65593
 GYPSUM    +          9.87472
 CALCITE             -2.35946
 NaCl      +          8.96211
 ALBITE    +          3.47172
 K-MONT    -         -3.72888
 BIOTITE   +          1.16438
               Computed    Observed
Carbon-13      -10.8453    -11.3020
C-14 (% mod)    84.2164*    57.2500
Sulfur-34        7.9830   Undefined
Strontium-87      Insufficient data
Nitrogen-15      0.0000   Undefined
-------------------------------------------------------------------------
Adjusted C-14 age in years:   3191.*     * = based on Original Data

          MODEL  68
 CO2 GAS              3.74721
 GYPSUM    +          9.87472
 CALCITE             -2.45074
 PLAGAN45  +          6.88292
 K-MONT    -         -6.39167
 EXCHANGE             4.32411
 BIOTITE   +          2.04310
               Computed    Observed
Carbon-13      -10.8990    -11.3020
C-14 (% mod)    84.6104*    57.2500
Sulfur-34        7.9830   Undefined
Strontium-87      Insufficient data
Nitrogen-15      0.0000   Undefined
-------------------------------------------------------------------------
Adjusted C-14 age in years:   3229.*     * = based on Original Data
```

TR-7 + ES-28 = MW-25

```
           MODEL   9
 Init 1    + F        0.75595
 Init 2    + F        0.24405
 CO2 GAS              7.23131
 GYPSUM    +          8.03822
 CALCITE             -5.54873
 NaCl      +          8.88772
 ALBITE    +          7.87327
 Ca-MONT   -         -8.04233
 K-SPAR    +          2.09782
 EXCHANGE            -3.08963
                Computed    Observed
Carbon-13      -12.7882    -13.2570
C-14 (% mod)    95.6482*    64.9900
Sulfur-34        9.5087   Undefined
Strontium-87      Insufficient data
Nitrogen-15      0.0000   Undefined
-------------------------------------------------------------------------
Adjusted C-14 age in years:   3195.*     * = based on Original Data

           MODEL  10
 Init 1    + F        0.75595
 Init 2    + F        0.24405
 CO2 GAS              6.10515
 GYPSUM    +          8.03822
 CALCITE             -4.42258
 NaCl      +          8.88772
 ALBITE    +          1.69402
 Ca-MONT   -         -2.99118
 K-SPAR    +          1.35121
 BIOTITE   +          0.74662
                Computed    Observed
Carbon-13      -12.5351    -13.2570
C-14 (% mod)    93.4997*    64.9900
Sulfur-34        9.5087   Undefined
Strontium-87      Insufficient data
Nitrogen-15      0.0000   Undefined
-------------------------------------------------------------------------
Adjusted C-14 age in years:   3007.*     * = based on Original Data
```

TR-7 + ES-28 = MW-25

```
           MODEL  11
 Init 1    + F        0.75595
 Init 2    + F        0.24405
 CO2 GAS              6.26794
 GYPSUM    +          8.03822
 CALCITE             -4.58537
 NaCl      +          8.88772
 ALBITE    +          1.69402
 MONT-FEL  -         -3.36737
 K-SPAR    +          0.89100
 BIOTITE   +          1.64458
                Computed    Observed
Carbon-13      -12.5780    -13.2570
C-14 (% mod)    93.8691*    64.9900
Sulfur-34        9.5087   Undefined
Strontium-87      Insufficient data
Nitrogen-15      0.0000   Undefined
-------------------------------------------------------------------------
Adjusted C-14 age in years:   3039.*     * = based on Original Data

           MODEL  15
 Init 1    + F        0.75595
 Init 2    + F        0.24405
 CO2 GAS              6.60468
 GYPSUM    +          8.03822
 CALCITE             -4.92210
 NaCl      +          8.88772
 ALBITE    +          1.69402
 K-SPAR    +          2.70293
 K-MONT    -         -4.09612
 BIOTITE   +          0.74662
                Computed    Observed
Carbon-13      -12.6594    -13.2570
C-14 (% mod)    94.5653*    64.9900
Sulfur-34        9.5087   Undefined
Strontium-87      Insufficient data
Nitrogen-15      0.0000   Undefined
-------------------------------------------------------------------------
Adjusted C-14 age in years:   3100.*     * = based on Original Data
```

TR-7 + ES-28 = MW-25

```
           MODEL  27
 Init 1    + F        0.75595
 Init 2    + F        0.24405
 CO2 GAS              7.36502
 GYPSUM    +          8.03822
 CALCITE             -5.68245
 NaCl      +          8.88772
 PLAGAN45  +          3.08003
 Ca-MONT   -         -3.74650
 K-SPAR    +          1.35121
 BIOTITE   +          0.74662
                Computed    Observed
Carbon-13      -12.8123    -13.2570
C-14 (% mod)    95.8481*    64.9900
Sulfur-34        9.5087   Undefined
Strontium-87      Insufficient data
Nitrogen-15      0.0000   Undefined
-------------------------------------------------------------------------
Adjusted C-14 age in years:   3212.*     * = based on Original Data

           MODEL  28
 Init 1    + F        0.75595
 Init 2    + F        0.24405
 CO2 GAS              7.56892
 GYPSUM    +          8.03822
 CALCITE             -5.88635
 NaCl      +          8.88772
 PLAGAN45  +          3.08003
 MONT-FEL  -         -4.21768
 K-SPAR    +          0.77479
 BIOTITE   +          1.87133
                Computed    Observed
Carbon-13      -12.8471    -13.2570
C-14 (% mod)    96.1342*    64.9900
Sulfur-34        9.5087   Undefined
Strontium-87      Insufficient data
Nitrogen-15      0.0000   Undefined
-------------------------------------------------------------------------
Adjusted C-14 age in years:   3236.*     * = based on Original Data
```

TR-7 + ES-28 = MW-25

```
           MODEL  32
 Init 1    + F        0.75595
 Init 2    + F        0.24405
 CO2 GAS              7.99069
 GYPSUM    +          8.03822
 CALCITE             -6.30812
 NaCl      +          8.88772
 PLAGAN45  +          3.08003
 K-SPAR    +          3.04426
 K-MONT    -         -5.13046
 BIOTITE   +          0.74662
               Computed    Observed
Carbon-13      -12.9119    -13.2570
C-14 (% mod)    96.6609*    64.9900
Sulfur-34        9.5087   Undefined
Strontium-87      Insufficient data
Nitrogen-15      0.0000   Undefined
---------------------------------------------------------------------
Adjusted C-14 age in years:   3282.*     * = based on Original Data

           MODEL  34
 Init 1    + F        0.75595
 Init 2    + F        0.24405
 CO2 GAS              9.72546
 GYPSUM    +          8.03822
 CALCITE             -8.04288
 NaCl      +          8.88772
 PLAGAN45  +          6.93507
 K-SPAR    +          1.35121
 NA-MONT   -         -6.42507
 BIOTITE   +          0.74662
               Computed    Observed
Carbon-13      -13.1016    -13.2570
C-14 (% mod)    98.1299*    64.9900
Sulfur-34        9.5087   Undefined
Strontium-87      Insufficient data
Nitrogen-15      0.0000   Undefined
---------------------------------------------------------------------
Adjusted C-14 age in years:   3406.*     * = based on Original Data
```

TR-7 + ES-28 = MW-25

```
           MODEL  37
 Init 1    + F        0.75595
 Init 2    + F        0.24405
 CO2 GAS              6.06469
 GYPSUM    +          8.03822
 CALCITE             -4.38212
 NaCl      +          8.88772
 SiO2                -5.89556
 K-SPAR    +          1.14652
 EXCHANGE             0.84701
 BIOTITE   +          0.95130
                Computed    Observed
Carbon-13      -12.5241    -13.2570
C-14 (% mod)    93.4044*    64.9900
Sulfur-34        9.5087   Undefined
Strontium-87      Insufficient data
Nitrogen-15      0.0000   Undefined
-------------------------------------------------------------------------
Adjusted C-14 age in years:   2998.*     * = based on Original Data

           MODEL  43
 Init 1    + F        0.75595
 Init 2    + F        0.24405
 CO2 GAS              5.79642
 GYPSUM    +          8.03822
 CALCITE             -4.11384
 NaCl      +          8.88772
 Ca-MONT   -         -1.60642
 K-SPAR    +          1.14652
 EXCHANGE             0.84701
 BIOTITE   +          0.95130
                Computed    Observed
Carbon-13      -12.4469    -13.2570
C-14 (% mod)    92.7341*    64.9900
Sulfur-34        9.5087   Undefined
Strontium-87      Insufficient data
Nitrogen-15      0.0000   Undefined
-------------------------------------------------------------------------
Adjusted C-14 age in years:   2939.*     * = based on Original Data
```

TR-7 + ES-28 = MW-25

```
           MODEL  44
 Init 1    + F        0.75595
 Init 2    + F        0.24405
 CO2 GAS              5.88384
 GYPSUM    +          8.03822
 CALCITE             -4.20127
 NaCl      +          8.88772
 MONT-FEL  -         -1.80846
 K-SPAR    +          0.89937
 EXCHANGE             0.84701
 BIOTITE   +          1.43355
                Computed    Observed
Carbon-13      -12.4729    -13.2570
C-14 (% mod)    92.9600*    64.9900
Sulfur-34        9.5087   Undefined
Strontium-87      Insufficient data
Nitrogen-15      0.0000   Undefined
-------------------------------------------------------------------------
Adjusted C-14 age in years:   2959.*     * = based on Original Data

           MODEL  47
 Init 1    + F        0.75595
 Init 2    + F        0.24405
 CO2 GAS              5.89571
 GYPSUM    +          8.03822
 CALCITE             -4.21314
 NaCl      +          8.88772
 K-SPAR    +          1.08247
 NA-MONT   -         -1.60642
 EXCHANGE             1.11207
 BIOTITE   +          1.01535
               Computed    Observed
Carbon-13      -12.4763    -13.2570
C-14 (% mod)    92.9901*    64.9900
Sulfur-34        9.5087   Undefined
Strontium-87      Insufficient data
Nitrogen-15      0.0000   Undefined
-------------------------------------------------------------------------
Adjusted C-14 age in years:   2962.*     * = based on Original Data
```

TR-7 + ES-28 + PC-157A = MW-224

```
           MODEL   4
 Init 1    + F        0.21373
 Init 2    + F        0.38813
 Init 3    + F        0.39814
 CO2 GAS              -0.36883
 GYPSUM    +           5.06267
 CALCITE              -1.72323
 NaCl      +           1.60648
 PLAGAN45  +           0.00000
 K-SPAR    +           3.67016
 K-MONT    -          -3.03297
 EXCHANGE             -4.87832
                Computed    Observed
Carbon-13      -13.3164    -13.3650
C-14 (% mod)    83.8233*    71.5100
Sulfur-34        4.8437   Undefined
Strontium-87      Insufficient data
Nitrogen-15      0.0000   Undefined
-------------------------------------------------------------------------
Adjusted C-14 age in years:   1313.*     * = based on Original Data
```

```
           MODEL  18
 Init 1    + F        0.13261
 Init 2    + F        0.55550
 Init 3    + F        0.31189
 CO2 GAS              -0.12961
 GYPSUM    +           0.00000
 CALCITE              -1.68074
 NaCl      +           1.01761
 MONT-FEL  -          -4.27711
 K-SPAR    +           3.20642
 ANORTH    +           2.89637
 EXCHANGE             -6.64375
                Computed    Observed
Carbon-13      -13.4479    -13.3650
C-14 (% mod)    85.4900*    71.5100
Sulfur-34        0.0000   Undefined
Strontium-87      Insufficient data
Nitrogen-15      0.0000   Undefined
-------------------------------------------------------------------------
Adjusted C-14 age in years:   1476.*     * = based on Original Data
```

TR-7 + ES-28 + PC-157A = MW-224

```
           MODEL  90
 Init 1    + F         0.13261
 Init 2    + F         0.55550
 Init 3    + F         0.31189
 GYPSUM    +           0.00000
 CALCITE               -1.81035
 NaCl      +           1.01761
 PLAGAN45  +           5.10603
 MONT-FEL  -          -6.49418
 K-SPAR    +           3.20622
 EXCHANGE              -8.04791
 BIOTITE   +           0.28842
                Computed    Observed
Carbon-13      -13.9084    -13.3650
C-14 (% mod)    85.4102*    71.5100
Sulfur-34        0.0000   Undefined
Strontium-87      Insufficient data
Nitrogen-15      0.0000   Undefined
-------------------------------------------------------------------------
Adjusted C-14 age in years:   1468.*     * = based on Original Data

           MODEL 107
 Init 1    + F         0.13261
 Init 2    + F         0.55550
 Init 3    + F         0.31189
 GYPSUM    +           0.00000
 CALCITE               -1.90210
 NaCl      +           1.01761
 DOLOMITE  +           0.04588
 MONT-FEL  -          -4.39181
 K-SPAR    +           3.22133
 ANORTH    +           3.08332
 EXCHANGE              -6.64375
                Computed    Observed
Carbon-13      -13.4686    -13.3650
C-14 (% mod)    82.2925*    71.5100
Sulfur-34        0.0000   Undefined
Strontium-87      Insufficient data
Nitrogen-15      0.0000   Undefined
-------------------------------------------------------------------------
Adjusted C-14 age in years:   1161.*     * = based on Original Data
```

TR-7 + ES-28 + PC-157 A = MW-105

```
           MODEL  14
 Init 1    + F        0.30815
 Init 2    + F        0.28824
 Init 3    + F        0.40360
 CO2 GAS              0.00000
 GYPSUM    +          9.97922
 CALCITE             -1.80348
 NaCl      +          3.92156
 MONT-FEL  -         -5.48448
 ANORTH    +          1.24030
 BIOTITE   +          5.93489
               Computed    Observed
Carbon-13      -14.2552    -13.8330
C-14 (% mod)    80.5162*    66.6300
Sulfur-34        8.9258   Undefined
Strontium-87      Insufficient data
Nitrogen-15      0.0000   Undefined
-------------------------------------------------------------------
Adjusted C-14 age in years:   1565.*     * = based on Original Data

           MODEL  42
 Init 1    + F        0.26493
 Init 2    + F        0.37743
 Init 3    + F        0.35765
 CO2 GAS              0.00000
 GYPSUM    +          7.28173
 CALCITE             -1.65337
 PLAGAN45  +          3.13906
 MONT-FEL  -         -8.37332
 ANORTH    +          1.94088
 BIOTITE   +          6.30038
               Computed    Observed
Carbon-13      -13.9152    -13.8330
C-14 (% mod)    81.3171*    66.6300
Sulfur-34        6.5131   Undefined
Strontium-87      Insufficient data
Nitrogen-15      0.0000   Undefined
-------------------------------------------------------------------
Adjusted C-14 age in years:   1647.*     * = based on Original Data
```

TR-7 + ES-28 + PC-157 A = MW-105

```
           MODEL 379
 Init 1    + F        0.14825
 Init 2    + F        0.61817
 Init 3    + F        0.23358
 CO2 GAS              0.00000
 CALCITE             -1.24818
 Ca-MONT   -          -8.36496
 K-SPAR    +          2.80361
 ANORTH    +          7.62832
 EXCHANGE            -2.09951
 BIOTITE   +          2.38108
                Computed    Observed
Carbon-13      -12.8491    -13.8330
C-14 (% mod)    83.8559*    66.6300
Sulfur-34        0.0000   Undefined
Strontium-87      Insufficient data
Nitrogen-15      0.0000   Undefined
-------------------------------------------------------------------------
Adjusted C-14 age in years:   1901.*     * = based on Original Data

           MODEL 526
 Init 1    + F        0.28639
 Init 2    + F        0.33315
 Init 3    + F        0.38046
 GYPSUM    +          8.62103
 CALCITE             -1.72790
 NaCl      +          0.00000
 PLAGAN45  +          5.12061
 SiO2                -5.84115
 MONT-FEL  -          -6.93901
 BIOTITE   +          6.11892
                Computed    Observed
Carbon-13      -14.0873    -13.8330
C-14 (% mod)    80.9113*    66.6300
Sulfur-34        7.7110   Undefined
Strontium-87      Insufficient data
Nitrogen-15      0.0000   Undefined
-------------------------------------------------------------------------
Adjusted C-14 age in years:   1605.*     * = based on Original Data
```

TR-7 + ES-28 + PC-157 A = MW-105

```
          MODEL 531
 Init 1    + F        0.29020
 Init 2    + F        0.32529
 Init 3    + F        0.38451
 GYPSUM    +          8.85860
 CALCITE              -1.74112
 NaCl      +          0.00000
 PLAGAN45  +          5.47210
 Ca-MONT   -         -2.06153
 MONT-FEL  -         -6.68459
 BIOTITE   +          6.08673
               Computed    Observed
Carbon-13      -14.1171    -13.8330
C-14 (% mod)    80.8410*    66.6300
Sulfur-34        7.9235   Undefined
Strontium-87      Insufficient data
Nitrogen-15      0.0000   Undefined
-------------------------------------------------------------------------
Adjusted C-14 age in years:   1598.*     * = based on Original Data

          MODEL 532
 Init 1    + F        0.29462
 Init 2    + F        0.31617
 Init 3    + F        0.38922
 GYPSUM    +          9.13466
 CALCITE              -1.75648
 NaCl      +          0.00000
 PLAGAN45  +          5.88054
 Ca-MONT   -         -8.28281
 K-SPAR    +          0.87316
 BIOTITE   +          4.34561
               Computed    Observed
Carbon-13      -14.1515    -13.8330
C-14 (% mod)    80.7599*    66.6300
Sulfur-34        8.1704   Undefined
Strontium-87      Insufficient data
Nitrogen-15      0.0000   Undefined
-------------------------------------------------------------------------
Adjusted C-14 age in years:   1590.*     * = based on Original Data
```

TR-7 + ES-28 + PC-157 A = MW-105

```
           MODEL 535
 Init 1    + F        0.28806
 Init 2    + F        0.32970
 Init 3    + F        0.38224
 GYPSUM    +          8.72521
 CALCITE              -1.73370
 NaCl      +          0.00000
 PLAGAN45  +          5.27475
 MONT-FEL  -         -8.33719
 K-MONT    -         -0.62525
 BIOTITE   +          6.50740
                Computed    Observed
Carbon-13      -14.1004    -13.8330
C-14 (% mod)    80.8804*    66.6300
Sulfur-34        7.8042   Undefined
Strontium-87      Insufficient data
Nitrogen-15      0.0000   Undefined
-------------------------------------------------------------------
Adjusted C-14 age in years:   1602.*     * = based on Original Data

           MODEL 536
 Init 1    + F        0.28140
 Init 2    + F        0.34345
 Init 3    + F        0.37516
 GYPSUM    +          8.30943
 CALCITE              -1.71056
 NaCl      +          0.00000
 PLAGAN45  +          5.66305
 MONT-FEL  -         -7.27272
 NA-MONT   -         -1.67245
 BIOTITE   +          6.16114
                Computed    Observed
Carbon-13      -14.0478    -13.8330
C-14 (% mod)    81.0042*    66.6300
Sulfur-34        7.4323   Undefined
Strontium-87      Insufficient data
Nitrogen-15      0.0000   Undefined
-------------------------------------------------------------------
Adjusted C-14 age in years:   1615.*     * = based on Original Data
```

TR-7 + ES-28 + PC-157 A = MW-105

```
           MODEL 538
 Init 1    + F        0.27810
 Init 2    + F        0.35024
 Init 3    + F        0.37166
 GYPSUM    +          8.10400
 CALCITE              -1.69913
 NaCl      +          0.00000
 PLAGAN45  +          4.35563
 K-SPAR    +          4.28878
 K-MONT    -         -9.89326
 BIOTITE   +          4.19091
                Computed    Observed
Carbon-13      -14.0216    -13.8330
C-14 (% mod)    81.0660*    66.6300
Sulfur-34        7.2486   Undefined
Strontium-87      Insufficient data
Nitrogen-15      0.0000   Undefined
-------------------------------------------------------------------------
Adjusted C-14 age in years:   1621.*     * = based on Original Data

           MODEL 539
 Init 1    + F        0.24861
 Init 2    + F        0.41109
 Init 3    + F        0.34030
 GYPSUM    +          6.26348
 CALCITE              -1.59671
 NaCl      +          0.00000
 PLAGAN45  +          7.12168
 K-SPAR    +          1.29339
 NA-MONT   -         -9.14862
 BIOTITE   +          3.91467
                Computed    Observed
Carbon-13      -13.7799    -13.8330
C-14 (% mod)    81.6372*    66.6300
Sulfur-34        5.6023   Undefined
Strontium-87      Insufficient data
Nitrogen-15      0.0000   Undefined
-------------------------------------------------------------------------
Adjusted C-14 age in years:   1679.*     * = based on Original Data
```

TR-7 + ES-28 + PC-157 A = MW-105

```
           MODEL 569
 Init 1    + F        0.26080
 Init 2    + F        0.38594
 Init 3    + F        0.35326
 GYPSUM    +          7.02415
 CALCITE              -1.63904
 NaCl      +          0.00000
 MONT-FEL  -         -7.08044
 ANORTH    +          3.83521
 EXCHANGE             0.75844
 BIOTITE   +          6.13135
                Computed    Observed
Carbon-13      -13.8814    -13.8330
C-14 (% mod)    81.3971*    66.6300
Sulfur-34        6.2827   Undefined
Strontium-87      Insufficient data
Nitrogen-15      0.0000   Undefined
-------------------------------------------------------------------------
Adjusted C-14 age in years:   1655.*     * = based on Original Data

           MODEL 575
 Init 1    + F        0.30430
 Init 2    + F        0.29619
 Init 3    + F        0.39951
 GYPSUM    +          9.73894
 CALCITE              -1.79011
 NaCl      +          0.00000
 ANORTH    +          2.45325
 NA-MONT   -         -5.53307
 EXCHANGE             2.77597
 BIOTITE   +          5.22102
                Computed    Observed
Carbon-13      -14.2260    -13.8330
C-14 (% mod)    80.5849*    66.6300
Sulfur-34        8.7109   Undefined
Strontium-87      Insufficient data
Nitrogen-15      0.0000   Undefined
-------------------------------------------------------------------------
Adjusted C-14 age in years:   1572.*     * = based on Original Data
```

TR-7 + ES-28 + PC-157 A = MW-105

```
           MODEL 630
 Init 1    + F        0.26916
 Init 2    + F        0.36870
 Init 3    + F        0.36214
 GYPSUM    +          7.54565
 CALCITE              -1.66806
 PLAGAN45  +          6.35524
 SiO2                 0.00000
 MONT-FEL  -         -9.69797
 EXCHANGE             -0.77707
 BIOTITE   +          6.47357
                Computed    Observed
Carbon-13      -13.9496    -13.8330
C-14 (% mod)    81.2358*    66.6300
Sulfur-34        6.7491   Undefined
Strontium-87      Insufficient data
Nitrogen-15      0.0000   Undefined
-------------------------------------------------------------------------
Adjusted C-14 age in years:   1638.*     * = based on Original Data

           MODEL 648
 Init 1    + F        0.23093
 Init 2    + F        0.44757
 Init 3    + F        0.32150
 GYPSUM    +          5.16009
 CALCITE              -1.53532
 PLAGAN45  +          0.00000
 Ca-MONT   -         -6.99099
 K-SPAR    +          1.45488
 ANORTH    +          5.11845
 BIOTITE   +          3.74906
                Computed    Observed
Carbon-13      -13.6286    -13.8330
C-14 (% mod)    81.9957*    66.6300
Sulfur-34        4.6154   Undefined
Strontium-87      Insufficient data
Nitrogen-15      0.0000   Undefined
-------------------------------------------------------------------------
Adjusted C-14 age in years:   1715.*     * = based on Original Data
```

STANDING DISTRIBUTION LIST

Weiquan Dong
Professional Engineering Specialist
Nevada Division of Environmental Protection
Department of Conservation and Natural Resources
375 E Warm Springs Rd, Suite 200
Las Vegas, NV 89119

Alan Pineda
Civil Engineer
Nevada Division of Environmental Protection
Department of Conservation and Natural Resources
375 E Warm Springs Rd, Suite 200
Las Vegas, NV 89119

Danielle D. Ward
Administrative Assistant
Nevada Division of Environmental Protection
Department of Conservation and Natural Resources
375 E Warm Springs Rd, Suite 200
Las Vegas, NV 89119

Steve Clough
Remediation Director
Nevada Environmental Response Trust
510 S. Fourth Street
Henderson, NV 89012

Alka Singhal
Senior Managing Consultant
Ramboll
2200 Powell St Suite 700
Emeryville, CA 94608

Nevada State Library and Archives
State Publications
100 North Stewart Street
Carson City, NV 89701-4285
NSLstatepubs@admin.nv.gov

Archives Getchell Library
University of Nevada, Reno
1664 N. Virginia St.
Reno, NV 89557
cklenke@unr.edu

Document Section, Library
University of Nevada, Las Vegas
4505 Maryland Parkway
Las Vegas, NV 89154
sue.wainscott@unlv.edu

†Library
Southern Nevada Science Center
Desert Research Institute
755 E. Flamingo Road
Las Vegas, NV 89119-7363

All on distribution list receive one PDF copy, unless otherwise noted.

† 2 copies; CD with pdf (from which to print)